5-21-2007

Protein Binding Sites and Cis-acting Sequences on the West Nile Virus 3' (+) SL RNA

William G. Davis
Georgia State University

West Nile Virus 3' (+) SL RNA Protein Binding Sites and *Cis*-acting Sequences

by

William G. Davis

Under the Direction of Dr. Margo A. Brinton

Abstract

The 3' terminal 96 nts of the West Nile virus (WNV) genomic RNA are predicted to form two stem loop (SL) stuctures, a short SL (SSL) of 16 nts and a longer terminal SL of 80 nts. These two structures are referred to collectively as the WNV 3' (+) SL RNA and have been shown to contain *cis*-acting elements during virus replication. RNase footprinting and nitrocellulose filter-binding assays were previously used to map one major and two minor binding sites for the cell protein, eukaryote elongation factor 1 A (eEF1A), on the WNV 3' (+) SL RNA. Various base substitutions were engineered into a WNV cDNA infectious clone within the major eEF1A binding site on the terminal SL or within the minor binding site on the SSL and the affect on viral growth was assessed. None of these mutations affected the efficiency of translation of the viral polyprotein from the genomic RNA, but all of the mutations that decreased eEF1A binding to the 3' SL RNA *in vitro* also decreased viral minus strand RNA synthesis in transfected cells. Mutations to the major eEF1A binding site that increased the efficiency of eEF1A binding to the 3' SL RNA *in vitro* increased viral minus strand RNA synthesis, which resulted in decreased synthesis of genomic RNA. These results strongly suggest that the interaction between eEF1A and the WNV 3'

SL promotes viral minus-strand synthesis. eEF1A colocalized with viral replication complexes (RC) in infected cells and antibody to eEF1A coimmunoprecipitated viral RC proteins, suggesting that eEF1A may facilitates an interaction between the 3' end of the genome and the RC. eEF1A was also shown to bind to the 3' terminal SL RNAs of four divergent flaviviruses with similar efficiency and colocalized with RC in dengue infected cells, suggesting that this cell protein plays a similar role in RNA replication for all flaviviruses.

INDEX WORDS: West Nile virus, RNA-protein interaction, 3' Untranslated Region, RNA replication

West Nile Virus 3' (+) SL RNA Protein Binding Sites and *Cis*-acting Sequences

by

Willam G. Davis

A Dissertation Submitted in Partial Fulfillment of the Requirements for the

Degree of Doctor of Philosophy

in the College of Arts and Sciences

Georgia State University

2007

West Nile Virus 3' (+) SL RNA Protein Binding Sites and *Cis*-acting Sequences

by

William G. Davis

Major Professor: Margo A. Brinton

Committee Members: W. David Wilson
Teryl Frey

Electronic Version Approved by:

Office of Graduate Studies
College of Arts and Sciences
Georgia State University
August 2007

Acknowledgements

This dissertation is dedicated to my family. To my daughter, Madeline, and my wife, Deborah, who have persevered through out my studies and to my parents for their continuous support and encouragement. My thanks to all the members of the Brinton lab past and present and to my committee members Dr. Frey and Dr. Wilson. And of course, my thanks to my mentor Dr. Brinton for all of her help and support.

Table of Contents

LIST OF FIGURES

CHAPTER I

Introduction

General Characteristics

WNV is a member of the family *flaviviridae*, which is comprised of three genera, the *flaviviruses*, the *pestviruses* and the *hepaciviruses* and the as yet unclassified viruses, GBV-A and GBV-C. Members of the flavivirus genus are further divided into antigenic serogroups such as the tick-borne encephalitis virus (TBE) group, the Japanese encephalitis virus (JE) group, the yellow fever virus (YFV) group and the dengue virus (Den) group. Ticks are the vectors for the members of the TBE group, while the vectors for the members of the JE, YFV and Den serogroups are mosquitoes (Lindenbach, 2007).

WNV was first isolated from a patient in the West Nile Province of Uganda (Smithburn, 1940). WNV is classified in the JE serogroup. There are two WNV lineages based on sequence comparisons. Lineage I viruses are distributed throughout Africa, the Middle East, Europe, India, Australia, and North America. Lineage II viruses are found in sub-Saharan Africa and Madagascar (Lanciotti et al., 2002). Most lineage II viruses are non-pathogenic, while infection with lineage I viruses can result in more severe disease and have been associated with major epidemics outside Africa (Lanciotti et al., 1999; Murgue, Zeller, and Deubel, 2002).

WNV is maintained in a mosquito-bird cycle in nature (Gubler, 2007). Although *Culex* mosquitoes are the main vectors of WNV transmission, WNV has

been recovered from 60 different species of mosquitoes (Hayes et al., 2005). After mosquitoes ingest virus during a blood meal, the virus infects the cells of the midgut. The virus disseminates to the hemocele and then to the salivary glands. Virus particles present in the salivary glands of infectious mosquitoes are transmitted to susceptible birds during a blood meal. In vertebrates, primary replication of the virus takes place at the site of the mosquito bite and spreads to the regional lymph nodes. Once in the lymph system, the virus enters the vascular system and spreads to peripheral organs. Replication occurs in the central nervous system if the virus is able to pass the blood-brain barrier. High viral titers in the blood of infected birds are necessary for virus transmission back to mosquitoes. WNV has been isolated from over 300 species of birds, which exhibit different levels of viremia and disease susceptibility (Komar et al., 2003). Humans are considered dead end hosts and do not play a part in maintaining the viral transmission life cycle in nature because viral titers are not high enough in human blood to infect mosquitoes.

The majority of WNV infections in humans are asymptomatic. Fever, headache and the occasional rash are observed in about 20% of infected individuals and less than 1% of infected individuals develop meningitis or encephalitis which is sometimes fatal (Petersen, Marfin, and Gubler, 2003). Disease usually clears within 3-6 days. However, in rare cases, infection can result in a long term paralytic polio-like syndrome (Saad et al., 2005).

VIRION STRUCTURE

The WN virion is small, enveloped and spherical with a diameter of 40-60 nm, and contains a positive-sense, single-stranded RNA genome. The surface of the virion contains two viral structural proteins, the envelope (E) and membrane (M) proteins (Lindenbach, 2007). The interaction between the E homodimers is proposed to give the virus its icosahedral symmetry (Kuhn et al., 2002). The capsid is formed by the capsid (C) protein and surrounds the viral RNA genome (Lindenbach, 2007).

FLAVIVIRAL REPLICATION CYCLE

Attachment of the E protein on the surface of the virion to the host cell is mediated by an unknown receptor(s). Entry into the cell by endocytosis and is mediated by clathrin coated pits, the virions are directed into prelysosomal vesicles where fusion between the host and virion membranes is induced by low pH, and the viral nucleocapsid is released (Fig. 1.1 A) (Chu and Ng, 2004; Gollins and Porterfield, 1985; Stiasny et al., 2004). The release of the viral genome from the nucleocapsid occurs by an unknown mechanism, but the viral genome has been shown to be accessible for translation immediately after host and cell membrane fusion (Koschinski et al., 2003). The single open reading frame is translated and the viral polyprotein produced is then cleaved by host and viral proteases into 3 structural and 7 nonstructural proteins (Fig. 1.1 B and C). The viral genome serves as a template for the generation of viral minus strand RNA (Fig. 1.1 D). The minus strand RNA in turn is the template for the synthesis of viral genomic RNA (Fig. 1.1 E). RNA synthesis of viral plus and minus strand RNAs is disproportionate and after the initial

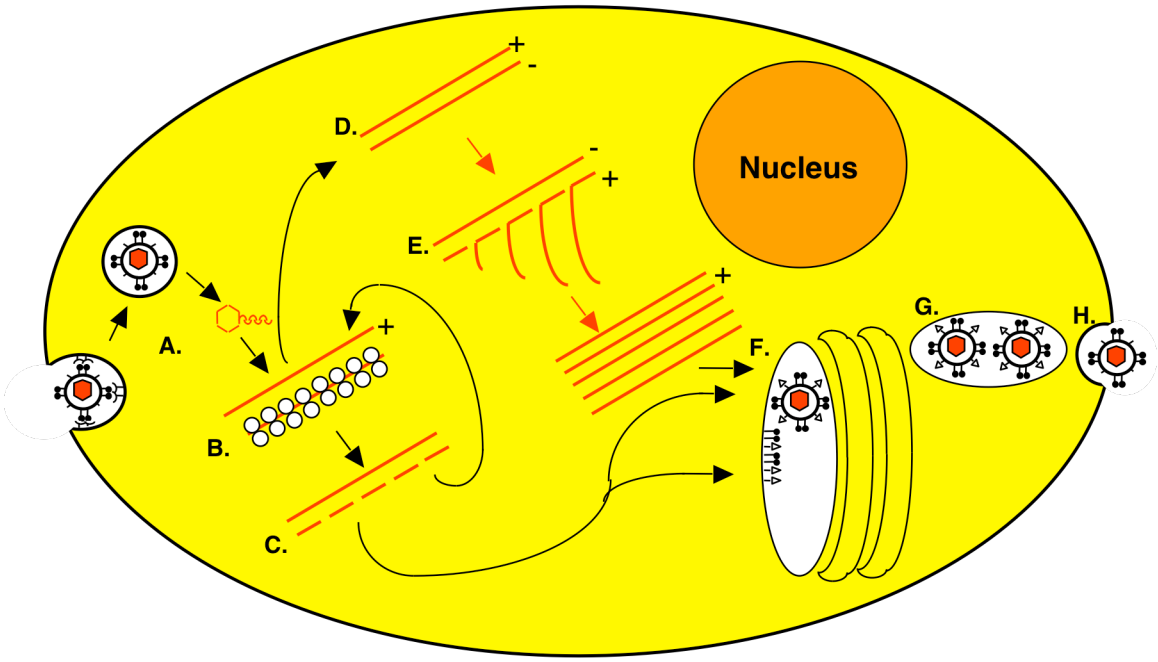

Figure 1.1. Flavivirus replication cycle.
A. Attachment and entry of the virion and uncoating of the virion RNA. **B.** Translation of the virion RNA. **C.** Proteolytic proccessing of the viral polyprotein. **D.** Synthesis of minus strand RNA. **E.** Synthesis of genomic RNA from the minus strand RNA. **F.** Encapsidation of the viral genome and assembly of immature virions. **G.** Transport of the virions to plasma membrane. **H.** Exocytosis of the virions. Figure from (Brinton, 2002)

phase of RNA replication, the ratio of plus to minus strand RNA in infected cells is about 100 to 1 (Browning et al., 1990). Replication of the viral genome takes place in envaginations of perinuclear membranes (Mackenzie, Kenney, and Westaway, 2007; Miller, Sparacio, and Bartenschlager, 2006). Virion assembly occurs in the endoplasmic reticulum vesicles. Mature virions are produced by the cleavage of the precursor viral structural protein, prM, to M in the Golgi (Fig. 1.1 F and G) (Lindenbach, 2007). Virions are transported in vesicles to the plasma membrane and then released by the fusion of virion containing vesicles with the plasma membrane (Fig 1.1 H) (Mackenzie and Westaway, 2001).

GENOME RNA

The genomic RNA is an mRNA. The single open-reading-frame (ORF) codes for a polyprotein of approximately 3000 amino acids in length (Fig. 1.2). The genome contains a 5' type I cap, but no 3' poly A tail. Translation of the genome ORF is cap-dependent and is initiated by ribosomal scanning. The 5' end of the genome codes for the structural proteins, and the 3' end of the genome codes for the nonstructural (NS) proteins. The polyprotein is cleaved by viral and cellular proteases. The gene order of the WNV ORF is 5' C-prM-E-NS1-NS2A-NS2B-NS3-NS4A- NS4B- NS5 3'.

VIRION STRUCTURAL PROTEINS

Dimers of the C protein assemble to form the viral nucleocapsid. The C protein is a small, highly basic protein of about 11 kDa. Interaction between the nucleocapsid and the viral genomic RNA is achieved through charged interactions between the negatively charged RNA and the positively charged amino acid residues

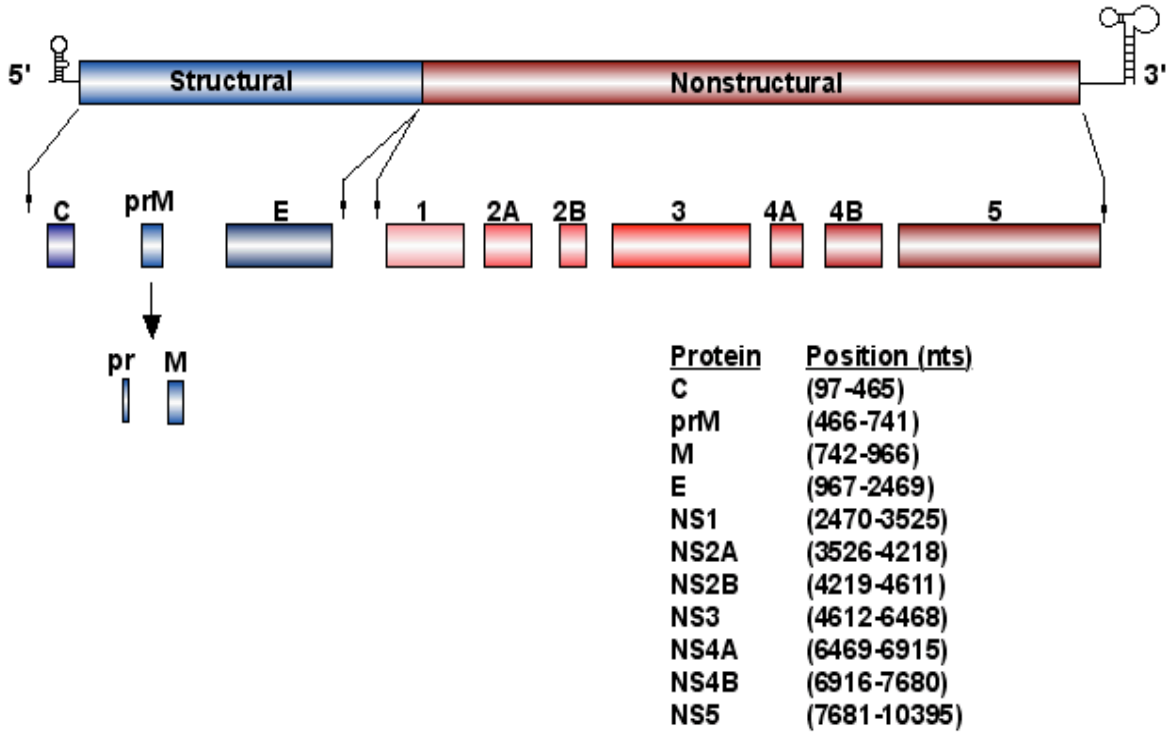

Protein	Position (nts)
C	(97-465)
prM	(466-741)
M	(742-966)
E	(967-2469)
NS1	(2470-3525)
NS2A	(3526-4218)
NS2B	(4219-4611)
NS3	(4612-6468)
NS4A	(6469-6915)
NS4B	(6916-7680)
NS5	(7681-10395)

Figure 1.2. Schematic drawing of the flavivirus genome RNA and the mature viral proteins encoded in the polyprotein. Not drawn to scale

located at the N and C terminus of the protein which are separated by a hydrophobic region thought to interact with the viral membrane (Ma et al., 2004).

The M protein is cleaved from the viral precursor protein, prM. The prM protein assists with the folding of the E proteins. The formation of prM-E heterodimers prevents E from undergoing an acid catalyzed rearrangement during secretory transport of nascent immature virions to the plasma membrane of the host cell (Guirakhoo, Bolin, and Roehrig, 1992). In the immature virion, prM is cleaved releasing the pr fragment. This allows the E proteins to form homodimers that lie close to the virion surface in the mature virion (Wengler and Wengler, 1989).

The viral E protein is the major antigenic structural protein in the envelope and mediates cell receptor binding and membrane fusion. Upon exposure to low pH, the E homodimers in the mature virion dissociate and form trimers (Allison et al., 1995; Stiasny et al., 2004).

VIRAL NONSTRUCTURAL PROTEINS

NS1 is translocated into the ER membrane during synthesis (Falgout and Markoff, 1995). NS1 is also found within the cytoplasm, on the surface of plasma membranes, and is secreted from infected cells (Lindenbach, 2007). Even though NS1 is a hydrophilic protein and lacks a transmembrane domain, NS1 homodimers associate with cell membranes and are not secreted (Winkler et al., 1989). Mutations that prevented the formation of NS1 homodimers had no effect on NS1 secretion, but reduced viral titers on Vero cells by 100 fold (Hall et al., 1999). NS1 colocalizes with

viral replication complexes and the interaction between NS1 and NS4A has been shown to be required for viral RNA replication, but the exact function of NS1 in viral RNA replication is not known (Lindenbach and Rice, 1999; Mackenzie, Jones, and Young, 1996). The function of NS1 on the surface of the plasma membrane is not known, but antibody directed against NS1 initiated complement-mediated lysis of infected cells and the secreted form of NS1 has been shown to be a complement-fixing antigen (Brandt et al., 1970; Lindenbach and Rice, 2003). The secreted and plasma membrane bound forms of NS1 have recently been shown to bind to complement regulatory protein factor H and block activation of the complement system (Chung et al., 2006).

NS2A and NS2B are small hydrophobic proteins. NS2A has been shown to have a role in the assembly of the virus (Liu, Chen, and Khromykh, 2003). NS2A has also been reported to inhibit interferon signaling by acting as an interferon antagonist (Munoz-Jordan et al., 2003). Interferon inhibition could be reversed by mutation of a single alanine to a proline at position 30 (Liu et al., 2006). NS2B forms a complex with NS3 and is a cofactor for the NS2B-NS3 serine protease, which auto-proteolytically cleaves the viral polyprotein at the NS2A/NS2B, NS2B/NS3, NS3/NS4A, and NS4B/NS5 junctions (Amberg et al., 1994; Chambers et al., 1990).

NS3 is a large multifunctional protein. The N-terminus of this protein is the catalytic domain of the NS2B-NS3 serine-protease complex. The NS3 protease domain, without the NS2B cofactor, has been crystallized and the structure showed homology to that of other enzymes in the serine protease family (Murthy, Clum, and

Padmanabhan, 1999). The NS3 C-terminus resembles the super group 2 RNA helicases both in sequence homology and crystal structure. These RNA helicases have been shown to have both RNA unwinding and RNA-stimulated nucleoside triphosphatase (NTPase) enzymatic activities (Gorbalenya et al., 1989; Wengler and Wengler, 1991; Wu et al., 2005; Xu et al., 2005). NS3 has also been shown to have RNA triphosphatase activity, which may be used to dephosphorylate the 5' end of the genome prior to the addition of the cap by NS5 (Wengler and Wengler, 1993). NS3 has also been shown to induce apoptosis via the caspase-8 pathway when over-expressed (Prikhod'ko et al., 2002; Ramanathan et al., 2006).

NS4A and NS4B are small membrane associated hydrophobic proteins. Both have been shown to colocalize with viral replication complexes. NS4A has been shown to be required for viral-induced membrane rearangements in the cell (Mackenzie et al., 1998; Miller, Sparacio, and Bartenschlager, 2006). NS4A and NS4B have been reported to block interferon signaling in replicon containing cells (Munoz-Jordan et al., 2003).

NS5 is a large multifunctional protein. The N terminal domain of NS5 contains the methyltransferase enzymatic activities for capping the genome RNA and was shown to bind specifically to the 5' UTR of the flaviviral genome (Dong et al., 2007; Filomatori et al., 2006). The C terminal domain of NS5 contains the viral RNA dependant RNA polymerse (RDRP). Similar RDRP motifs are found in RDRPs of all positive strand RNA viruses (Koonin, 1991; Lindenbach and Rice, 2003; Malet et al., 2007). The RNA secondary structures present at the 3' end of the genome have been

shown to be required for *de novo* initiation of RNA synthesis (Ackermann and Padmanabhan, 2001).

THE GENOME NONCODING REGIONS

The flavivirus genomic RNA coding region is flanked by 5' and 3' noncoding sequences. The 5' noncoding region of WNV is 96 nt long and the 3' noncoding region is 632 nt long (Brinton, Fernandez, and Dispoto, 1986). The 3' terminal 96 nts of the WNV genomic RNA are predicted to form two stem loop (SL) structures, a short SL (SSL) of 16 nts and a longer 3' terminal SL of 80 nts. These two structures will be collectively referred to as the WNV 3' (+) SL RNA and are predicted to be conserved among divergent flaviviruses (Brinton, Fernandez, and Dispoto, 1986; Hahn et al., 1987; Shi et al., 1996). Previously, three cellular proteins with molecular masses of 105, 84 and 52 kDa were reported to bind specifically to the WNV 3' (+) SL RNA. The 52 kDa protein was subsequently identified as eEF1A (Blackwell and Brinton, 1997). The dissociation constant (kD) for the interaction between eEF1A and the WNV 3' SL RNA is 10^{-9} M and is similar to that of the interaction between eEF1A and charged tRNAs (Riis et al., 1990). One major and two minor eEF1A binding sites were previously mapped on the WNV 3' (+) SL RNA (Blackwell and Brinton, 1997). The major binding site is located on the 5' side and in the middle of the terminal SL and accounts for 60% of the binding activity. One minor binding site was found to be the pentanucleotide sequence, which is conserved among divergent flaviviruses and found in the top loop of the 3' terminal SL. The other minor binding site is the SSL. (Blackwell and Brinton, 1997; Elghonemy, Davis, and Brinton, 2005;

Tilgner, Deas, and Shi, 2005). Each minor binding site accounted for 20% of the binding activity of eEF1A to the WNV 3' (+) SL RNA. The 3' terminal region is thought to function as a promoter for viral minus strand synthesis and to contain *cis*-acting elements, since deletion of this region is lethal for flavivirus infectious clones (Mandl et al., 1998; Men et al., 1996; Zeng et al., 1998).

The 3' end of the WNV viral genome may also be involved in the regulation of viral translation. The WNV genome is an mRNA as well as a template for viral transcription. The initiation of translation and RNA replication must be regulated so that "collisions" of a ribosome and the RDRP moving in opposite directions do not occur. According to the closed loop model of eukaryotic translation, the 5' and 3' termini of cell mRNAs are brought close together by the interactions between cap and poly A binding proteins (reviewed in Gray and Wickens, 1998). Poly A binding protein (PABP) interacts with eukaryotic translation initiation factor 4F (eIF4F) and PABP-interacting protein 1 (Paip-1). Paip-1 and eIF4F interact with the components of the mRNA cap binding complex, which include eIF4G and eIF4A. The close proximity of the 5' and 3' ends of the genome are thought to promote the stability of the mRNA and to improve the efficiency of the recruitment and recycling of the ribosomal subunits (Gale, Tan, and Katze, 2000; Ishii et al., 1999; McKnight and Lemon, 1998; Michel et al., 2000). Since WNV does not have a poly A tail, but does have a 5' cap structure, host factors binding to the 3' end might take over the role of PABP and mediate an interaction between the 3' end of the genome and the cap binding complex.

EUKARYOTIC ELONGATION FACTOR 1 A

eEF1A constitutes 1-4% of the total soluble protein in actively dividing cells and is second only to actin in abundance (Browning et al., 1990; Condeelis, 1995). eEF1A delivers aminoacylated tRNAs (aa-tRNA) and GTP to the A site on the ribosome during protein synthesis. The eEF1A:GTP:aa-tRNA complex then moves to the P site. eEF1A hydrolyzes GTP to GDP, which results in the release of eEF1A:GDP from the ribosome. In addition to its role in peptide chain elongation, eEF1A has been reported to bind to mRNA (Lui, 2002; Mickleburgh et al., 2006), to bind to and bundle actin filaments (Ejiri, 2002; Lui, 1996; Lui, 2002), to sever microtubules (Shiina, 1994), and to mediate protein degradation via ubiquitin-dependant pathways (Gonen, 1996; Gonen, 1994).

For the positive-strand RNA bacteriophage, Qβ, the bacterial homolog of eEF1A functions as part of the viral replicase holoenzyme and for the negative-strand RNA virus, vesicular stomatitis virus (VSV), eEF1A was shown to be a component of the viral transcriptase complex and required for replicase activity *in vitro* (Blumenthal and Carmichael, 1979; Brown, 1996; Miranda, 1997; Qanungo, 2004; Schuppli, 2000; Schuppli, 1998). eEF1A was also shown to interact with viral nonstructural proteins of two members of the family *Flaviviridae*, bovine viral diarrhea virus (NS5A) and hepatitis C virus (NS4A) , and with the Gag polyprotein of HIV type I (Cimarelli, 1999; Johnson, 2001; Kou et al., 2006).

eEF1A was reported to bind to the 3' terminal tRNA-like structure (TLS) of the of turnip yellow mosaic virus (TYMV) genome, and to act as both a translational

enhancer and a minus strand synthesis repressor (Matsuda, 2003a; Matsuda, 2003b). For the positive strand RNA plant virus, tobacco mosaic virus (TMV), eEF1A has also been reported to bind to both the genomic 3' TLS and the viral polymerase (Yamaji et al., 2006)

GOALS OF THIS DISSERTATION

Many flaviviruses are significant human pathogens and the RNA SL structures present at the termini of the WNV genome are found in divergent flaviviruses (Markoff, 2003; Olsthoorn and Bol, 2001). eEF1A has been shown to bind specifically to the WNV 3' (+) SL structures and has also been shown to bind to the 3' terminus of divergent flavivirus genomes (Blackwell and Brinton, 1997). The regulation of viral RNA synthesis is poorly understood for flaviviruses and it is also not known how the switching of the virus genome RNA from translation of the viral proteins to initiation of minus strand RNA synthesis is controlled. It is likely that the 3'(+) terminal region of the genome contains *cis*-acting signals for the initiation of negative sense RNA of the genome, but the 3'(+) terminal region could also contain *cis*-acting signals that enhance or suppress translation or facilitate the switch from genomic RNA translation to transcription. *Cis*-acting elements that are necessary for WNV replication and/or translation would likely be conserved in all flaviviruses. The further definition of these elements will help to elucidate the replication and translation strategies used by all the flaviviruses. These regions also provide targets for the development of new antivirals that would be effective against all flaviviruses.

1. Determine whether the major eEF1A binding site is *cis*-acting for WNV replication.

To obtain data on the functional importance of eEF1A binding to the WNV 3' (+) SL, mutations will be made in the major eEF1A binding site in a WNV infectious clone. Full-length mutant WNV infectious clone RNAs will be produced by *in vitro* transcription and used to transfect baby hamster kidney (BHK) cells. The viruses produced will then be analyzed for their replication efficiency. If particular mutations have a negative effect on virus replication, virus progeny will be passaged and then analyzed for reversions to the introduced mutations.

2. Determine whether the previously predicted 3' tertiary interaction is *cis*-acting for WNV replication.

The SSL is predicted to be a minor binding site for eEF1A as well as involved in a tertiary interaction with the stem of the terminal SL. The SSL as well as the sequences in the 3' terminal SL predicted to be involved in this tertiary interaction will be mutated in the WNV infectious clone to determine if these nts are *cis*-acting and whether the predicted pseudoknot is functionally important.

3. Determine whether mutations to the WNV 3'(+) SL RNA affect the relative binding activity of recombinant eEF1A for the WNV 3'(+) SL RNA.

Recombinant eEF1A purified from *E. coli* will be used to test the relative *in vitro* binding activity of eEF1A to 3' (+) SL RNAs with mutations in the major eEF1A binding site and the SSL.

4. Determine whether mutations to the WNV 3'(+) SL RNA affect the translation or replication of the viral RNA.

Mutations and deletions engineered into a WNV infectious clone will be tested for their effect on translation of the viral polyprotein in BHK cells three hours after transfection by relative quantification of viral antigen immunoflourescence. The effect of mutations and/or deletions on the efficiency of viral plus-strand and minus-strand RNA synthesis will be assessed by real-time RT-PCR.

5. Determine whether eEF1A colocalizes with viral replication complexes in infected BHK cells.

Antibodies against dsRNA, WNV NS3 and WNV NS5 will be used as markers for viral replication complexes. The colocalization of eEF1A with viral replication complexes will be assessed in BHK cells by confocal microscopy. Anti-eEF1A antibody will also be used in coimmunoprecipitation experiments to determine whether viral replication complexes interact with eEF1A in infected BHK cell lysates.

REFERENCES

Ackermann, M., and Padmanabhan, R. (2001). De novo synthesis of RNA by the dengue virus RNA-dependent RNA polymerase exhibits temperature dependence at the initiation but not elongation phase. *J Biol Chem* **276**(43)**,** 39926-37.

Allison, S. L., Schalich, J., Stiasny, K., Mandl, C. W., Kunz, C., and Heinz, F. X. (1995). Oligomeric rearrangement of tick-borne encephalitis virus envelope proteins induced by an acidic pH. *J Virol* **69**(2)**,** 695-700.

Amberg, S. M., Nestorowicz, A., McCourt, D. W., and Rice, C. M. (1994). NS2B-3 proteinase-mediated processing in the yellow fever virus structural region: in vitro and in vivo studies. *J Virol* **68**(6)**,** 3794-802.

Blackwell, J. L., and Brinton, M. A. (1997). Translation elongation factor-1 alpha interacts with the 3' stem-loop region of West Nile virus genomic RNA. *J Virol* **71**(9)**,** 6433-44.

Blumenthal, T., and Carmichael, G. G. (1979). RNA replication: function and structure of Qbeta-replicase. *Annu Rev Biochem* **48,** 525-48.

Brandt, W. E., Chiewslip, D., Harris, D. L., and Russell, P. K. (1970). Partial purification and characterization of a dengue virus soluble complement-fixing antigen. *J Immunol* **105**(6)**,** 1565-8.

Brinton, M. A. (2002). THE MOLECULAR BIOLOGY OF WEST NILE VIRUS: A New Invader of the Western Hemisphere. *Annual Review of Microbiology* **56**(1)**,** 371-402.

Brinton, M. A., Fernandez, A. V., and Dispoto, J. H. (1986). The 3'-nucleotides of flavivirus genomic RNA form a conserved secondary structure. *Virology* **153**(1)**,** 113-21.

Brown, D., and Gold, L. (1996). RNA replication by Qβ replicase: A working model. *Proc. Natl. Acad. Sci. USA* **93,** 11558-11562.

Browning, K. S., Humphreys, J., Hobbs, W., Smith, G. B., and Ravel, J. M. (1990). Determination of the amounts of the protein synthesis initiation and elongation factors in wheat germ. *J Biol Chem* **265**(29)**,** 17967-73.

Chambers, T. J., Weir, R. C., Grakoui, A., McCourt, D. W., Bazan, J. F., Fletterick, R. J., and Rice, C. M. (1990). Evidence that the N-terminal domain of nonstructural protein NS3 from yellow fever virus is a serine protease responsible for site-specific cleavages in the viral polyprotein. *Proc Natl Acad Sci U S A* **87**(22)**,** 8898-902.

Chu, J. J., and Ng, M. L. (2004). Infectious entry of West Nile virus occurs through a clathrin-mediated endocytic pathway. *J Virol* **78**(19)**,** 10543-55.

Chung, K. M., Liszewski, M. K., Nybakken, G., Davis, A. E., Townsend, R. R., Fremont, D. H., Atkinson, J. P., and Diamond, M. S. (2006). West Nile virus nonstructural protein NS1 inhibits complement activation by binding the regulatory protein factor H. *Proc Natl Acad Sci U S A* **103**(50)**,** 19111-6.

Cimarelli, A., and Luban, J. (1999). Translation elongation factor 1-alpha interacts specifically with the human immunodeficiency virus type 1 Gag polyprotein. *Journal of Virology* **73,** 5388-5401.

Condeelis, J. (1995). Elongation factor 1 alpha, translation and the cytoskeleton. *Trends Biochem Sci* **20**(5)**,** 169-70.

Dong, H., Ray, D., Ren, S., Zhang, B., Puig-Basagoiti, F., Takagi, Y., Ho, C. K., Li, H., and Shi, P. Y. (2007). Distinct RNA elements confer specificity to flavivirus RNA cap methylation events. *J Virol* **81**(9)**,** 4412-21.

Ejiri, S. (2002). Moonlighting Functions of Polypeptide Elongation factor 1: From Actin Bundling to Zinc Finger Protein R1-Associated Nuclear Localization. *Biosciences, Biotechnology, and Biochemistry* **66,** 1-21.

Elghonemy, S., Davis, W. G., and Brinton, M. A. (2005). The majority of the nucleotides in the top loop of the genomic 3' terminal stem loop structure are cis-acting in a West Nile virus infectious clone. *Virology* **331**(2)**,** 238-246.

Falgout, B., and Markoff, L. (1995). Evidence that flavivirus NS1-NS2A cleavage is mediated by a membrane-bound host protease in the endoplasmic reticulum. *J Virol* **69**(11)**,** 7232-43.

Filomatori, C. V., Lodeiro, M. F., Alvarez, D. E., Samsa, M. M., Pietrasanta, L., and Gamarnik, A. V. (2006). A 5' RNA element promotes dengue virus RNA synthesis on a circular genome. *Genes Dev* **20**(16)**,** 2238-49.

Gale, M., Jr., Tan, S. L., and Katze, M. G. (2000). Translational control of viral gene expression in eukaryotes. *Microbiol Mol Biol Rev* **64**(2)**,** 239-80.

Gollins, S. W., and Porterfield, J. S. (1985). Flavivirus infection enhancement in macrophages: an electron microscopic study of viral cellular entry. *J Gen Virol* **66 (Pt 9),** 1969-82.

Gonen, H., Dickman, D.,Schwartz, A.L. and Ciechanover, A. (1996). Protein synthesis elongation factor EF-1α is an isopeptidase essential for ubiquitin-dependent degradation of certain proteolytic substrates. *Adv. Exp. Med. Biol* **389,** 209-219.

Gonen, H., Smith, C.E., Siegel, N.R., Kahana, C., Merrick, W.C., Chakraburtty, K., Schwartz, A.L. and Ciechanover, A. (1994). Protein synthesis elongation factor factor EF-1α is essential for ubiquitin-dependent degredation of certain Na-acetylated proteins and may be substituted for by the bacterial elongation factor EF-Tu. *Proceedings from the National Academy of Sciences USA* **91,** 7648-7652.

Gorbalenya, A. E., Koonin, E. V., Donchenko, A. P., and Blinov, V. M. (1989). Two related superfamilies of putative helicases involved in replication, recombination, repair and expression of DNA and RNA genomes. *Nucleic Acids Res* **17**(12)**,** 4713-30.

Gray, N. K., and Wickens, M. (1998). Control of translation initiation in animals. *Annu Rev Cell Dev Biol* **14,** 399-458.

Gubler, D. J., Kuno, G., and Markoff, J. (2007). Flaviviruses. *In* "Fields Virology" (P. M. H. David M Knipe, Ed.), pp. 1153-1252. Lippincott Williams and Wilkins, Philadelphia.

Guirakhoo, F., Bolin, R. A., and Roehrig, J. T. (1992). The Murray Valley encephalitis virus prM protein confers acid resistance to virus particles and alters the expression of epitopes within the R2 domain of E glycoprotein. *Virology* **191**(2)**,** 921-31.

Hahn, C. S., Hahn, Y. S., Rice, C. M., Lee, E., Dalgarno, L., Strauss, E. G., and Strauss, J. H. (1987). Conserved elements in the 3' untranslated region of flavivirus RNAs and potential cyclization sequences. *J Mol Biol* **198**(1)**,** 33-41.

Hall, R. A., Khromykh, A. A., Mackenzie, J. M., Scherret, J. H., and Khromykh, T. I. (1999). Loss of dimerisation of the nonstructural protein NS1 of Kunjin virus delays viral replication and reduces virulence in mice, but still allows secretion of NS1. *Virology* **264,** 66.

Hayes, E. B., Komar, N., Nasci, R. S., Montgomery, S. P., O'Leary, D. R., and Campbell, G. L. (2005). Epidemiology and transmission dynamics of West Nile virus disease. *Emerg Infect Dis* **11**(8)**,** 1167-73.

Ishii, T., Shiroki, K., Iwai, A., and Nomoto, A. (1999). Identification of a new element for RNA replication within the internal ribosome entry site of poliovirus RNA. *J Gen Virol* **80 (Pt 4),** 917-20.

Johnson, C. M., Perz, D.R., French, R., Merrick, W.C., and Donis, R.O. (2001). The NS5A protein of bovine viral diarrhoea virus interacts with the a subunit of translation elongation factor-1. *Journal of General Virology* **82,** 2935-2943.

Komar, N., Langevin, S., Hinten, S., Nemeth, N., Edwards, E., Hettler, D., Davis, B., Bowen, R., and Bunning, M. (2003). Experimental infection of North American birds with the New York 1999 strain of West Nile virus. *Emerg Infect Dis* **9**(3)**,** 311-22.

Koonin, E. V. (1991). The phylogeny of RNA-dependent RNA polymerases of positive-strand RNA viruses. *J Gen Virol* **72 (Pt 9),** 2197-206.

Koschinski, A., Wengler, G., Wengler, G., and Repp, H. (2003). The membrane proteins of flaviviruses form ion-permeable pores in the target membrane after fusion: identification of the pores and analysis of their possible role in virus infection. *J Gen Virol* **84**(Pt 7)**,** 1711-21.

Kou, Y. H., Chou, S. M., Wang, Y. M., Chang, Y. T., Huang, S. Y., Jung, M. Y., Huang, Y. H., Chen, M. R., Chang, M. F., and Chang, S. C. (2006). Hepatitis C virus NS4A inhibits cap-dependent and the viral IRES-mediated translation through interacting with eukaryotic elongation factor 1A. *J Biomed Sci*.

Kuhn, R. J., Zhang, W., Rossmann, M. G., Pletnev, S. V., Corver, J., Lenches, E., Jones, C. T., Mukhopadhyay, S., Chipman, P. R., Strauss, E. G., Baker, T. S., and Strauss, J. H. (2002). Structure of dengue virus: implications for flavivirus organization, maturation, and fusion. *Cell* **108**(5)**,** 717-25.

Lanciotti, R. S., Ebel, G. D., Deubel, V., Kerst, A. J., Murri, S., Meyer, R., Bowen, M., McKinney, N., Morrill, W. E., Crabtree, M. B., Kramer, L. D., and Roehrig, J. T. (2002). Complete genome sequences and phylogenetic analysis of West Nile virus strains isolated from the United States, Europe, and the Middle East. *Virology* **298**(1)**,** 96-105.

Lanciotti, R. S., Roehrig, J. T., Deubel, V., Smith, J., Parker, M., Steele, K., Crise, B., Volpe, K. E., Crabtree, M. B., Scherret, J. H., Hall, R. A., MacKenzie, J. S., Cropp, C. B., Panigrahy, B., Ostlund, E., Schmitt, B., Malkinson, M., Banet, C., Weissman, J., Komar, N., Savage, H. M., Stone, W., McNamara, T., and

Gubler, D. J. (1999). Origin of the West Nile virus responsible for an outbreak of encephalitis in the northeastern United States. *Science* **286**(5448)**,** 2333-7.

Lindenbach, B. D., and Rice, C. M. (1999). Genetic interaction of flavivirus nonstructural proteins NS1 and NS4A as a determinant of replicase function. *J Virol* **73**(6)**,** 4611-21.

Lindenbach, B. D., and Rice, C. M. (2003). Molecular biology of flaviviruses. *Adv Virus Res* **59,** 23-61.

Lindenbach, B. D., Thiel, H. J, and Rice, C. M. (2007). Flaviviridae: The Viruses and Their Replication. *In* "Fields Virology" (D. M. Knipe, and Howley, P. M., Ed.), pp. 1101-1152. Lippincott Williams and Wilkins, Philadelphia.

Liu, W. J., Chen, H. B., and Khromykh, A. A. (2003). Molecular and functional analyses of Kunjin virus infectious cDNA clones demonstrate the essential roles for NS2A in virus assembly and for a nonconservative residue in NS3 in RNA replication. *J Virol* **77**(14)**,** 7804-13.

Liu, W. J., Wang, X. J., Clark, D. C., Lobigs, M., Hall, R. A., and Khromykh, A. A. (2006). A single amino acid substitution in the West Nile virus nonstructural protein NS2A disables its ability to inhibit alpha/beta interferon induction and attenuates virus virulence in mice. *J Virol* **80**(5)**,** 2396-404.

Lui, G., Tang, J., Edmonds, B.T., Murray, J., Levin, S., and Condeelis, J. (1996). F-actin Sequesters Elangation Factor 1α from Interaction with Aminoacyl-tRNA in a pH-dependent Reaction. *The Journal of Cell Biology* **135,** 953-963.

Lui, G. G., W.M., Persky, D., Latham, V.M., Singer, R.H. and Condeelis, J. (2002). Interaction of Elongation Factor 1α with F-Actin and β-Actin mRNA: Implications for Anchoring mRNA in Cell Protrusions. *Molecular Biology of the Cell* **13,** 579-592.

Ma, L., Jones, C. T., Groesch, T. D., Kuhn, R. J., and Post, C. B. (2004). Solution structure of dengue virus capsid protein reveals another fold. *Proc Natl Acad Sci U S A* **101**(10)**,** 3414-9.

Mackenzie, J. M., Jones, M. K., and Young, P. R. (1996). Immunolocalization of the dengue virus nonstructural glycoprotein NS1 suggests a role in viral RNA replication. *Virology* **220**(1)**,** 232-40.

Mackenzie, J. M., Kenney, M. T., and Westaway, E. G. (2007). West Nile virus strain Kunjin NS5 polymerase is a phosphoprotein localized at the cytoplasmic site of viral RNA synthesis. *J Gen Virol* **88**(Pt 4)**,** 1163-8.

Mackenzie, J. M., Khromykh, A. A., Jones, M. K., and Westaway, E. G. (1998). Subcellular localization and some biochemical properties of the flavivirus Kunjin nonstructural proteins NS2A and NS4A. *Virology* **245**(2)**,** 203-15.

Mackenzie, J. M., and Westaway, E. G. (2001). Assembly and maturation of the flavivirus Kunjin virus appear to occur in the rough endoplasmic reticulum and along the secretory pathway, respectively. *J Virol* **75**(22)**,** 10787-99.

Malet, H., Egloff, M. P., Selisko, B., Butcher, R. E., Wright, P. J., Roberts, M., Gruez, A., Sulzenbacher, G., Vonrhein, C., Bricogne, G., Mackenzie, J. M., Khromykh, A. A., Davidson, A. D., and Canard, B. (2007). Crystal Structure of the RNA Polymerase Domain of the West Nile Virus Non-structural Protein 5. *J Biol Chem* **282**(14)**,** 10678-89.

Markoff, L. (2003). 5'- and 3'-noncoding regions in flavivirus RNA. *Adv Virus Res* **59,** 177-228.

Matsuda, D., and T.W. Dreher (2003a). The tRNA-like structure of Turnip yellow mosaic virus RNA is a 3'-translational enhancer. *Virology* **321,** 36-46.

Matsuda, D., S. Yoshinari and T.W. Dreher (2003b). eEF1a binding to aminoacylated viral RNA represses minus strand synthesis by TYMV RNA-dependant RNA polymerase. *Virology* **321,** 47-56.

McKnight, K. L., and Lemon, S. M. (1998). The rhinovirus type 14 genome contains an internally located RNA structure that is required for viral replication. *Rna* **4**(12)**,** 1569-84.

Michel, Y. M., Poncet, D., Piron, M., Kean, K. M., and Borman, A. M. (2000). Cap-Poly(A) synergy in mammalian cell-free extracts. Investigation of the requirements for poly(A)-mediated stimulation of translation initiation. *J Biol Chem* **275**(41)**,** 32268-76.

Mickleburgh, I., Chabanon, H., Nury, D., Fan, K., Burtle, B., Chrzanowska-Lightowlers, Z., and Hesketh, J. (2006). Elongation factor 1alpha binds to the region of the metallothionein-1 mRNA implicated in perinuclear localization--importance of an internal stem-loop. *Rna* **12**(7)**,** 1397-407.

Miller, S., Sparacio, S., and Bartenschlager, R. (2006). Subcellular localization and membrane topology of the Dengue virus type 2 Non-structural protein 4B. *J Biol Chem* **281**(13)**,** 8854-63.

Miranda, G., Schuppli, D., Barrera, I., Hausherr, C., Sogo, J., and Weber, H. (1997). Recognition of bacteriophage Qb replicase: role of RNA interactions mediated

by ribosomal proteins S1 and host factor. *Journal of Molecular Biology* **267,** 1089-1103.

Munoz-Jordan, J. L., Sanchez-Burgos, G. G., Laurent-Rolle, M., and Garcia-Sastre, A. (2003). Inhibition of interferon signaling by dengue virus. *Proc Natl Acad Sci U S A* **100**(24)**,** 14333-8.

Murgue, B., Zeller, H., and Deubel, V. (2002). The ecology and epidemiology of West Nile virus in Africa, Europe and Asia. *Curr Top Microbiol Immunol* **267,** 195-221.

Murthy, H. M., Clum, S., and Padmanabhan, R. (1999). Dengue virus NS3 serine protease. Crystal structure and insights into interaction of the active site with substrates by molecular modeling and structural analysis of mutational effects. *J Biol Chem* **274**(9)**,** 5573-80.

Olsthoorn, R. C., and Bol, J. F. (2001). Sequence comparison and secondary structure analysis of the 3' noncoding region of flavivirus genomes reveals multiple pseudoknots. *Rna* **7**(10)**,** 1370-7.

Petersen, L. R., Marfin, A. A., and Gubler, D. J. (2003). West Nile virus. *Jama* **290**(4)**,** 524-8.

Prikhod'ko, G. G., Prikhod'ko, E. A., Pletnev, A. G., and Cohen, J. I. (2002). Langat flavivirus protease NS3 binds caspase-8 and induces apoptosis. *J Virol* **76**(11)**,** 5701-10.

Qanungo, K. R., D. Shaji, M. Mathur, and A.K. Banerjee (2004). Two RNA polymerase complexes from vesicular stomatitis virus-infected cells that carry out transcription and replication of genome RNA. *Proceedings from the National Academy of Sciences USA* **101,** 5952-5957.

Ramanathan, M. P., Chambers, J. A., Pankhong, P., Chattergoon, M., Attatippaholkun, W., Dang, K., Shah, N., and Weiner, D. B. (2006). Host cell killing by the West Nile Virus NS2B-NS3 proteolytic complex: NS3 alone is sufficient to recruit caspase-8-based apoptotic pathway. *Virology* **345**(1)**,** 56-72.

Riis, B., Rattan, S. I., Clark, B. F., and Merrick, W. C. (1990). Eukaryotic protein elongation factors. *Trends Biochem Sci* **15**(11)**,** 420-4.

Saad, M., Youssef, S., Kirschke, D., Shubair, M., Haddadin, D., Myers, J., and Moorman, J. (2005). Acute flaccid paralysis: the spectrum of a newly recognized complication of West Nile virus infection. *J Infect* **51**(2)**,** 120-7.

Schuppli, D., Geogijevic, J., and Weber, H. (2000). Synergism of mutations in the bacteriophage Qb RNA affecting host factor dependence of Qb replicase. *Journal of Molecular Biology* **295,** 149-154.

Schuppli, D., Miranda, G., Qiu, S., and Weber, H (1998). A branched stem-loop structure in the M-site of bacteriophage Qb RNA is important for template recognition by Qb replicase holoenzyme. *Journal of Molecular Biology* **283,** 585-593.

Shi, P. Y., Brinton, M. A., Veal, J. M., Zhong, Y. Y., and Wilson, W. D. (1996). Evidence for the existence of a pseudoknot structure at the 3' terminus of the flavivirus genomic RNA. *Biochemistry* **35**(13)**,** 4222-30.

Shiina, N., Gotoh, y., Kubomura, N., Iwamatsu, A., and Nishida, E. (1994). Microtubule severingby elongation factor 1a. *Science* **266,** 282-285.

Smithburn, K. C., Hughes, T.P., Burke, A.W., and Paul, J.H. (1940). A neurotropic virus isolated from the blood of a native of Uganda. *Am. J. Trop. Med. Hyg.* **20,** 471-492.

Stiasny, K., Bressanelli, S., Lepault, J., Rey, F. A., and Heinz, F. X. (2004). Characterization of a membrane-associated trimeric low-pH-induced Form of the class II viral fusion protein E from tick-borne encephalitis virus and its crystallization. *J Virol* **78**(6)**,** 3178-83.

Tilgner, M., Deas, T. S., and Shi, P. Y. (2005). The flavivirus-conserved penta-nucleotide in the 3' stem-loop of the West Nile virus genome requires a specific sequence and structure for RNA synthesis, but not for viral translation. *Virology* **331**(2)**,** 375-86.

Wengler, G., and Wengler, G. (1989). Cell-associated West Nile flavivirus is covered with E+pre-M protein heterodimers which are destroyed and reorganized by proteolytic cleavage during virus release. *J Virol* **63**(6)**,** 2521-6.

Wengler, G., and Wengler, G. (1991). The carboxy-terminal part of the NS 3 protein of the West Nile flavivirus can be isolated as a soluble protein after proteolytic cleavage and represents an RNA-stimulated NTPase. *Virology* **184**(2)**,** 707-15.

Wengler, G., and Wengler, G. (1993). The NS 3 nonstructural protein of flaviviruses contains an RNA triphosphatase activity. *Virology* **197**(1)**,** 265-73.

Winkler, G., Maxwell, S. E., Ruemmler, C., and Stollar, V. (1989). Newly synthesized dengue-2 virus nonstructural protein NS1 is a soluble protein but

becomes partially hydrophobic and membrane-associated after dimerization. *Virology* **171**(1)**,** 302-5.

Wu, J., Bera, A. K., Kuhn, R. J., and Smith, J. L. (2005). Structure of the Flavivirus helicase: implications for catalytic activity, protein interactions, and proteolytic processing. *J Virol* **79**(16)**,** 10268-77.

Xu, T., Sampath, A., Chao, A., Wen, D., Nanao, M., Chene, P., Vasudevan, S. G., and Lescar, J. (2005). Structure of the Dengue virus helicase/nucleoside triphosphatase catalytic domain at a resolution of 2.4 A. *J Virol* **79**(16)**,** 10278-88.

Yamaji, Y., Kobayashi, T., Hamada, K., Sakurai, K., Yoshii, A., Suzuki, M., Namba, S., and Hibi, T. (2006). In vivo interaction between Tobacco mosaic virus RNA-dependent RNA polymerase and host translation elongation factor 1A. *Virology* **347**(1)**,** 100-8

CHAPTER II

Interaction between the cellular protein eEF1A and the 3' terminal stem loop of the West Nile virus genomic RNA facilitates viral RNA minus strand initiation.

INTRODUCTION

The eukaryotic translation elongation factor, eEF1A, constitutes 1-4% of the total soluble protein in actively dividing cells and is second only to actin in abundance (Browning et al., 1990; Condeelis, 1995). eEF1A delivers aminoacylated tRNAs (aa-tRNA) and GTP to the A site on the ribosome during protein synthesis. The eEF1A:GTP:aa-tRNA complex then moves to the P site. eEF1A hydrolyzes GTP to GDP, which results in the release of eEF1A:GDP from the ribosome. In addition to its role in peptide chain elongation, eEF1A has been reported to bind to mRNA (Lui, 2002; Mickleburgh et al., 2006), to bind to and bundle actin filaments (Ejiri, 2002; Lui, 1996; Lui, 2002), to sever microtubules (Shiina, 1994), and to mediate protein degradation via ubiquitin-dependant pathways (Gonen, 1996; Gonen, 1994).

West Nile virus (WNV) is a member of the family *Flaviviridae* in the genus *Flavivirus*. WNV is transmitted by arthropods and is maintained in a mosquito-bird cycle in nature with humans as incidental hosts. WNV infection in humans is usually asymptomatic or causes a mild febrile illness. Less than 1% of all infections result in a severe central nervous system disease, that can sometimes be fatal (Petersen, Marfin, and Gubler, 2003; Weaver and Barrett, 2004).The WNV genome is a positive-polarity, single-stranded RNA of about 11 kb in length. Translation and

replication of the viral genome occur in the cytoplasm of infected cells. The genome contains a single open reading frame (ORF) encoding a polyprotein of approximately 3000 amino acids that is cleaved by host and viral proteases into 3 structural and 7 nonstructural proteins. The genome is flanked by 5' and 3' untranslated regions (UTR). The WNV 5' UTR is 96 nt long while the 3' UTR is 632 nt long. The genomic 3' terminal nt form a SL that is predicted to be highly conserved among all flaviviruses (Brinton, Fernandez, and Dispoto, 1986; Hahn et al., 1987; Markoff, 2003; Wengler and Castle, 1986). This 3' terminal region is thought to function as a promoter for viral minus-strand synthesis; deletion of the 3' SL in a flavivirus infectious clone was lethal providing evidence that *cis*-acting elements were present in this region (Bredenbeek et al., 2003). Previously, three cellular proteins with molecular masses of 105, 84 and 52 kDa were reported to bind specifically to the WNV 3' terminal SL RNA (Blackwell and Brinton, 1995). The 52 kDa protein was subsequently identified as eEF1A (Blackwell and Brinton, 1997). The dissociation constant (kD) for the interaction between eEF1A and the WNV 3' SL RNA is 10^{-9} M, which is similar to that of the interaction between eEF1A and individual charged tRNAs (Riis et al., 1990). One major and two minor eEF1A binding sites were previously mapped on the WNV 3' SL RNA using RNase footprinting and nitrocellulose filter binding assays (Blackwell and Brinton, 1997).

eEF1A has also been reported to bind to the genomic 3' terminal tRNA-like structure (TLS) of the positive-strand RNA plant virus, turnip yellow mosaic virus (TYMV), and to act as both a translational enhancer and a repressor of minus-strand

synthesis (Matsuda, 2003a; Matsuda, 2003b). eEF1A has been reported to bind to both the 3' TLS and the viral polymerase of the positive strand RNA plant virus, tobacco mosaic virus (TMV) (Yamaji et al., 2006). The bacterial homolog of eEF1A was shown to be a functional part of the viral replicase holoenzyme of the positive-strand RNA bacteriophage, Qβ (Blumenthal and Carmichael, 1979; Brown, 1996; Miranda, 1997; Schuppli, 2000; Schuppli, 1998). Similarly, for the negative-strand RNA virus, vesicular stomatitis virus (VSV), eEF1A was reported to be a component of the viral transcriptase complex and was required for replicase activity *in vitro* (Qanungo, 2004). eEF1A was also reported to interact with the bovine viral diarrhea virus nonstructural protein, NS5A; the hepatitis C virus nonstructural protein, NS4A; and the HIV type 1 Gag polyprotein (Cimarelli, 1999; Johnson, 2001; Kou et al., 2006).

Various mutations were introduced into the previously mapped major binding site of the WNV 3' SL RNA in a WNV infectious clone and the effect of these mutations on virus production, viral RNA translation, and viral RNA synthesis was assessed. All of the mutations that altered eEF1A binding *in vitro* had a negative effect on virus production in cell culture. None of the mutations had an effect on the translation of viral proteins. Mutations that decreased the binding efficiency of eEF1A to the viral 3'(+) SL *in vitro* had a negative effect on viral minus-strand RNA synthesis, while mutations that increased the binding efficiency of eEF1A to the viral 3' SL *in vitro*, increased the production of minus-strand RNA synthesis. The results

strongly suggest that eEF1A plays a role in the initiation of flavivirus minus-strand synthesis.

RESULTS

Effect of mutation of the major eEF1A binding site in a WNV infectious clone on progeny virus production.

Two minor and one major binding sites for eEF1A on the 3'(+) SL RNA of WNV were previously reported (Blackwell and Brinton, 1997). The major eEF1A binding site (5'CACA 3', nts 62 to 65 from the 3' end of the genomic RNA), was predicted to consist of an unpaired A at position 62 and the base paired nts 63 to 65 (CAC) (Fig. 1A). In a WNV infectious clone, one or more of the four nts of the major eEF1A binding site were changed (shown in bold). In Mutant A, the unpaired A62 was substituted with a U changing the binding site to 5'CAC**U** 3' and creating a G-U base pair that removed the bulge and further stabilized the stem in this region. In Mutant B (5'**UGG**A 3'), three of the four binding site nts were changed. This mutation was predicted to widen the bulge by one nt on each side, but to maintain the base pairing of the two 5' mutated nts of the binding site. In Mutant C (5'**UGG**A 3'+ 5' G**CCA** 3'), the nts on the opposite side of the stem from the binding site were mutated in Mutant B RNA to restore the predicted secondary structure. In Mutant D (5'**UGUG** 3'), only the four binding site nts were changed. The parental predicted secondary structure was preserved, but the unpaired nt in the binding site was now mutated to a G instead of an A (Fig. 2.1A). WNV 3'(+) RNA probes with the Mutant B or C substitutions were previously reported to decrease *in vitro* binding

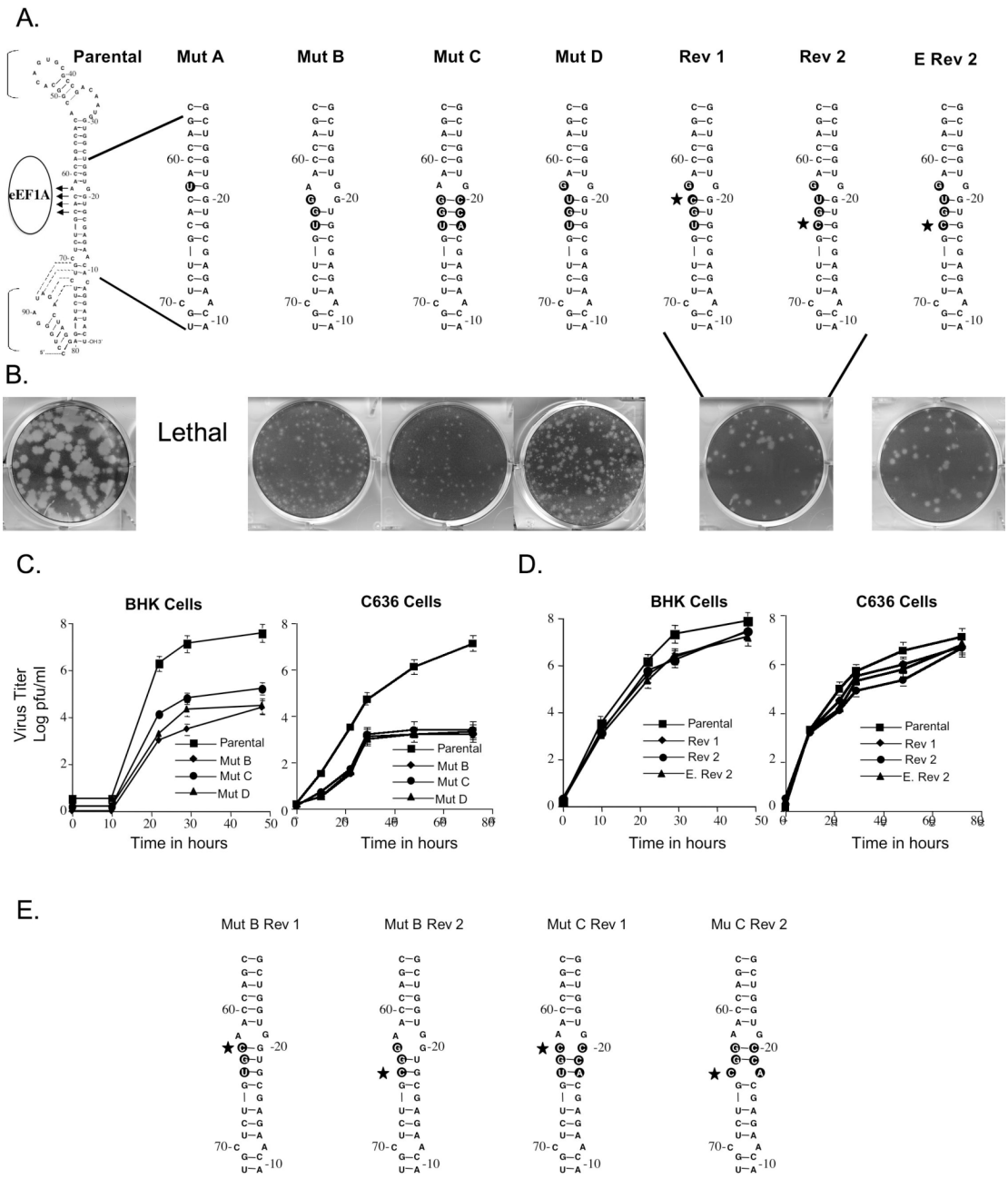

Figure 2.1. Mutation of the major eEF1A binding site in the 3' (+) SL of a WNV infectious clone.
(A) The engineered nt substitutions are indicated by black circles and revertant nt are indicated with a star. (B) Plaques produced by progeny virus 72 hr after RNA transfection. (C) Mutant virus growth in BHK and C6/36 cell monolayers infected with an MOI of 0.1. (D) Revertant virus growth in BHK and C6/36 cells infected with an MOI of 0.1. Error bars represent the SE (n=4). (E) Predicted secondary structures of Mutant B and C revertant viruses.

of purified BHK eEF1A by about 60% in filter binding studies (Blackwell and Brinton, 1997). The parental and mutant viral RNAs were *in vitro* transcribed by SP6 RNA polymerase and used to transfect 90% confluent BHK monolayers in a 6-well tissue culture plate. At 72 hr after transfection, the plaque phenotype of progeny virus was assessed on an agarose-overlaid transfection well.

No plaques were observed in wells transfected with Mutant A or after three sequential blind passages of culture fluid harvested from transfection wells of BHK cells. Also, viral RNA was not detected by RT-PCR in any of these fluids. Mutants B, C and D each produced pinpoint plaques (less than 0.1 mm in diameter) on the transfection well (Fig. 2.1B). The diameter of plaques produced by parental virus was 2-3 mm (Fig. 2.1B). Virus harvested from replicate non-overlayed transfection plates was titered by plaque assay and then used to analyze virus kinetics in both a mammalian (BHK) and a mosquito (C3/36) cell line. The growth of mutant viruses B, C, and D was reduced by 100 to 1000 fold as compared to the parental infectious clone virus. The titer at 48 hr after infection of BHK cells was 3.5×10^4 PFU/ml for Mutant B, 9×10^4 PFU/ml for Mutant C, 4.35×10^4 PFU/ml for Mutant D and 5.5×10^7 PFU/ ml for parental infectious clone virus (Fig. 2.1C). These mutants also displayed a 10,000 fold reduction in growth in C6/36 cells. In these cells, the titer at 72 hr was 2×10^3 PFU/ml for Mutant B, 4×10^3 PFU/ml for Mutant C, 3×10^3 PFU/ml for Mutant D and was 1.2×10^7 for parental infectious clone virus (Fig. 2.1C).

After three passages in either BHK or C6/36 cells, some intermediate sized plaques (1mm in diameter) were observed among the pinpoint plaques with Mutants B, C, and D. Intermediate size plaques were individually picked, virus from each picked plaque was amplified by growth for 48 hr in individual wells of a 24-well tissue culture plate and then viral RNA in harvested culture fluid was extracted and amplified by RT-PCR. The PCR products were cloned into pTOPO TA 2.1 (Invitrogen) and 10 clones for each mutant were sequenced. Analysis of the sequences showed that reversion to the parental nt (C) had occurred in the intermediate plaque virus from Mutants B, C, and D at either position 63 or 65 from the 3' end of the genome. The two types of partial revertants were found in approximately equal frequency for each of the three mutants. The predicted structures of the two revertants obtained for Mutant D are shown in figure 2.1A (Rev 1 and Rev 2). The growth kinetics of the two Mutant D partial revertants was next compared in BHK and C6/36 monolayers infected at an MOI of 0.1 These revertant viruses maintained an intermediate sized plaque phenotype during passage. Although both revertants replicated significantly more efficiently than the original Mutant D, neither revertant produced wild type yields. The plaque and growth characteristics of these revertants remained stable during three additional passages. The virus titer produced in BHK cells at 48 hr after infection by Revertant 1 was 4.3 x 10^7 PFU/ml and by Revertant 2 was 3.9 x 10^7 PFU/ml, while parental infectious clone virus produced a yield of 8.8 x 10^7 PFU/ml (Fig. 1D). In C6/36 cells, the yields of Revertant 1 and Revertant 2 at 72 hr after infection were 8 x 10^6 PFU/ml and 6 x 10^6 PFU/ml,

respectively, while the yield of the parental infectious clone virus was 1.2 x 10^7 PFU/ml (Fig. 2.1D).

To ensure that the increased replication efficiency observed for the partial revertants was not due to a second site mutation located elsewhere in the viral genomic RNA, site-directed mutagenesis was performed on Mutant D plasmid DNA to engineer a partial revertant sequence (5'UGUG 3' changed to 5'CGUG 3'). This mutant was designated Engineered Revertant 2 (Fig. 2.1A). After transfection, this RNA produced an intermediate plaque phenotype (1 mm) (Fig. 2.1B). Virus recovered from transfection wells was titered and used to infect either BHK or C6/36 cell monolayers at an MOI of 0.1. The virus yields were similar to those obtained with the original Revertant 2 that arose in infected cells. The Engineered Revertant 2 produced 1.5 x 10^7 PFU/ml at 48 hr after infection in BHK cells and 8.8 x 10^6 PFU/ml at 72 hr in C6/36 cells. These results indicate that the phenotype of the Revertant 2 virus was due solely to the reversion of a single C within the major eEF1A binding site.

In the case of Mutant D, the two revertant Cs replaced Us and changed a U-G base pair back to a stronger G-C base pair. The predicted secondary structures of the Mutants B and C revertants are shown in figure 2.1E. In the Mutant B Revertant 1, the G·G bulge was replaced with a G-C base pair and in Mutant B Revertant 2; the G-U base pair reverted to a G-C base pair. In Mutant C, the two revertant Cs changed the more stable G-C and U-A base pairs to C·C and C·A bulges, respectively. While the reversions found in Mutants B and D were predicted to stabilize the predicted

RNA secondary structure in the major eEF1A binding site, the reversions found in Mutant C destabilized the predicted secondary structure in this binding site. The lack of correlation observed between the stability of the stem in the region of the major eEF1A binding site (nts 63-65) and the efficiency of virus growth strongly suggests that the revertant Cs are important for another function.

Mutagenesis of the nts base paired with the major eEF1A binding site.

A previous study showed that when the pairing partners of the major eEF1A binding site nts were mutated so that the binding site nts were in a single stranded context, the resulting mutant RNA bound about 20% more efficiently to eEF1A than did the wild type 3' SL RNA (Blackwell and Brinton, 1997). The same set of substitutions and another similar set of mutations were introduced into the infectious clone. Nts 18-21 were mutated to 5'CCCA 3' (Mutant E) or nts 18-20 were mutated to 5'CCA 3' (Mutant F) (Fig. 2.2A) and the effect of these mutations on virus growth efficiency was analyzed. After transfection of BHK monolayers with either Mutant E or F viral RNA, the plaque phenotype of the progeny virus was similar to that of the parental infectious clone virus (2-3 mm). Analysis of the growth of these mutant viruses in BHK and C6/36 cell monolayers infected with an MOI of 0.1 (Fig. 2.2B) showed that both mutant grew about 10 fold less efficiently than the parental virus. At 48 hr after infection in BHK cells, Mutant E produced a titer of 7×10^6 PFU/ml, Mutant F produced a titer of 6×10^6 PFU/ml, and the parental infectious clone virus produced a titer of 5.5×10^7 PFU/ml. At 72 hr after infection in C6/36

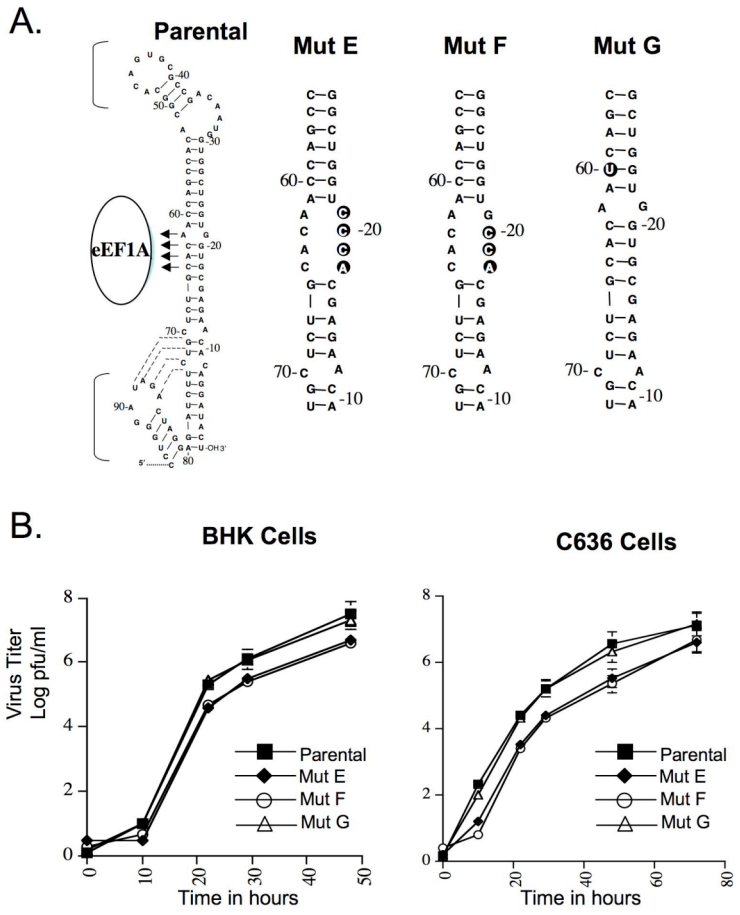

Figure 2.2. Mutation of the pairing partners of the major eEF1A binding site.
(A) The engineered nt substitutions are indicated by black circles. (B) Virus growth in BHK and C6/36 cells infected with an MOI of 0.1. Error bars represent the SE (n=4).

cells, Mutant E produced a titer of 6 x 10^6 PFU/ml, Mutant F produced a titer of 6.6 x 10^6 PFU/ml, and the parental virus produced a titer of 1.5 x 10^7 PFU/ml.

Mutagenesis of a C adjacent to the major eEF1A binding site.

The equivalent frequency with which the same two partial revertants were generated after passage of Mutants A, B and C and the observation that either of the two Cs in the 4 nt binding site increased the efficiency of viral growth in cell culture to similar levels suggests that there is a redundancy in this binding sequence. To determine whether mutations of other cytidines in the vicinity of the major eEF1A binding site would also have a negative effect on viral growth, the C located just above the major eEF1A binding site at nt 60 from the 3' end was mutated to a U (Mutant G) to maintain base pairing (Fig. 2.2A). Mutant G produced wild type plaques (2-3 mm) at 72 hr after RNA transfection (data not shown) and the virus yields observed after infection of BHK or C6/36 cell cultures with Mutant G at an MOI of 0.1 were similar to those obtained with parental infectious clone virus. At 48 hr after infection in BHK cells, parental virus produced a titer of 5.5 x 10^7 PFU/ml, while the yield for Mutant G virus was of 3.7 x 10^7 PFU/ml (Fig. 2.2B). At 72 hr after infection in C6/36 cells, the yield for the Mutant G was 1.2 x 10^7 PFU/ml, while that for the parental virus was 1.5 x 10^7 PFU/ml. In contrast to the two conserved Cs in the eEF1A binding site, mutation of the C in Mutant G had no observable effect on the efficiency of virus replication.

Relative binding activity.

Although the relative efficiency of the WNV 3'(+) SL RNA probes with Mutant B and C substitutions had been previously analyzed in filter binding assays, the binding efficiency of eEF1A to the 3' (+) SL RNAs with Mutant A, Mutant D, Mutant E and the Engineered Revertant 2 substitutions had not been previously reported. A gel mobility shift assay was used to compare the relative binding activity of purified recombinant eEF1A for the various 3' (+) SL RNAs and the parental 3' (+) SL RNA. Each of the radiolabeled 3' (+) SL RNA probes (2000 CPM) was incubated with 0, 4, 8, 20, or 40 ng of purified recombinant eEF1A for 30 min at room temperature. The RNA-protein complexes formed were separated on 5% non-denaturing polyacrylamide gels and detected by phosphorimaging. The percent of the free probe shifted was calculated as described in the Materials and Methods. A representative gel from at least three replicate assays with each RNA probe is shown in Figure 3A. Relative binding activity as measured by the percent of the free probe shifted by recombinant eEF1A for each of the RNA probes is shown in Fig. 2.3B. With 40 ng of recombinant eEF1A, 67% of the parental 3' SL RNA probe was shifted, but only 20% of the mutant A probe, 27% of Mutant C, 30% of the Mutant D probe and 54% of the Engineered Revertant 2 RNA probe was shifted. In contrast, 80% of the Mutant E RNA probe was shifted with 40 ng of recombinant eEF1A. The results obtained with the gel mobility shift assays with Mutant A, Mutant C, Mutant D, and Mutant E 3' (+) SL RNAs correlated well with those obtained previously with filter binding assays (Blackwell and Brinton, 1997). In the case of Mutants C and D,

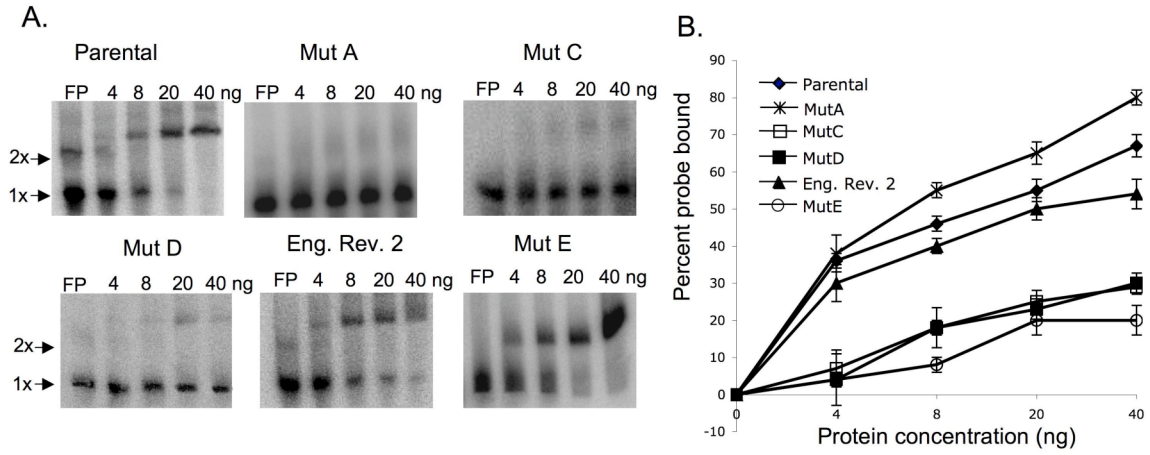

Figure 2.3. Comparison of the binding activity of recombinant eEF1A to parental, mutant and revertant virus 3 ' (+) SL RNA probes.
(A) A gel mobilty shift assay done with 32P-radiolabeled 3'(+) SL RNAs (2000 CPM) and recombinant eEF1A purified from E. coli extracts. (B) The percent of 32P RNA shifted by recombinant eEF1A. Error bars represent the SE (n=3).

the relative decrease in the binding efficiency correlated with the decrease in viral replication efficiency. Also, the increased binding efficiency of the Engineered Revertant 2 RNA compared to Mutant C and D RNAs correlated with the observed increase in virus replication efficiency. Only with Mutant E was there a lack of correlation between eEF1A binding efficiency and the virus replication efficiency observed.

Effect of eEF1A binding site mutations on viral RNA translation.

All of the mutations made in the major eEF1A binding site reduced viral growth efficiency in cell culture. These mutations could negatively affect either viral RNA translation and/or replication. To analyze the effect of mutations on viral RNA translation, parental infectious clone and Mutant A, D and E RNAs were *in vitro* transcribed and used to transfect BHK cells grown on coverslips. At 3 hr after RNA transfection, the cells were fixed and permeabilized. WNV antigen (red) was detected by immunoflourescence using an anti-WNV MHIAF as described in the Materials and Methods. Even though the phenotypes of these mutants differed, Mutant A (lethal), Mutant D (0.1 mm plaques) and Mutant E (2-3 mm plaques), similar high levels of virus-specific antigen were detected in over 80-90% of the cells with the parental infectious clone RNA and also with each of the three mutant RNAs (Fig. 2.4A). These results indicate that none of these mutations negatively affected the translation of the viral RNA.

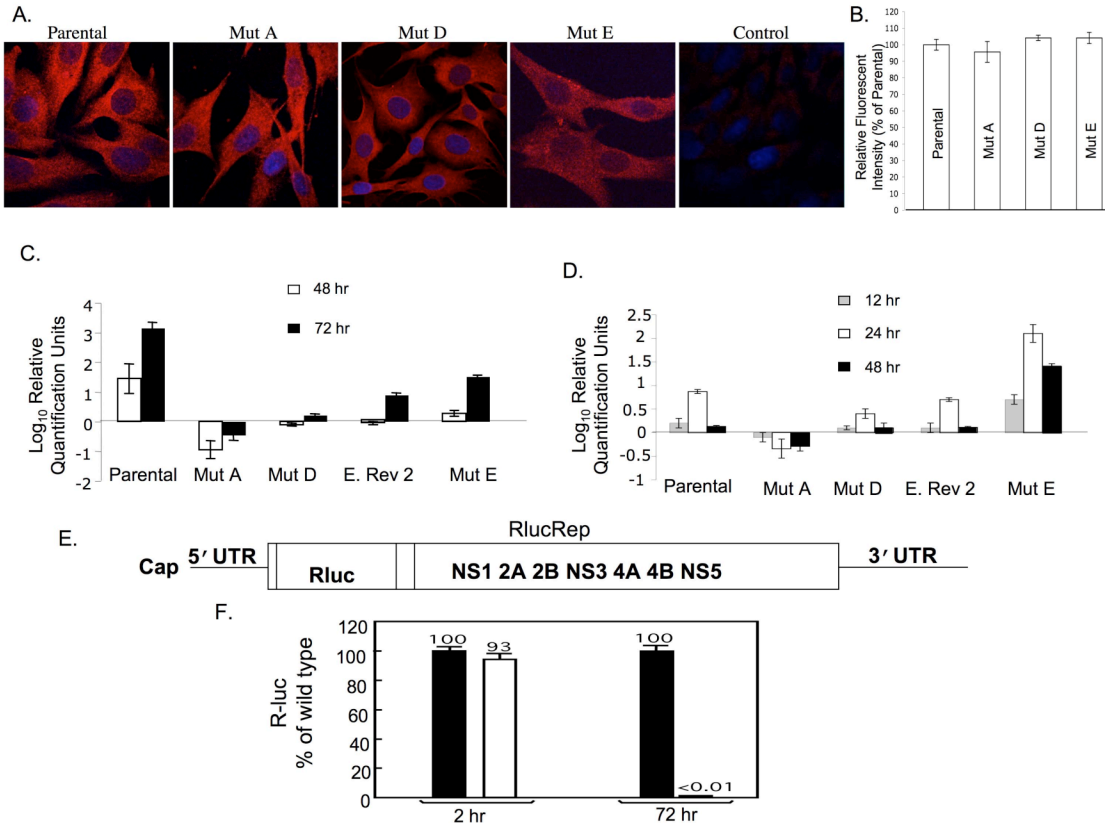

Figure 2.4. Effect of mutations in the major eEF1A binding site on the translation and replication efficiency of the viral genome.
(A) As a measure of translation efficiency, WNV antigens (red) were detected by confocal microscopy in BHK cells 3 hr after transfection of genomic RNA with anti-WNV MHIAF. (B) Relative fluorescent intensities of WNV proteins in the cytoplasm of transfected BHK cells. (C) Relative quantification of intracellular WNV genomic RNA by Real-Time RT-PCR. RNA detected at 48 and 72 hr after transfection. Error bars represent the SE (n=3). (D) Relative quantification of intracellular WNV minus-strand RNA by strand specific Real-Time RT-PCR. RNA detected at 12, 24 and 48 hr after transfection. Error bars represent the SE (n=3). (E) Schematic of a WNV reporting replicon containing an Rluc gene fused in-frame with the ORF (RlucRep). (E) Equal amounts of wild-type (black bar) and mutant (white bar) RlucRep RNAs (10 μg) were transfected into BHK cells and cell lysates were quantified for Rluc activity at 2 h and 72 h post-transfection as a measure of viral RNA translation and replication, respectively. An average value obtained from four independent experiments is shown.

Effect of eEF1A binding site mutations on viral RNA replication.

The effect of mutations in the major eEF1A binding site on viral RNA replication was next assayed. Relative real time RT-PCR was used to quantify the intracellular levels of genomic viral RNA within BHK cells 48 and 72 hr after transfection. Viral RNA levels measured at each of these times were normalized to the amount of viral genomic RNA (primarily input viral RNA) present in cell extracts at 6 hr after transfection and also to the levels of the cellular GAPDH mRNA to control for sample variation. Increases in the levels of viral genomic RNA above transfected input RNA were observed at 48 and 72 hr after transfection with the parental infectious clone RNA (Fig. 2.4C). At both 48 and 72 hr after transfection of Mutant A (lethal) RNA, the intracellular genomic RNA levels were lower than the viral RNA input at 6 hr after transfection, indicating degradation of the input RNA and little if any RNA replication (Fig. 2.4C). With Mutant D, the level of genomic RNA produced was also lower than input RNA at 48 hr after transfection, but to a lesser extent than seen with Mutant A, suggesting some RNA replication had occurred. An increase observed at 72 hr after transfection confirmed that this RNA was replicating, but at a lower level than the parental infectious clone RNA. These results were consistent with the low virus yields and small size plaques observed with Mutant D in figure 2.1. At 48 hr, the Engineered Revertant 2 genomic RNA level detected was similar to that observed after transfection of Mutant D RNA at 48 hr, but by 72 hr there was a greater increase in the Engineered Revertant 2 genomic RNA

that was seen with Mutant D. With Mutant E, an increase in genomic RNA levels was observed at both 48 and 72 hr after transfection, but the levels were lower than those observed with the parental infectious clone RNA (Fig. 2.4C). These results indicate that each of the major eEF1A binding site mutations had a negative effect on viral genomic RNA replication whether or not they increased or decreased *in vitro* eEF1A binding efficiency.

The WNV 3'(+) SL RNA is thought to contain promoter elements for minus-strand RNA synthesis. The effects of the major eEF1A binding site mutations on viral minus-strand RNA synthesis were next investigated using minus-strand specific real time RT-PCR. Intracellular levels of minus strand RNA in BHK cells were quantified at 12, 24 and 48 hr after transfection. Minus strand RNA levels at these time points were normalized to viral minus strand RNA detected at 2 hr after transfection and to cellular GAPDH mRNA. The majority of the minus strand signal detected at 2 hr was due to non-specific detection of plus strand input RNA. Therefore, this normalization stringently removed nonspecific background. After transfection of parental infectious clone RNA, minus-strand RNA levels peaked at 24 hr and then decreased by 48 hr (Fig. 2.4D). No minus-strand RNA amplification was detected for Mutant A (lethal) RNA at 12, 24 or 48 hr after transfection (Fig. 2.4D). A decreased level of minus-strand synthesis with was observed after transfection of Mutant D RNA as compared to the parental virus. With Engineered Revertant 2, an intermediate level of minus-strand synthesis was detected that was between that for the parental and Mutant D RNAs (Fig. 2.4D). Interestingly, Mutant E, which bound to eEF1A more efficiently

in vitro, showed a significantly increased level of minus strand synthesis at 12, 24 and 48 hr after transfection as compared to the parental infectious clone RNA even though the amount of Mutant E genomic RNA synthesis detected was lower than that of the parental infectious clone RNA (Fig. 2.4C and D). All of the mutations in the major eEF1A binding site that reduced *in vitro* RNA-protein binding activity also reduced *in vivo* synthesis of minus strand RNA. In contrast, a mutation that increased *in vitro* RNA-protein activity also increased *in vivo* minus strand RNA synthesis.

As an alternate means of analyzing the effect of mutations in the major eEF1A binding site on translation and viral RNA replication data was obtained by a collaborator, P.Y. Shi, using a luciferase-reporting NY-99 replicon (RlucRep, Fig. 2.4E). RlucRep contains an Rluc gene fused in-frame with the viral nonstructural gene ORF. This gene was inserted into the position where the majority of the viral structural gene region had been deleted (Fig. 2.4E). After transfection of BHK cells with RlucRep RNA, two distinct Rluc peaks were detected, one at 2-10 hr after transfection and another beginning at 24 hr after transfection. The initial peak represents translation from the input RNA while the second peak represents translation from replicated replicon RNA (Lo et al., 2003). After transfection of BHK cells with an equal amount of parental or Mutant D RlucRep RNA, similar levels of Rluc activity were observed at 2 hr after transfection, indicating that translation was not affected by the mutation (Fig. 2.4F). In contrast, at 72 hr after transfection, a background level of Rluc activity was observed for the Mutant D RlucRep (Fig. 2.4F). Also, an immunofluorescence assay was used to detect viral antigen expressing

cells. Antigen positive cells were observed at 72 hr after transfection of BHK cells with the parental RlucRep RNA, but no positive cells were observed in cultures transfected with the Mutant D RlucRep RNA (data not shown). The data show that in the replicon the Mutant D substitutions caused a lethal phenotype. In contrast, although the Mutant D infectious clone showed a reduced level of RNA replication (Fig. 2.4C and D), sufficient levels of viral RNA replication occurred to generate a revertant (Fig. 2.1A).

Colocalization of WNV proteins and eEF1A within BHK cells.

The observation that mutations made in the major eEF1A binding site in a WNV infectious clone RNA had a negative effect on viral growth suggested this viral RNA-cell protein interaction occurred in infected cells. Confocal microscopy was used to determine whether eEF1A and viral RC colocalized in the cytoplasm of cells infected with either WNV or the divergent flavivirus, Den 2. BHK cells were infected with WNV or Den 2 at an MOI of 0.1, or mock infected. Cells grown on coverslips were permeabilized and fixed 36 hrs after infection with WNV or 72 hrs after infection with Den 2. Den 2 was fixed at a later time point due to the slower growth kinetics of Den 2 virus. Anti-NS3/NS5 (red) and anti-eEF1A (green) were both used at a 1:200 dilution. Due to the high degree of conservation of NS3 and NS5 among divergent flaviviruses, antibodies made against the WNV NS3/NS5 were used to detect RC in both WNV and Den 2 infected cells. In uninfected cells, eEF1A was found throughout the cytoplasm and NS3/NS5 was not detected (Fig. 2.5A). Although eEF1A was detected throughout the cytoplasm in infected cells, it was found to

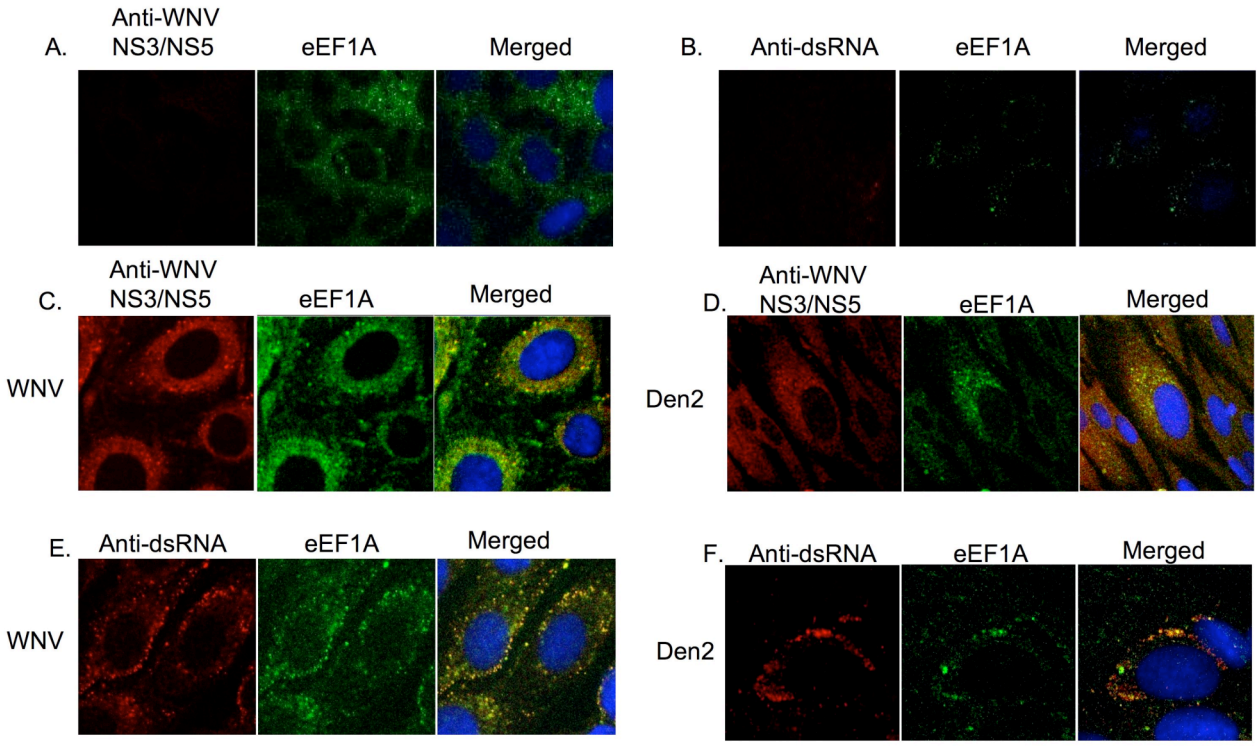

Figure 2.5. Colocalization of eEF1A and flaviviral RC in infected BHK cells.
BHK cells were infected with WNV, strain Eg101, (panels C and E) and Den 2, strain Bangkok, (panels D and F) at an MOI of 0.1, or were mock infected (panels A and B). Cells were fixed and permeabilized at 36 hr (WNV) or 72 hr (Den 2) and then incubated a rabbit antibody specific for WNV NS3 and NS5 proteins at a 1:50 dilution (panels A, C and E) or mouse monoclonal anti-dsRNA antibody at a 1:200 dilution (panels B, D, and F) and a goat polyclonal anti-eEF1A antibody at a 1:200 (panels A, C and D) or a 1:800 dilution (panels B, E and F). The anti-NS3/NS5 and anti-dsRNA antibodies were conjugated with secondary antibody that fluoresced red and the anti-eEF1A antibody was conjugated with a secondary antibody that fluoresced green. Hoechst Dye was used to stain the nuclear DNA blue. Coverslips were mounted on glass slides and cells were visualized using a LSM 510 laser confocal microscope (Carl Zeiss Inc., Thornwood, NY) with a 100X oil immersion objective.

concentrate in discrete foci in the perinuclear region as well as in a ring around the nucleus in these cells. Colocalization (yellow) of eEF1A and WNV NS3/NS5 proteins in a ring around the nucleus as well as in discrete foci was observed by 36 hrs after infection (Fig. 2.5C), and a similar pattern of colocalization in Den 2 infected cells was observed at 72 hr after infection (Fig. 2.5D). Previous studies indicated that these foci in the perinuclear region represent the viral RC (Mackenzie et al., 1998; Miller, Sparacio, and Bartenschlager, 2006; Westaway et al., 1997). The broad ring observed could be due to high levels of anti-EF1A antibody or alternatively to the interaction of eEF1A and NS3/NS5 outside of the RC. In subsequent experiments, done with a higher dilution of anti-eEF1A antibody (1:800) only the discrete perinuclear foci of eEF1A were detected.

Antibodies directed against dsRNA (red) were also used in separate experiments to detect viral RNA in RC. The anti-dsRNA antibody is specific for dsRNA and does not detect ribosomal RNA. In both WNV and Den 2 virus infected cells, colocalization of dsRNA and eEF1A was observed in perinuclear foci (Fig. 2.5E and F). The colocalization of eEF1A with two of the flavivirus nonstructural proteins, and also with dsRNA in infected cells strongly suggests that eEF1A is recruited into viral RC in infected cells.

Co-immunoprecipitation of viral NS3 and NS5 by anti-eEF1A antibodies.

eEF1A was previously reported to bind to the viral nonstructural proteins of bovine viral diarrhea virus and hepatitis C virus and the polymerase and 3'UTR of tobacco mosaic virus (Johnson, 2001; Kou et al., 2006; Yamaji et al., 2006) and the colocalization experiments described above indicated that eEF1A might interact with one of the WNV nonstructural proteins. The WNV 3'(+) SL RNA is thought to contain promoter elements for minus strand synthesis, but there has been no conclusive evidence that the viral polymerase and/or other viral RC proteins bind efficiently to the 3'(+) SL RNA even though this has been reported by other labs (Chen et al., 1997; Cui et al., 1998). Antibodies against eEF1A were used in co-immunoprecipitation experiments to determine whether eEF1A was able to pull down WNV nonstructural proteins. The cellular proteins NFAR-1 and NFAR-2 were previously reported to bind to the 3' terminus of bovine viral diarrhea virus genomic RNA (Isken et al., 2003). Antibodies to these proteins were also used in co-immunoprecipitation experiments. HSP105 was not previously reported to bind to any viral proteins and antibody to this protein was used as a negative control. BHK cells were either infected with the parental infectious clone virus at an MOI of 5 or mock infected. S2 lysates were harvested and immunoprecipitated with antibodies against the cellular proteins eEF1A, NFAR-1, NFAR-2 or HSP105. The immunoprecipitated complexes were analyzed by Western blotting as described in the Materials and Methods. NS3 and NS5 were detected in the infected, but not in the uninfected cell lysates with an anti-NS3/NS5 antibody (Fig. 2.6A). WNV NS3 and

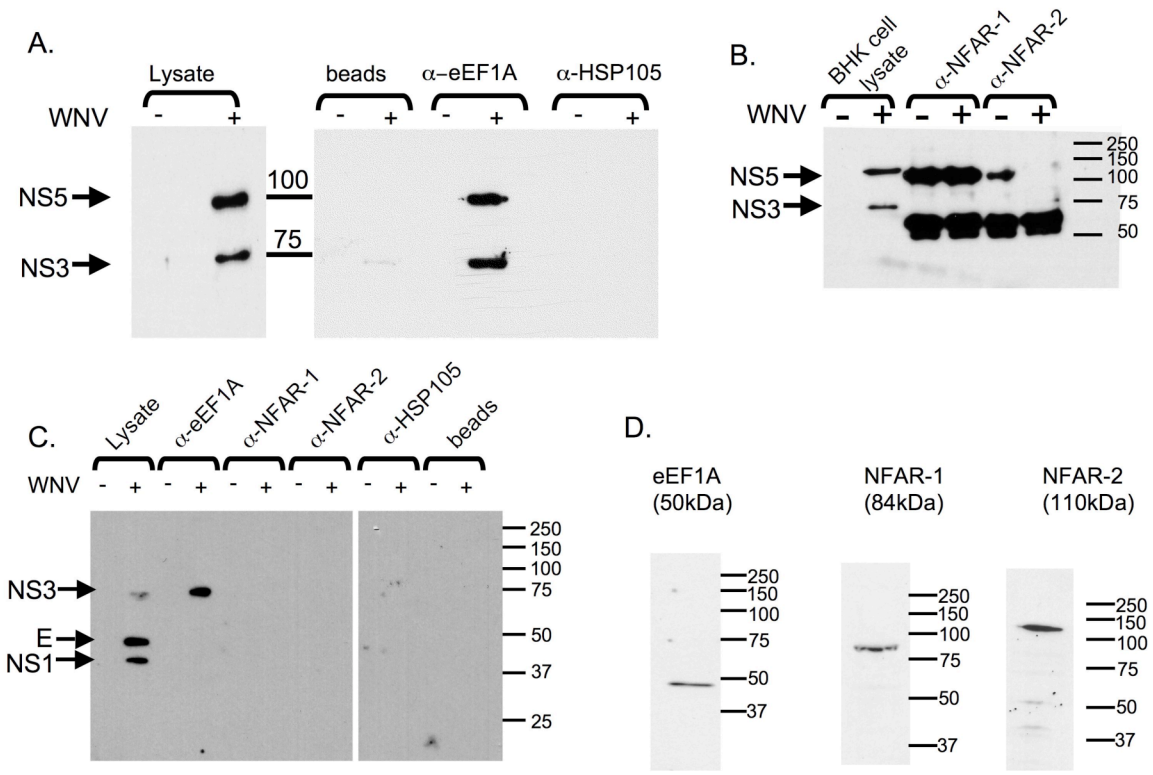

Figure 2.6. Co-immunoprecipitation of NS3 and NS5 with anti-eEF1A antibodies. (A) Antibodies against the cellular proteins eEF1A or HSP105 were incubated with WNV infected or uninfected BHK cell lysates and coprecipitated viral proteins were detected by Western blot using anti-NS3/NS5 antibody. (B) Anti-NFAR-1 or anti-NFAR-2 were incubated with uninfected or infected BHK cell lysates and coprecipitated viral proteins were detected by Western blot using anti-NS3/NS5 antibody. (C) Anti-eEF1A, NFAR-1, NFAR-2 or HSP105 were used in pull down experiments with WNV infected or uninfected BHK cell lysates and coprecipitated viral proteins were detected by Western blot using anti-WNV MHIAF (D) Proteins in BHK cell lysates were separated by SDS-PAGE and analyzed by Western blotting using anti-eEF1A, NFAR-1, or NFAR-2 antibodies.

NS5 were coprecipitated by anti-eEF1A antibody, but not by anti-HSP105 antibody (Fig. 2.6A) or anti-NFAR-1 or NFAR-2 antibodies (Fig. 2.6B). Since the anti-NFAR-1 and the anti-NFAR-2 antibodies were generated in rabbits as was the anti-WNV NS3/NS5 antibody, heavy and light chain antibody bands were detected in both uninfected and infected immunoprecipitates. Viral proteins in immunoprecipitates were also analyzed with a hyperimmune anti-WNV sera made in mice (MHIAF). In the infected cell lysate, NS1, E, and NS3 were detected on a Western blot with this antibody (Fig. 2.6C). NS3, but not E or NS1, was coprecipitated by anti-eEF1A antibody, but not by NFAR-1, NFAR-2, or HSP105 antibodies (Fig. 2.6C). Control Westerns performed on the cell lysates with the eEF1A, NFAR-1 and NFAR-2 antibodies detected only a single band of the expected size (Fig. 2.6D). When cell lysates were run on 1% agarose gels, no ribosomal RNA bands were detected by ethidium bromide staining, suggesting that polysomes were not present in the lysates. eEF1A interacts with one or more proteins present in WNV RC. Although an interaction between eEF1A and either E or NS1 was ruled out, the observation that both NS3 and NS5 were coprecipitated strongly suggests that eEF1A interacts with one or more of the viral proteins in the RC. Since antibodies to the four other RC proteins NS2A, NS2B, NS4A, and NS4B were not available, it was also not possible to determine whether these proteins were also coprecipitated by eEF1A antibody.

DISCUSSION

The 3' terminal 96 nts of the WNV genomic RNA were predicted to form two adjacent SL structures which were confirmed by structure probing experiments and these structures are predicted to be conserved among divergent flaviviruses (Brinton, Fernandez, and Dispoto, 1986; Hahn et al., 1987; Olsthoorn and Bol, 2001; Wengler and Castle, 1986). One major and two minor binding sites for the cellular protein eEF1A within the 3' terminal 96 nts of the WNV genomic RNA were previously mapped (Blackwell and Brinton, 1997). One minor binding site is located in the top left loop (nts 41-47 from the 3' end) of the 3' terminal SL, while the other is in the small adjacent SL (nts 81-96), (Blackwell and Brinton, 1997). The majority of the primary sequences and predicted structures of the two minor binding sites are conserved among divergent mosquito-borne flaviviruses. Previous studies showed that mutation of the top left loop of the 3' terminal SL in an infectious clone or a replicon negatively affected virus growth or viral RNA replication, respectively (Elghonemy, Davis, and Brinton, 2005; Tilgner, Deas, and Shi, 2005). Mutation or deletion of the small SL also negatively affected viral growth and viral RNA replication (Davis and Brinton, unpublished data). These studies indicated that both of the eEF1A minor binding sites are functionally important.

In the present study, the functional relevance of the major eEF1A binding site, which accounts for 60% of the *in vitro* eEF1A binding activity, was analyzed. The major eEF1A binding site consists of 4 adjacent nts (nts 62-65 from the 3' end) located on the 5' side in the middle region of the stem of the 3' terminal structure.

A62 is unpaired while and nts 63-65 (CAC) are base paired. Substitution of A62 with a U to create a G-U base pair was lethal for the virus and *in vitro* eEF1A binding to an RNA probe with this mutation was reduced by 40% as compared to the parental SL RNA, suggesting that a bulge in this region is essential for both virus viability and efficient eEF1A binding. In a previous study, two alternative substutions that caused A62 to be base paired, the substitution of A62 with C or the substitution of the G on the opposite side of the stem with a U, were also found to be essential (Yu and Markoff, 2005).The presence of a bulge may facilitate the opening of the major groove of an RNA stem allowing sequence specific binding to occur (Weeks and Crothers, 1991).

Although nts 63-65 are base paired in the parental WNV 3'SL RNA structure, mutations that made one or more of these three nts single stranded, such as in Mutants E and F, were viable but they did not grow as efficiently as the parental virus. Mutant C and D RNA probes, in which nts 63-65 were double stranded showed decreased eEF1A binding efficiency in vitro and decreased levels of virus growth was observed when these mutations were introduced into an infectious clone. All of the partial revertants generated by Mutants B, C and D had a revertant C at either nt 63 or 65. Although these partial revertants grew slightly less efficiently than the parental virus, they all grew with equal efficiency whether or not the revertant C was in a single stranded or double stranded context. *In vitro* binding of eEF1A to the Engineered Revertant 2 RNA probe, which had nt 65 in a double stranded context, did show a 24% increase in eEF1A binding compared to Mutant D, but this RNA still

bound 13% less efficiently than the parental RNA. Consistent with its increased eEF1A binding efficiency, this revertant grew more efficiently than Mutant D but less efficiently than the parental virus. The results indicate that a C at nt 63 or 65 allows efficient enough eEF1A binding to facilitate virus replication levels to be that are only slightly less efficient than when Cs are present at both positions and suggests that two adjacent functional eEF1A binding sites may be present in the major binding site in the WNV 3' (+) SL RNA. This redundancy may be an advantage in protecting this critical site from being inactivated by random mutations.

A correlation was consistently observed between the extent of the decrease in the *in vitro* binding activity of eEF1A to a mutant WNV 3' (+) SL RNA and the extent of the decrease in the level of viral intracellular minus strand RNA produced by an infectious clone with the same mutation. When a decrease in intracellular viral genomic RNA was detected, a decreased virus yield was also observed. Conversely, with Mutant D 3' (+) SL RNA, which bound 13% more efficiently to eEF1A in *in vitro* binding assays than the parental probe, 10 times higher levels of intracellular viral minus strand RNA were observed in transfected cells. In flavivirus infected cells, the levels of plus and minus strand RNA synthesis are tightly regulated. After the initial phase of RNA replication, the ratio of plus to minus strand RNA in infected cells is about 100 to 1 (Cleaves, Ryan, and Schlesinger, 1981). As might be expected, dissregulation of this ratio by the increased level of minus strand RNA produced by Mutant D resulted in less efficient synthesis of genomic RNA and a reduced virus

yield. Together, these results provide strong support for a direct role for eEF1A in the initiation of WNV minus strand RNA synthesis.

eEF1A was found to colocalize with NS3, NS5 and dsRNA in both WNV and Den 2 infected BHK cells. Also, anti-eEF1A antibody coimmunoprecipitated WNV NS3 and NS5 from infected cell lysates. It is not currently known whether eEF1A interacts directly with only one or both of these proteins and/or with another RC protein, but these data suggest that eEF1A does interact with the viral RC as well as with the 3' (+) SL RNA. Previous studies with several other RNA viruses, including Qβ, VSV, BVDV and HCV have reported interactions between eEF1A and viral RC proteins (Blumenthal and Carmichael, 1979; Cimarelli, 1999; Johnson, 2001; Kou et al., 2006; Qanungo, 2004). The roles of various host factors in the positive sense RNA bacteriophage Qβ RC have been well characterized (Blumenthal and Carmichael, 1979). The bacterial homolog of eEF1A, EF-Tu, binds the Qβ viral genomic RNA at the S2 binding site and to viral proteins in the replication holoenzyme and both of these interactions were reported to be required for specific initiation of synthesis minus-strand RNA synthesis (Brown, 1996; Kita et al., 2006). In contrast, the binding of eEF1A to the 3' TLS of TYMV was shown to enhance translation and repress minus-strand RNA synthesis (Matsuda, 2003a; Matsuda, 2003b). The data obtained in the present study, support the hypothesis that eEF1A plays similar roles in facilitating the initiation of WNV and Qβ viral minus strand synthesis.

Data obtained with purified viral RNA-dependent-RNA-polymerases from poliovirus and hepatitis C virus suggest that these enzymes have a low affinity for their template RNAs (Beckman and Kirkegaard, 1998; Lohmann et al., 1998). The flavivirus RdRp, NS5, must recognize the 3'(+) and 3'(-) strand terminal RNA sequences to initiate the synthesis of viral minus and plus strand RNAs, respectively. NS5 has only been reported to bind with high affinity to the 5'(+) sequence of the viral genomic RNA presumably as part of its RNA capping function (Filomatori et al., 2006; Zhou et al., 2007). eEF1A binds to the WNV 3'(+) SL RNA with a high affinity (Blackwell and Brinton, 1997) and the strength of the interaction between eEF1A and the viral 3' (+) SL RNA consistently correlated with the efficiency of the initiation of viral minus stand RNA synthesis. eEF1A also interacts with WNV RC proteins. These observations strongly suggest that eEF1A provides specific recognition of the 3'(+) SL template RNA and facilitates its interaction with the RdRp in the RC. Initiation of minus strand synthesis may be directly coupled with translation. The binding of eEF1A to both a newly made viral RC protein and to the 3' end of a translating genomic RNA may facilitate the switch of a viral genome from translation to RNA replication. The three contact sites for eEF1A in the 3'(+) SL RNA each appear to be functionally important, which suggests that the binding of eEF1A to these three sites on the viral 3'(+) SL RNA may result in a conformation change in this RNA template that is necessary for the RC to efficiently recognize and bind to it in the correct orientation for the initiation of minus strand RNA synthesis.

eEF1A was shown to bind with a similar efficiency to the 3' (+) SL RNAs of four divergent flaviviruses (Blackwell and Brinton, unpublished data). While the 3' terminal genomic RNA sequences are not well conserved among these divergent flaviviruses, the RNA secondary structures as well as several short sequences, including the minor eEF1A binding sites, are conserved. Although the major binding sites for eEF1A on these divergent flaviviral RNAs have not yet been functionally mapped, eEF1A was found to colocalize to RC in both Den 2 and WNV infected cells. These results support a role for eEF1A in the initiation of minus strand RNA synthesis by all flaviviruses. Several characteristics of eEF1A make it an ideal protein to serve as a viral host factor. eEF1A is constitutively expressed and distributed throughout the cytoplasm and attached to actin filaments and so would be readily available for use by an incoming viral genome. After actin, eEF1A is the second most abundant protein in cells and therefore competition between the viral RNA and the host cell for this protein would not be an issue. eEF1A is highly conserved among different eukaryotic species (Condeelis, 1995). Flaviviruses replicate in both insect and a variety of vertebrate hosts during their natural transmission cycles and the eEF1As available in these various hosts would be quite similar. During its normal cell functions, eEF1A interacts specifically with the other host elongation complex proteins and with ribosomal RNA. Both RNA/RNA and RNA/protein interaction appear to be functionally important for the role of eEF1A in flavivirus minus strand RNA initiation.

None of the mutations made in the major eEF1A binding site in either a WNV infectious clone or a replicon had any effect on the translation of the viral RNA. Data obtained in a previous study showed that the presence of the WNV 3' (+) SL on a chimeric reporter mRNA decreased *in vitro* translation efficiency under conditions of limiting concentrations of translation factors (Li and Brinton, 2001) suggesting that under these conditions, 3'(+) SL RNAs and ribosomes were competing for a translation factor, such as eEF1A (Blackwell and Brinton, 1997). However, the abundance of eEF1A in cells makes it unlikely that eEF1A concentrations would be limiting. The observed colocalization of eEF1A to the viral RC, which are thought to be located within invaginations of the perinuclear membranes suggests that the concentration of eEF1A to these complexes ensures continuing viral minus strand synthesis even during peak translation of viral proteins.

MATERIALS AND METHODS

Cells and virus.

Baby hamster kidney-21/WI2 cells (hereafter referred to as BHK cells) were grown at 37^{o} C with 5% CO_2 in Eagle's minimum essential media (MEM) containing 4.5% heat-inactivated fetal bovine serum (FBS) and 10 μg/ml gentamicin (Vaheri et al., 1965). C6/36 cells were grown at 27^{o}C in Eagle's MEM containing 10% FBS, 0.1 mM non-essential amino acids and 10 μg/ml of gentamicin. WNV strain Eg101 (2 x 10^8 PFU/ml) was prepared in BHK cells as described previously (Scherbik et al., 2006). Dengue virus 2 (Den 2), strain Bangkok, was provided by Walter Brandt

(Walter Reed Army Institute of Research, Washington DC) in a 10% W/V suckling mouse brain homogenate with a titer of 2 x 10^6 PFU/ml.

Preparation of S100 cell extracts.

Cells were grown to confluency in T150 tissue culture flasks, washed with ice-cold phosphate buffered saline (PBS), harvested by scraping and pelleted by centrifugation at 150 X g. The cells were resuspended in hypotonic cell lysis buffer [10 mM HEPES (pH 7.9), 5 mM DTT, 20% glycerol, 10 mM NaCl, 0.1 mM phenylmethylsulfonyl fluoride (PMSF), 10 μg/ml leupeptin] vortexed for 30 sec, kept on ice for 10 min and then lysed by the addition of 1% Triton X-100 (Sigma, St. Louis, MO.). The nuclei were removed by centrifugation at 2000 x g. The resulting supernatant was adjusted to 14 mM HEPES (pH 7.5), 1 mM EDTA, 6 mM Tris-Cl (pH 7.5), 1 mM $MgCl_2$, 1 mM DTT, 5 mM NaCl, 60 mM KCl, and 50% glycerol, clarified by centrifugation at 100,000 x g for 15 minutes and stored at –20^{o}C. The total protein concentration of the S100-supernatant was approximately 1 μg/μl.

Purification of eEF1A.

eEF1A was purified from BHK cell extracts by ammonium sulfate precipitation and fractionated on a MonoS HR5/5 column (Amersham Pharmacia Biotech, Piscataway, NJ.) as previously described (Blackwell and Brinton, 1997). eEF1A cDNA amplified by RT-PCR from BHK cells was cloned into the T7 expression vector pCR T7/CT-TOPO (Invitrogen, Carlsbad, CA.) (Smith, Blackwell, and Brinton, unpublished data). Recombinant eEF1A was expressed in Origami cells (Novagen, Madison, WI.) Protein expression was induced with 1 mM IPTG and cells

were harvested after 4 hr. The cell pellet was resuspended in Extraction buffer (50 mM sodium phosphate, 300 mM NaCl, pH 7.6) and lysed with a French pressure cell press (SIM-AMINCO Spectronic Instrument Inc., Rochester, NY.). The cell lysate was centrifuged at 3000 x g to pellet cell debris. Recombinant protein was bound to Talon metal affinity resin (BD Biosciences Clontech, Palo Alto, CA.) that was then applied to a 2 ml Talon disposable gravity column (Clontech). The column was washed with Wash buffer (50 mM sodium phosphate, 300 mM NaCl, 20 mM imidazole, pH 7.6). Recombinant protein was eluted with Elution buffer (50 mM sodium phosphate, 300 mM NaCl, 300 mM imidazole, pH 7.6), dialyzed against two liters of dialysis buffer (50 mM sodium phosphate, 50 mM NaCl, pH 7.6) in a Slide-A-Lyzer dialysis cassette (Pierce, Rockford, IL.) to remove imidazole and concentrated to 200-400 ng/μl using a Centricon 10 concentrator (Amicon, Beverly, MA.).

DNA templates for RNA transcription.

The WNV 3' SL template, pWNV(+)3' SL, contained the 3' terminal 111 nt of the WNV Eg101 genome RNA cloned into pCR1000 (Invitrogen) and its construction was described previously (Blackwell and Brinton, 1995). The plasmids described above were used to generate PCR templates that contained a T7 promoter for RNA transcription as described previously (Blackwell and Brinton, 1995). The primers used are available upon request. PCR products were purified using the Qiagen PCR clean up kit (Qiagen, Valencia, CA).

RNA transcripts.

The PCR products described above were used as templates for transcription of WNV 3'(+) SL RNAs done in the presence of (α-^{32}P) GTP using T7 RNA polymerase (50 U) according to the manufacturer's protocol (Ambion, Austin, TX.) for 1 hr at 37^{o} C. Transcription reactions were stopped by the addition of DNase (1 U) for 15 minutes at 37^{o} C, and the RNA was gel purified and precipitated with ethanol as described previously (D'Alessio, 1982). The purified RNAs were resuspended in 100µl of RNase free storage buffer (100 mM sodium phosphate (pH 7.2) 300 mM KCL, 5 mM EDTA, 5 mM DTT, 25% glycerol) or water. Radioactivity was measured using a scintillation counter (Beckman LS6500) and the specific activity (~1.3 x 10^{7} cpm/µg) was calculated as described previously (Blackwell and Brinton, 1997).

Gel mobility shift assays.

Purified recombinant eEF1A was incubated in Gel shift buffer (GS buffer) with a ^{32}P-labeled 3' viral RNA probe (2000 cpm or approximately 0.2 nM final concentration per reaction), poly I-C (50 ng), and RNase inhibitor (Ambion) (10 units) for 30 min at room temperature. The RNA-protein complexes were resolved by nondenaturing 5% polyacrylamide gel electrophoresis (PAGE) in 1X TBE buffer. The percent RNA bound was quantified with a Fuji BAS 1800 analyzer (Fuji Photo Film Co., Japan) and Image Gauge software (Science Lab, 98, version 3.12, Fuji Photo Film Co.). Analysis of UV-induced cross-linked RNA-protein complexes was performed as described previously (Blackwell and Brinton, 1997).

Mutagenesis of a WNV infectious clone.

The construction and characteristics of the chimeric full length WNV infectious clone were previously described (Yamshchikov, 2001). An extra A was inserted at nt position 11,019. This addition did not affect viral growth, but stabilized the plasmid in *E. coli.* Infectious clone DNA was amplified in TOP10 cells (Invitrogen) and purified using a plasmid miniprep kit (Qiagen). The strategy used to introduce mutations in the 3' SL was described previously (Elghonemy, Davis, and Brinton, 2005). Primer sequences used to generate the mutant viral cDNAs are available upon request. All mutations made to the infectious clone DNA were confirmed by sequencing.

***In vitro* transcription of WNV genomic RNA.**

Parental or mutant infectious clone plasmid DNA was linearized at the 3' end of the WNV cDNA with the restriction enzyme Xba I and then purified using a PCR cleanup kit (Qiagen). The *in vitro* transcription of capped RNA was performed using the Message Maker SP6 Transcription kit (Epicentre, Madison, WI) according to the manufacturer's protocol. RNase-free DNase was then added and the reaction mixture was incubated at 37^{o} C for 30 min. DNase was heat-inactivated at 65^{o}C for 15 min and the reaction mixture was used directly for transfection of BHK cells.

Transfection of WNV genomic RNA into BHK cells.

RNA transfection was performed as described previously (Elghonemy, Davis, and Brinton, 2005). Briefly, genomic RNA was transfected into BHK cells in 6-well dishes with DMRIE-C according to the manufacturer's protocol (Invitrogen). After a

2 hr incubation at 37^{o}C, the transfection media was removed and the cells were overlayed with either 2 ml of 5% FCS MEM or a 1:1 mixture of 1% agarose and 2X MEM containing 5% FBS. At 72 hr after transfection, the agarose was removed and plaques were visualized using a methyl violet stain (10% ethanol, 0.5% methyl violet). Alternatively, when plaques were to be picked, the initial overlay was not removed and a second overlay of 0.05% neutral red solution, 0.5% agarose in 1X MEM was added and plaques were visible 8 hr later. Virus in media harvested from duplicate wells was titrated by plaque assay on BHK cells.

Viral growth curves.

Growth curves were performed as described previously (Elghonemy, Davis, and Brinton, 2005). Briefly, duplicate confluent BHK or C6/36 monolayers in T25 flasks were infected at a multiplicity of infection (MOI) of 0.1. Aliquots of culture fluid were taken at 0, 10, 22, 29 and 48 hr after infection of BHK cells and at 0, 10, 22, 29, 48, and 72 hr after infection of C6/36 cells and stored at -80^{o}C until titrated by plaque assay.

Analysis of virus revertant.

Revertant virus was first plaque purified and then viral RNA was extracted and purified using TRI Reagent LS (Molecular Research Center, Inc., Cincinnati, OH.) according to the manufacturer's protocol. A cDNA copy of the desired region of the revertant virus was amplified by RT-PCR and cloned into pTOPO-TA 2.1 (Invitrogen). Ten clones for each revertant virus were checked by DNA sequencing.

Analysis of intracellular viral RNA by real-time RT-PCR.

Full-length genomic RNAs were generated as described above. Replicate BHK monolayers in 6-well tissue culture plates (80% confluency) were washed once with 2 ml of Opti-MEM (Invitrogen) and then transfected with 200 ng of RNA in DMRIE-C (Invitrogen). At the indicated times after transfection, each well was washed 3 times with 5 ml of growth media and total RNA within the cell was extracted using TRI Reagent (Molecular Research Center, Inc.). The relative amount of intracellular viral genomic RNA was determined by real-time RT-PCR on an Applied Biosystems 7500 real-time PCR system using 200 ng of total RNA, and the TaqMan one-step RT-PCR kit according to the manufacturer's protocol (Applied Biosystem). The NS1 region primers used were 5'GGCGGTTCTAGGAGAAGTCA-3'and 5'-CTCCTGTTGTGGTTGCTTCT-3' and the FRET probe was 5' Fam-TGCACCTGGCCAGAAACCCACACTCTGT3' TAMRA.

For specific detection of minus-strand RNA, T7-tagged primer real-time RT-PCR was performed as previously described (Lanford et al., 1994; Samuel and Diamond, 2005). Briefly, 2 pmol of the minus-strand primer, 5'-**GCGTAATACGACTCACTATA**gagggcggttctaggagaagt-3', [T7 tag sequence (the uppercase, bold); NS1 sequence (lower case, non-bold)] was incubated with 800 ng of total RNA in a Taqman one-step RT-PCR reaction mixture and incubated at 50^{o}C for 30 min and then at 95^{o}C for 30 min to inactivate the reverse transcriptase. Then, 20 pmol of each of the following primers were added 5'-

GCGTAATACGACTCACTATA-3', 5'-ctcctgttgtggttgcttc-3' and 5 pmol of the probe, 5'Fam-TGCACCTGGCCAGAAACCCACACTCTGT3'-TAMRA, and the PCR reaction was performed as follows: 40 cycles at 95°C for 15 sec and then 60°C for 1 min.

Analysis of all real-time RT-PCR reactions was done using the relative quantification software from Applied Biosystems and the cellular mRNA GAPDH (Applied Biosystems) as the endogenous control. The genomic RNA levels at 48 and 72 hr after transfection were normalized against input RNA present at 6 hr after transfection to remove background. Levels of minus strand RNA at 12, 24 and 48 hr after transfection were also normalized to viral RNA levels present at 2 hr after transfection to remove nonspecific amplification of genomic strand RNA

Confocal Microscopy.

BHK cells grown to 60% confluency on 15 mm glass coverslips were either transfected with 1 μg of viral RNA as described above or infected with WNV or Den 2 at an MOI of 0.1. The cells were fixed by incubation with 4% paraformaldehyde in PBS for 10 min at room temperature and then permeabilized at the indicated times with methanol at -20°C for 10 min. Coverslips were washed with PBS and then blocked overnight with 5% horse serum (Invitrogen) in PBS. Primary antibodies used were: mouse hyper-immune ascitic fluid (MHIAF) against WNV (a gift from Dr. Robert Tesh, UTMB, Galveston, TX) at a 1:100 dilution, rabbit anti-WNV NS3/NS5 made to gel-purified viral proteins as described previously (21) at a 1:50 dilution, a mouse anti-dsRNA antibody (English and Scientific Consulting, Szirak, Hungary) at

a 1:200 dilution and a goat anti-eEF1A antibody (Santa Cruz Biotechnology, Santa Cruz, CA.) at a 1:200 dilution in the NS3/NS5 colocalization experiments or a 1:700 dilution in the dsRNA colocalization experiments. Coverslips were incubated with primary antibody in PBS with 5% horse serum for 1 hr at 37^{o}C and then washed 4 times with PBS. Coverslips were next incubated with the appropriate secondary antibody (chicken anti-rabbit IgG-TR, chicken anti-mouse IgG-TR, or donkey anti-goat IgG FITC, Santa Cruz Biotechnology) in PBS with 5% horse serum at a 1:300 dilution and Hoechst Dye to stain the nuclei. After washing with PBS, the coverslips were mounted on glass slides with Prolong mounting media (Invitrogen) and visualized with a 100 X oil immersion objective on a LSM 510 laser confocal microscope using LSM 5 (Ver. 3.2) software (Carl Zeiss Inc., Thornwood, NY). Relative fluorescence intensity was measured in 7 μm diameter circles in 3 locations in the cytoplasm of 10 representative transfected BHK cells for each viral RNA using LSM 5 (3.2) software. Images compared for each experimental series were collected using the same instrument settings.

Mutagenesis of a NY99 WNV replicon.

The construction and characterization of the luciferase-reporting replicon, RlucRep, was reported previously (Lo et al., 2003). A mutant RlucRep containing a 4-nt 5'-UGUG-3' substitution in the major binding site for eEF1A was constructed by swapping the parental 3' cDNA fragment located between the unique Mlu I (nt 10,436) and Xba I (3' terminus of the genomic cDNA) restriction sites with the PCR fragment containing the substitution. The PCR fragment containing the 4-nt change

was prepared via standard overlapping PCR. The cDNA clone of mutant RlucRep was verified by DNA sequencing. Conditions used for *in vitro* transcription, and transfection of replicon RNA, as well as for the luciferase reporter assays were as previously described (Shi et al., 2002)

Co-immunoprecipitation and Western blotting.

Confluent monolayers of BHK cells in 6 well tissue culture plates were mock-infected or infected with WNV (MOI of 5) for 24 hr. Cells were washed twice with 2 ml of PBS, scraped, pelleted at 700 x G and resuspended in Cell Lysis buffer [50 mM sodium-phosphate (pH 7.2), 150 mM NaCl, 10 mM DTT, 1% NP-40, and complete mini protease inhibitor (Roche)] at a concentration of 2.5 x 10^6 cells/ml. Cells were incubated on ice for 30 min and then sonicated 4 x 5 sec using a Branson Sonifier 450 (Danbury, CT). Cell debris was removed by centrifugation at 2000 x G for 5 min. The total protein concentration was approximately 200 ng/μl. Infected and mock-infected cell lysates (200 μl) were precleared by incubation with protein A/G magnetic beads (New England Biolabs) at 4^o C for 1 hr. The beads were then removed by applying a magnetic field and the cleared supernatant was used for subsequent experiments. Cleared supernatant was incubated for 1 hr at 4^oC with 2 μg of antibody against one the following cellular proteins, eEF1A (Santa Cruz), HSP105 (Santa Cruz), or NFAR-1 or NFAR-2 (a gift from Sven-Erik Behrens, Fox Chase Cancer Center, Philadelphia, PA). Fresh protein A/G magnetic beads (25 μl) were then added and incubated at 4^oC for 1 hr. Recovered beads were washed 7 times with 1 ml of Cell Lysis buffer, resuspended in 50 ml of 2X SDS loading buffer (0.5 M Tris-HCl, 20%

glycerol, 4% SDS, 2% mercaptoethanol, 0.5% bromophenol blue) and incubated at 70^{o}C for 5 min. Beads were removed with a magnetic field and the sample was separated by 10% SDS-PAGE. The separated proteins were then electrophoretically transferred to a nitrocellulose membrane. The membrane was blocked at 4^{o}C overnight with TBS [50 mM Tris (pH 7.6), 150 mM NaCl**]** containing 5% milk and 0.1% Tween 20 and then incubated with a rabbit polyclonal anti-NS3/NS5 antibody for 1 hr at room temperature or anti-WNV MHIAF. The blots were then washed with TBS and incubated with the secondary antibody (horseradish peroxidase-conjugated anti-rabbit or horseradish peroxidase conjugated anti-mouse (Santa Cruz) for 1 hr at room temperature. The washed blots were processed for enhanced chemiluminescence using the Super-Signal West Pico detection kit (Pierce, Rockford, Il) according to the manufacturer ' s instructions and exposed to film.

Computer analysis of predicted RNA secondary structure.

The predicted secondary structures of the terminal SL RNAs shown were analyzed by minimization of free energy using the M-Fold program (Zuker, 2003).

REFERENCES

Beckman, M. T., and Kirkegaard, K. (1998). Site size of cooperative single-stranded RNA binding by poliovirus RNA-dependent RNA polymerase. *J Biol Chem* **273**(12)**,** 6724-30.

Blackwell, J. L., and Brinton, M. A. (1995). BHK cell proteins that bind to the 3' stem-loop structure of the West Nile virus genome RNA. *J Virol* **69**(9)**,** 5650-8.

Blackwell, J. L., and Brinton, M. A. (1997). Translation elongation factor-1 alpha interacts with the 3' stem-loop region of West Nile virus genomic RNA. *J Virol* **71**(9)**,** 6433-44.

Blumenthal, T., and Carmichael, G. G. (1979). RNA replication: function and structure of Qbeta-replicase. *Annu Rev Biochem* **48,** 525-48.

Bredenbeek, P. J., Kooi, E. A., Lindenbach, B., Huijkman, N., Rice, C. M., and Spaan, W. J. (2003). A stable full-length yellow fever virus cDNA clone and the role of conserved RNA elements in flavivirus replication. *J Gen Virol* **84**(Pt 5)**,** 1261-8.

Brinton, M. A., Fernandez, A. V., and Dispoto, J. H. (1986). The 3'-nucleotides of flavivirus genomic RNA form a conserved secondary structure. *Virology* **153**(1)**,** 113-21.

Brown, D., and Gold, L. (1996). RNA replication by Qβ replicase: A working model. *Proc. Natl. Acad. Sci. USA* **93,** 11558-11562.

Browning, K. S., Humphreys, J., Hobbs, W., Smith, G. B., and Ravel, J. M. (1990). Determination of the amounts of the protein synthesis initiation and elongation factors in wheat germ. *J Biol Chem* **265**(29)**,** 17967-73.

Chen, C. J., Kuo, M. D., Chien, L. J., Hsu, S. L., Wang, Y. M., and Lin, J. H. (1997). RNA-protein interactions: involvement of NS3, NS5, and 3' noncoding regions of Japanese encephalitis virus genomic RNA. *J Virol* **71**(5)**,** 3466-73.

Cimarelli, A., and Luban, J. (1999). Translation elongation factor 1-alpha interacts specifically with the human immunodeficiency virus type 1 Gag polyprotein. *Journal of Virology* **73,** 5388-5401.

Cleaves, G. R., Ryan, T. E., and Schlesinger, R. W. (1981). Identification and characterization of type 2 dengue virus replicative intermediate and replicative form RNAs. *Virology* **111**(1)**,** 73-83.

Condeelis, J. (1995). Elongation factor 1 alpha, translation and the cytoskeleton. *Trends Biochem Sci* **20**(5)**,** 169-70.

Cui, T., Sugrue, R. J., Xu, Q., Lee, A. K., Chan, Y. C., and Fu, J. (1998). Recombinant dengue virus type 1 NS3 protein exhibits specific viral RNA binding and NTPase activity regulated by the NS5 protein. *Virology* **246**(2)**,** 409-17.

D'Alessio, J. A. (1982). "RNA sequencing." Gel electroporesis of nucleic acids (D. R. a. B. D. James, Ed.) IRL Press, Oxford.

Ejiri, S. (2002). Moonlighting Functions of Polypeptide Elongation factor 1: From Actin Bundling to Zinc Finger Protein R1-Associated Nuclear Localization. *Biosciences, Biotechnology, and Biochemistry* **66,** 1-21.

Elghonemy, S., Davis, W. G., and Brinton, M. A. (2005). The majority of the nucleotides in the top loop of the genomic 3' terminal stem loop structure are cis-acting in a West Nile virus infectious clone. *Virology* **331**(2)**,** 238-246.

Filomatori, C. V., Lodeiro, M. F., Alvarez, D. E., Samsa, M. M., Pietrasanta, L., and Gamarnik, A. V. (2006). A 5' RNA element promotes dengue virus RNA synthesis on a circular genome. *Genes Dev* **20**(16)**,** 2238-49.

Gonen, H., Dickman, D.,Schwartz, A.L. and Ciechanover, A. (1996). Protein synthesis elongation factor EF-1α is an isopeptidase essential for ubiquitin-dependent degradation of certain proteolytic substrates. *Adv. Exp. Med. Biol* **389,** 209-219.

Gonen, H., Smith, C.E., Siegel, N.R., Kahana, C., Merrick, W.C., Chakraburtty, K., Schwartz, A.L. and Ciechanover, A. (1994). Protein synthesis elongation factor factor EF-1α is essential for ubiquitin-dependent degredation of certain Na-acetylated proteins and may be substituted for by the bacterial elongation factor EF-Tu. *Proceedings from the National Academy of Sciences USA* **91,** 7648-7652.

Grun, J. B., and Brinton, M. A. (1988). Separation of functional West Nile virus replication complexes from intracellular membrane fragments. *J Gen Virol* **69 (Pt 12),** 3121-7.

Hahn, C. S., Hahn, Y. S., Rice, C. M., Lee, E., Dalgarno, L., Strauss, E. G., and Strauss, J. H. (1987). Conserved elements in the 3' untranslated region of flavivirus RNAs and potential cyclization sequences. *J Mol Biol* **198**(1)**,** 33-41.

Isken, O., Grassmann, C. W., Sarisky, R. T., Kann, M., Zhang, S., Grosse, F., Kao, P. N., and Behrens, S. E. (2003). Members of the NF90/NFAR protein group are involved in the life cycle of a positive-strand RNA virus. *Embo J* **22**(21)**,** 5655-65.

Johnson, C. M., Perz, D.R., French, R., Merrick, W.C., and Donis, R.O. (2001). The NS5A protein of bovine viral diarrhoea virus interacts with the a subunit of translation elongation factor-1. *Journal of General Virology* **82,** 2935-2943.

Kita, H., Cho, J., Matsuura, T., Nakaishi, T., Taniguchi, I., Ichikawa, T., Shima, Y., Urabe, I., and Yomo, T. (2006). Functional Qbeta replicase genetically fusing essential subunits EF-Ts and EF-Tu with beta-subunit. *J Biosci Bioeng* **101**(5)**,** 421-6.

Kou, Y. H., Chou, S. M., Wang, Y. M., Chang, Y. T., Huang, S. Y., Jung, M. Y., Huang, Y. H., Chen, M. R., Chang, M. F., and Chang, S. C. (2006). Hepatitis C virus NS4A inhibits cap-dependent and the viral IRES-mediated translation through interacting with eukaryotic elongation factor 1A. *J Biomed Sci*.

Lanford, R. E., Sureau, C., Jacob, J. R., White, R., and Fuerst, T. R. (1994). Demonstration of in vitro infection of chimpanzee hepatocytes with hepatitis C virus using strand-specific RT/PCR. *Virology* **202**(2)**,** 606-14.

Li, W., and Brinton, M. A. (2001). The 3' stem loop of the West Nile virus genomic RNA can suppress translation of chimeric mRNAs. *Virology* **287**(1)**,** 49-61.

Lo, M. K., Tilgner, M., Bernard, K. A., and Shi, P. Y. (2003). Functional analysis of mosquito-borne flavivirus conserved sequence elements within 3' untranslated region of West Nile virus by use of a reporting replicon that differentiates between viral translation and RNA replication. *J Virol* **77**(18)**,** 10004-14.

Lohmann, V., Roos, A., Korner, F., Koch, J. O., and Bartenschlager, R. (1998). Biochemical and kinetic analyses of NS5B RNA-dependent RNA polymerase of the hepatitis C virus. *Virology* **249**(1)**,** 108-18.

Lui, G., Tang, J., Edmonds, B.T., Murray, J., Levin, S., and Condeelis, J. (1996). F-actin Sequesters Elangation Factor 1α from Interaction with Aminoacyl-tRNA in a pH-dependent Reaction. *The Journal of Cell Biology* **135,** 953-963.

Lui, G. G., W.M., Persky, D., Latham, V.M., Singer, R.H. and Condeelis, J. (2002). Interaction of Elongation Factor 1α with F-Actin and β-Actin mRNA: Implications for Anchoring mRNA in Cell Protrusions. *Molecular Biology of the Cell* **13,** 579-592.

Mackenzie, J. M., Khromykh, A. A., Jones, M. K., and Westaway, E. G. (1998). Subcellular localization and some biochemical properties of the flavivirus Kunjin nonstructural proteins NS2A and NS4A. *Virology* **245**(2)**,** 203-15.

Markoff, L. (2003). 5'- and 3'-noncoding regions in flavivirus RNA. *Adv Virus Res* **59,** 177-228.

Matsuda, D., and T.W. Dreher (2003a). The tRNA-like structure of Turnip yellow mosaic virus RNA is a 3'-translational enhancer. *Virology* **321,** 36-46.

Matsuda, D., S. Yoshinari and T.W. Dreher (2003b). eEF1a binding to aminoacylated viral RNA represses minus strand synthesis by TYMV RNA-dependant RNA polymerase. *Virology* **321,** 47-56.

Mickleburgh, I., Chabanon, H., Nury, D., Fan, K., Burtle, B., Chrzanowska-Lightowlers, Z., and Hesketh, J. (2006). Elongation factor 1alpha binds to the region of the metallothionein-1 mRNA implicated in perinuclear localization--importance of an internal stem-loop. *Rna* **12**(7)**,** 1397-407.

Miller, S., Sparacio, S., and Bartenschlager, R. (2006). Subcellular localization and membrane topology of the Dengue virus type 2 Non-structural protein 4B. *J Biol Chem* **281**(13)**,** 8854-63.

Miranda, G., Schuppli, D., Barrera, I., Hausherr, C., Sogo, J., and Weber, H. (1997). Recognition of bacteriophage Qb replicase: role of RNA interactions mediated by ribosomal proteins S1 and host factor. *Journal of Molecular Biology* **267,** 1089-1103.

Olsthoorn, R. C., and Bol, J. F. (2001). Sequence comparison and secondary structure analysis of the 3' noncoding region of flavivirus genomes reveals multiple pseudoknots. *Rna* **7**(10)**,** 1370-7.

Petersen, L. R., Marfin, A. A., and Gubler, D. J. (2003). West Nile virus. *Jama* **290**(4)**,** 524-8.

Qanungo, K. R., D. Shaji, M. Mathur, and A.K. Banerjee (2004). Two RNA polymerase complexes from vesicular stomatitis virus-infected cells that carry out transcription and replication of genome RNA. *Proceedings from the National Academy of Sciences USA* **101,** 5952-5957.

Riis, B., Rattan, S. I., Clark, B. F., and Merrick, W. C. (1990). Eukaryotic protein elongation factors. *Trends Biochem Sci* **15**(11)**,** 420-4.

Samuel, M. A., and Diamond, M. S. (2005). Alpha/beta interferon protects against lethal West Nile virus infection by restricting cellular tropism and enhancing neuronal survival. *J Virol* **79**(21)**,** 13350-61.

Scherbik, S. V., Paranjape, J. M., Stockman, B. M., Silverman, R. H., and Brinton, M. A. (2006). RNase L plays a role in the antiviral response to West Nile virus. *J Virol* **80**(6)**,** 2987-99.

Schuppli, D., Geogijevic, J., and Weber, H. (2000). Synergism of mutations in the bacteriophage Qb RNA affecting host factor dependence of Qb replicase. *Journal of Molecular Biology* **295,** 149-154.

Schuppli, D., Miranda, G., Qiu, S., and Weber, H (1998). A branched stem-loop structure in the M-site of bacteriophage Qb RNA is important for template recognition by Qb replicase holoenzyme. *Journal of Molecular Biology* **283,** 585-593.

Shi, P. Y., Brinton, M. A., Veal, J. M., Zhong, Y. Y., and Wilson, W. D. (1996). Evidence for the existence of a pseudoknot structure at the 3' terminus of the flavivirus genomic RNA. *Biochemistry* **35**(13)**,** 4222-30.

Shi, P. Y., Tilgner, M., Lo, M. K., Kent, K. A., and Bernard, K. A. (2002). Infectious cDNA clone of the epidemic west nile virus from New York City. *J Virol* **76**(12)**,** 5847-56.

Shiina, N., Gotoh, y., Kubomura, N., Iwamatsu, A., and Nishida, E. (1994). Microtubule severingby elongation factor 1a. *Science* **266,** 282-285.

Tilgner, M., Deas, T. S., and Shi, P. Y. (2005). The flavivirus-conserved penta-nucleotide in the 3' stem-loop of the West Nile virus genome requires a specific sequence and structure for RNA synthesis, but not for viral translation. *Virology* **331**(2)**,** 375-86.

Vaheri, A., Sedwick, W. D., Plotkin, S. A., and Maes, R. (1965). Cytopathic effect of rubella virus in RHK21 cells and growth to high titers in suspension culture. *Virology* **27**(2)**,** 239-41.

Wallner, G., Mandl, C. W., Kunz, C., and Heinz, F. X. (1995). The flavivirus 3'-noncoding region: extensive size heterogeneity independent of evolutionary relationships among strains of tick-borne encephalitis virus. *Virology* **213**(1)**,** 169-78.

Weaver, S. C., and Barrett, A. D. (2004). Transmission cycles, host range, evolution and emergence of arboviral disease. *Nat Rev Microbiol* **2**(10)**,** 789-801.

Weeks, K. M., and Crothers, D. M. (1991). RNA recognition by Tat-derived peptides: interaction in the major groove? *Cell* **66**(3)**,** 577-88.

Wengler, G., and Castle, E. (1986). Analysis of structural properties which possibly are characteristic for the 3'-terminal sequence of the genome RNA of flaviviruses. *J Gen Virol* **67 (Pt 6),** 1183-8.

Westaway, E. G., Mackenzie, J. M., Kenney, M. T., Jones, M. K., and Khromykh, A. A. (1997). Ultrastructure of Kunjin virus-infected cells: colocalization of NS1 and NS3 with double-stranded RNA, and of NS2B with NS3, in virus-induced membrane structures. *J Virol* **71**(9)**,** 6650-61.

Yamaji, Y., Kobayashi, T., Hamada, K., Sakurai, K., Yoshii, A., Suzuki, M., Namba, S., and Hibi, T. (2006). In vivo interaction between Tobacco mosaic virus RNA-dependent RNA polymerase and host translation elongation factor 1A. *Virology* **347**(1)**,** 100-8.

Yamshchikov, V. F., G. Wengler, A.A. Perelygin, M.A. Brinton, and R.W. Compans (2001). An infectious clone of the West Nile flavivirus. *Virology* **281**(2)**,** 294-304.

Yu, L., and Markoff, L. (2005). The topology of bulges in the long stem of the flavivirus 3' stem-loop is a major determinant of RNA replication competence. *J Virol* **79**(4)**,** 2309-24.

Zhou, Y., Ray, D., Zhao, Y., Dong, H., Ren, S., Li, Z., Guo, Y., Bernard, K. A., Shi, P. Y., and Li, H. (2007). Structure and Function of Flavivirus NS5 Methyltransferase. *J Virol*.

Zuker, M. (2003). Mfold web server for nucleic acid folding and hybridization prediction. *Nucleic Acids Res* **31**(13)**,** 3406-15.

CHAPTER III

Mutagenesis of a Minor eEF1A binding Site on the West Nile Virus 3' (+) SL RNA

INTRODUCTION

West Nile virus (WNV) is a member of the family *Flaviviradae*, the genus *flavivirus* and the Japanese encephalitis serogroup. WNV is endemic to Asia and Africa and since 1999, also to North Amercia. WNV is maintained in a mosquito-bird-mosquito cycle in nature with mammals, including humans, as incidental hosts. WNV infections in humans are usually asymptomatic with about 20% of infected individuals developing a mild febrile illness, but in less than 1% of all cases, infection results in severe central nervous system disease that in rare instances can be fatal (Petersen, Marfin, and Gubler, 2003; Weaver and Barrett, 2004).

The single-stranded, positive sense WNV genomic RNA is 11,021 nts in length and contains a single open reading frame, which encodes a polyprotein that is cleaved by host and viral proteases into 3 structural and 7 nonstructural viral proteins. The 3' terminus of the flavivirus genomic RNA is predicted to contain promoter elements important for the synthesis of the viral minus strand RNA, since deletion or mutation of this region was previously shown to be lethal for virus replication (Bredenbeek et al., 2003; Elghonemy, Davis, and Brinton, 2005; Lo et al., 2003; Tilgner, Deas, and Shi, 2005; Tilgner and Shi, 2004; Yu and Markoff, 2005). The open reading frame is flanked by a 96 nt 5' noncoding region and a 632 nt 3'

noncoding region. The 3' terminal 96 nts of the WNV genomic RNA are predicted to form two stem loop (SL) stuctures, a short SL (SSL) of 16 nts and a longer terminal SL of 80 nts. These two structures will be referred to collectively as the WNV 3' (+) SL RNA and are predicted to be conserved among divergent flaviviruses (Brinton, Fernandez, and Dispoto, 1986; Hahn et al., 1987; Shi et al., 1996). Previously, three cellular proteins with molecular masses of 105, 84 and 52 kDa were reported to bind specifically to the WNV 3' (+) SL RNA. The 52 kDa protein was subsequently identified as eEF1A (Blackwell and Brinton, 1997). The dissociation constant (kD) for the interaction between eEF1A and the WNV 3' SL RNA is 10^{-9} M and is similar to that of the interaction between eEF1A and charged tRNAs (Blackwell and Brinton, 1997; Riis et al., 1990). One major and two minor eEF1A binding sites were previously mapped on the WNV 3' (+) SL RNA (Blackwell and Brinton, 1997). The major binding site is located on the 5' side in the middle of the terminal SL and accounts for 60% of the binding activity. One minor binding site was mapped to the pentanucleotide sequence, which is conserved among the divergent flaviviruses and located in the top left loop of the 3' terminal SL and the other is in the SSL (Blackwell and Brinton, 1997; Elghonemy, Davis, and Brinton, 2005; Tilgner, Deas, and Shi, 2005). Each minor binding site accounted for 20% of the *in vitro* binding activity of eEF1A for the WNV 3' (+) SL RNA.

The SSL consists of a 5 base pair stem and a 6 nt loop. The majority of the nts of this loop are conserved among divergent mosquito borne flaviviruses, the consensus sequence is (5' GA(U/A)AGA 3') (Olsthoorn and Bol, 2001; Shi et al.,

1996). This hexanucleotide loop resembles a GN_NRA tetra loop-like motif (R-purine and N-any nt). GN_NRA motifs have shown to be involved in both RNA-RNA and RNA-protein interactions (Abramovitz and Pyle, 1997; Gutell, Larsen, and Woese, 1994). A GN_NRA tetra loop was identified in the Sarcin/Ricin Loop (SRL) of ribosomal RNA which was previously reported to be a binding site for eEF1A (Szewczak et al., 1993). GN_NRA motifs have been shown to form RNA-RNA tertiary interactions in group I and group II self-splicing enzymes (Costa and Michel, 1995). A previous *in vitro* study of a truncated WNV model RNA predicted that the SSL loop nts at positions 86-89 counting from the 3' end of the RNA genome (3'AGAU 5') formed a tertiary interaction with nts 71-74 (3'UCUG 5') in the stem of the 3' terminal SL (Shi et al., 1996).

eEF1A, second only to actin in abundance in the cell, constitutes 1-4% of the total soluble protein in an actively dividing cell. During protein synthesis, eEF1A delivers aminoacylated tRNAs (aa-tRNA) along with GTP to the A site of the ribosome. The eEF1A:GTP:aa-tRNA complex then moves to the P site and after the hydrolysis of GTP to GDP, the eEF1A:GDP complex is released from the ribosome. eEF1A has also been shown to bind to mRNA (Lui, 2002; Mickleburgh et al., 2006), to bind to and bundle actin filaments (Ejiri, 2002; Lui, 1996; Lui, 2002), to sever microtubules (Shiina, 1994), and to mediate protein degradation via ubiquitin-dependant pathways (Gonen, 1996; Gonen, 1994).

For the positive-strand RNA bacteriophage, Qβ, the bacterial homolog of eEF1A functions as part of the viral replicase holoenzyme and for the negative-strand

RNA virus, vesicular stomatitis virus (VSV), eEF1A was shown to be a component of the viral replicase complex and required for activity of this complex *in vitro* (Blumenthal and Carmichael, 1979; Brown, 1996; Miranda, 1997; Qanungo, 2004; Schuppli, 2000; Schuppli, 1998). eEF1A was also shown to interact with viral nonstructural proteins of two members of the family *Flaviviridae*, bovine viral diarrhea virus (NS5A) and hepatitis C virus (NS4A), and also with the Gag polyprotein of HIV type I (Cimarelli, 1999; Johnson, 2001; Kou et al., 2006).

eEF1A was reported to bind to the 3' terminal tRNA-like structure (TLS) of the turnip yellow mosaic virus (TYMV) genome, and to act as both a translational enhancer and a repressor of minus strand synthesis (Matsuda, 2003a; Matsuda, 2003b). eEF1A has also been shown to bind to both the 3' TLS and the viral polymerase of another positive strand RNA plant virus, tobacco mosaic virus (TMV) (Yamaji et al., 2006)

The SSL and the region of the 3' terminal SL predicted to form a tertiary interaction with the SSL were mutated in an infectious clone. The results showed that the SSL is *cis*-acting and that two base pairs (U72-A10 and G71-C11) in the stem of the 3' terminal SL that are flanked by two symmetrical one base-pair internal loops are also *cis*-acting. Disruption of the previously predicted tertiary interaction had no affect on viral growth. None of the mutations introduced into the SSL or the 3' terminal SL affected the translational efficiency of the genomic RNA, but many of the mutations reduced the efficiency of minus strand RNA synthesis.

RESULTS

Mutagenesis of a minor binding site for eEF1A.

The WNV SSL was previously reported to be one of two minor binding sites for the cellular translation elongation factor eEF1A and some of the SSL loop nts were predicted to be involved in a putative tertiary interaction with the stem of the 3' terminal SL of the viral genomic RNA (Blackwell and Brinton, 1997; Shi et al., 1996). To determine whether nts in the SSL are *cis*-acting, a WNV infectious clone was used to introduce mutations into the SSL. The mutated WNV cDNAs were *in vitro* transcribed, the RNA produced was used to transfect BHK cell monolayers (either 0.1 μg or 1μg of RNA per well of a 6-well plate), and the effect of mutations on plaque size was assessed. The representative plaque plates shown in the figures were chosen to clearly indicate plaque size and do not indicate the efficiency of mutant virus growth. In Mutant 1, the entire SSL (nts 81-96) was deleted. No plaques were detected 72 hr after transfection of Mutant 1 RNA. Also, no progeny virus was detected by either plaque assay or RT-PCR after three blind passages on BHK cells indicating that this was a lethal mutation for the virus (Fig. 3.1). Next, individual nts in the loop of the SSL were substituted (Fig. 3.1). All mutations made preserved the predicted secondary structure of the WNV 3' (+) SL RNA with the exception of Mutant 9 and Mutant 10, in which nts 86 and 91 were predicted to pair. In Mutant 2, nt 87 was mutated from a G to a C (Fig. 3.1). This mutation was predicted to disrupt the formation of the only G-C base pair in the predicted tertiary interaction (see Fig. 3.1, parental). This mutation was also lethal. Plaques were not detected on the

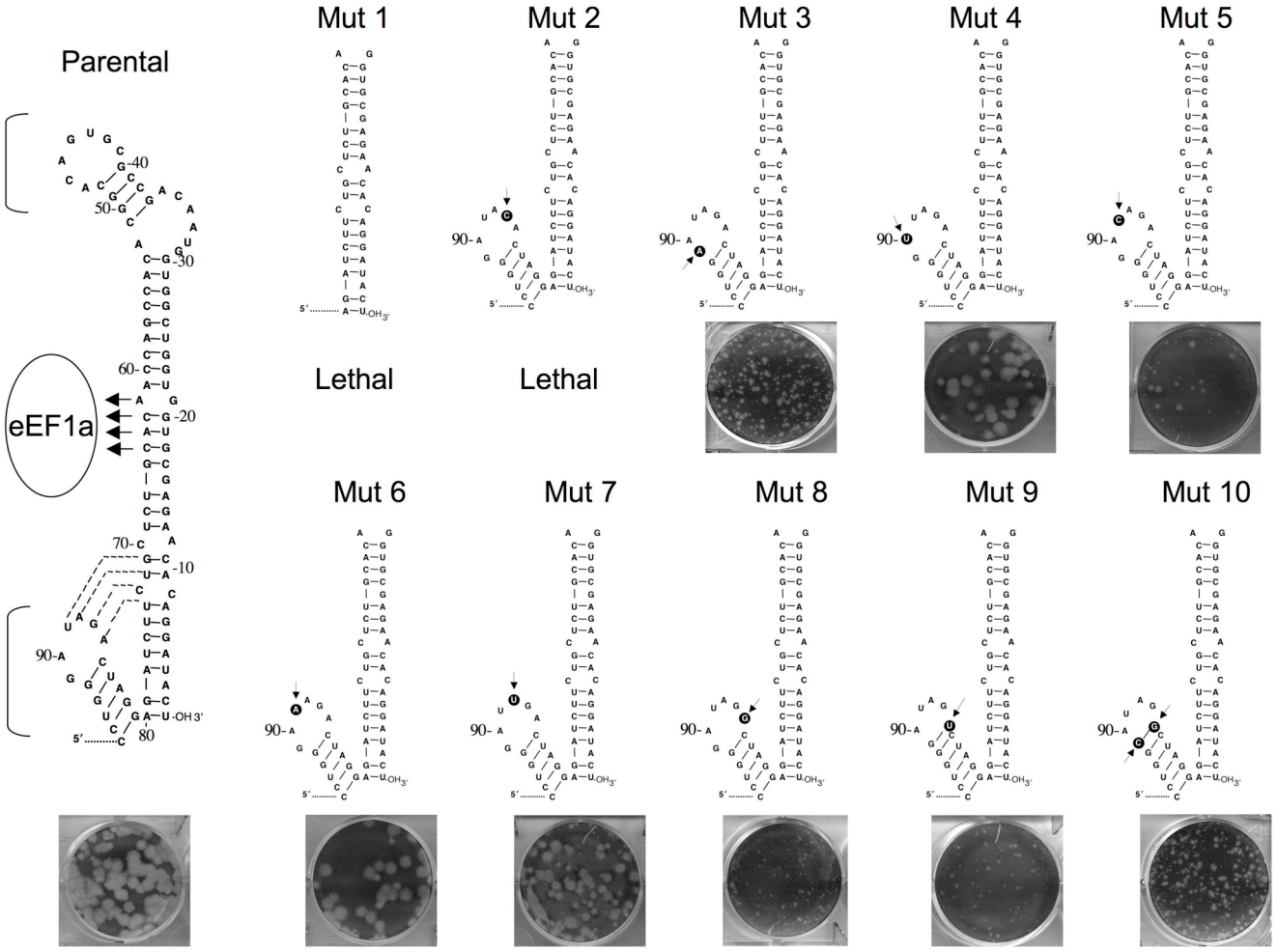

Figure 3.1. Mutagenesis of the WNV SSL.
The minor binding sites for eEF1A on the WNV 3'(+) SL RNA are indicated by brackets. The major binding site is indicated by arrows. Dashed lines show a predicted tertiary interaction between the SSL and the 3' terminal SL. Nt substitutions are indicated with an arrow and a black circle. Plaques formed 72 hr after transfection of either 1μg or 0.1 μg of RNA on a 6-well plate are shown.

transfection plate and no evidence of progeny virus was detected by either plaque assay or RT-PCR following three blind passages on BHK cell monolayers. When G91 was mutated to an A in Mutant 3, small plaques (0.1 mm) were observed on the transfection plate (Fig. 3.1). After a single passage on BHK cells, large parental-size plaques (2-3 mm) were detected. Viral RNA was purified from picked large plaques, amplified by RT-PCR, sequenced, and only the parental sequence was detected. In Mutant 4, A90 was substituted with a U and, parental-sized plaques (2-3 mm) were observed on the transfection plate and the mutated nt did not revert to the parental sequence after 3 passages. When U89 was mutated to a C in Mutant 5, small plaques were observed (Fig. 3.1). After a single passage on BHK cells, large plaques were detected and when these plaques were picked and sequenced, only the parental sequence was obtained. However, when U89 was changed to an A (Mutant 6), parental-size plaques were observed and the nt did not revert to the parental sequence after three passages on BHK cells (Fig. 3.1). The Mutant 6 sequence is characteristic of the 3' RNAs of divergent mosquito borne flaviviruses, such as dengue and yellow fever. In Mutant 7, A88 was changed to a U. While both small and large plaques were observed on the transfection plate (Fig. 3.1), only large plaques were observed after a single passage on BHK cells. Large plaques were picked and sequenced and only the parental sequence was detected. When A86 was mutated to either a G (Mutant 8) or to a U (Mutant 9), small plaques were observed on the transfection plate (Fig. 3.1). Mutant 8 maintained the predicted secondary structure of the loop while in Mutant 9, a G-U base pair was predicted to form between the first and last nts of the loop (Fig.

3.1). After a single passage on BHK cells, both Mutant 8 and Mutant 9 produced parental-sized plaques. These large plaques were picked and sequenced for both Mutant 8 and Mutant 9 and only the parental sequence was detected. To generate Mutant 10, A86 and G91 were changed to a G and a C, respectively. These two nts were predicted to form a G-C base pair (Fig. 3.1). On the transfection plate, small plaques were observed. After a single passage on BHK cells, both small and large plaques were detected. The large plaques were picked and sequenced and the results showed that both the mutated nts had reverted to the parental sequence. Together these data indicate that the SSL is *cis*-acting and that 3 of the 4 loop nts predicted to be involved in the putative tertiary interaction are *cis*-acting.

Mutational analysis of the lower stem of the 3' terminal SL.

As an additional means of testing the biological relevance of the predicted tertiary interaction, mutations were next made to nts in the stem of the 3' terminal SL predicted to be involved in this interaction in the WNV infectious clone. The tertiary interaction was previously reported not to be able to form in *in vitro* studies when the interaction site in the 3' terminal stem was completely base paired (Shi et al., 1996). The C at position 73 from the 3' end of the RNA was predicted to interact with G87 to form the strongest base pair in the predicted tertiary interaction (Fig. 3.2, parental). In Mutants 11, 12 and 13, the C at position 73 was mutated to either a G, an A or was deleted (Fig. 3.2). None of these mutations affected the size of the plaques produced on the transfection plate, and no revertant sequences were detected after three passages on BHK cells. The C at nt position 9 was next mutated to a G (Mutant 14).

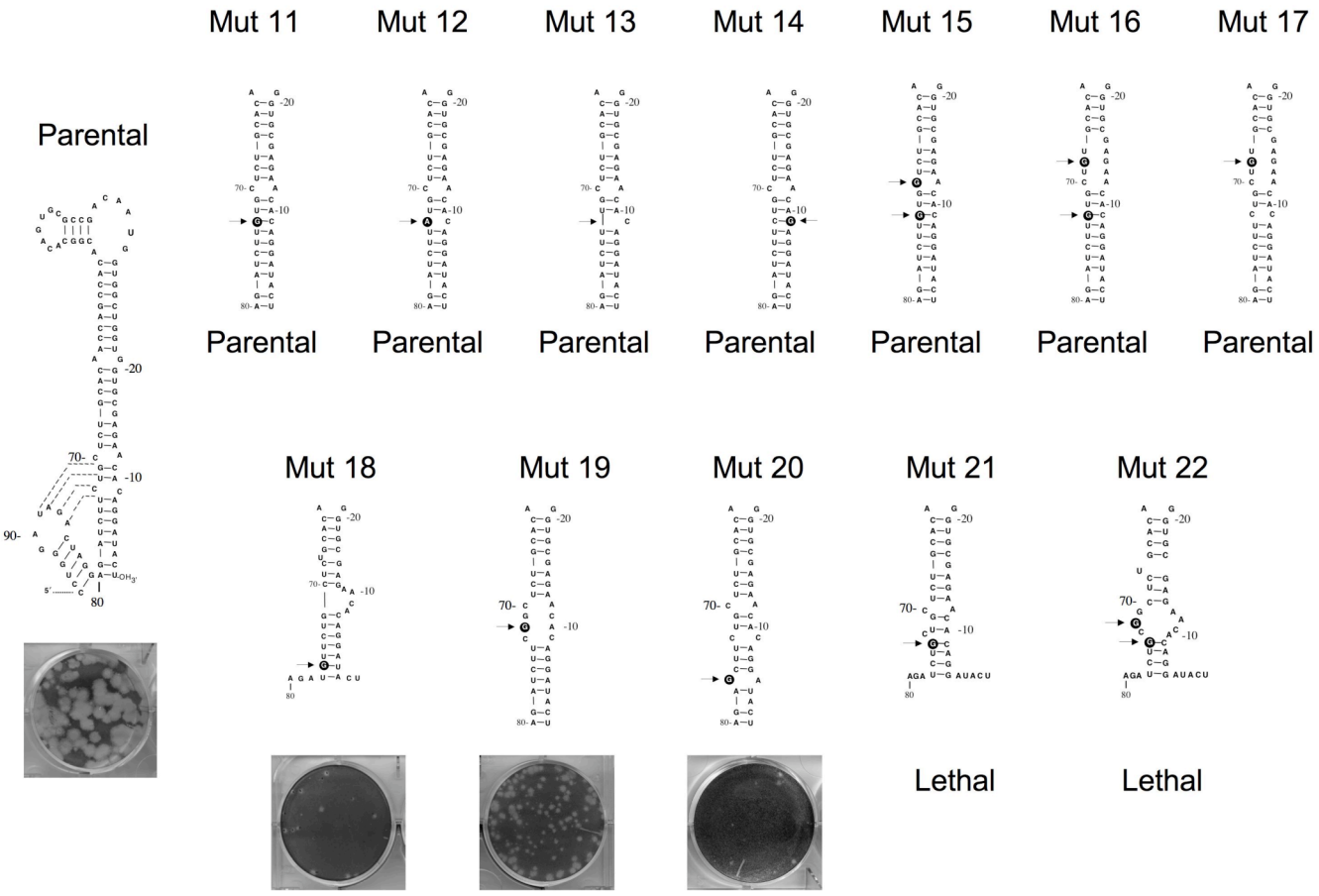

Figure 3.2. Mutagenesis of nts on the 3' side of the WNV terminal SL predicted to be involved in a tertiary interaction.
Dashed lines indicate the predicted tertiary interaction. Nt substitutions are indicated with an arrow and a black circle. Plaques formed 72 hr after transfection of either 1μg or 0.1 μg of RNA on a 6-well plate are shown.

This mutation was predicted to make the putative interaction site on the stem completely double stranded (Fig. 3.2). This mutation produced virus with parental-sized plaques that did not revert after three passages on BHK cells.

Since the C73 and C9 mutations predicted to disrupt the predicted tertiary interaction had no effect on viral growth, the possibility that the tertiary interaction might be able to shift to an alternate location on the stem of the 3' terminal SL in the context of the complete 3' terminal SL was next investigated. C70 or C68 were mutated to Gs in Mutant 11 to generate Mutants 15 and 16, respectively (Fig. 3.2). The mutations in Mutant 16 were predicted to create a large internal loop in the middle of the stem (Fig. 3.2). When only the C at position 68 was changed to a G (Mutant 17), the predicted structural change was the same for Mutant 16 (Fig. 3.2). All of these mutants produced parental-sized plaques that were stable through three passages on BHK cells. In Mutant 18, C76 was substituted with a G. This mutation not only created a large internal bulge on the 3' side of the stem, but also the two 3' terminal nts were predicted to be unpaired and the base pairs on either side of the bulge were different (Fig. 3.2). Small plaques were present on the Mutant 18 transfection plate and after a single passage on BHK cells only large plaques containing the parental sequence were detected. Introduction of the Mutant 18 substitution into a WNV replicon was previously reported to be lethal (Tilgner and Shi, 2004). The results indicate that the tertiary interaction did not shift to an alternate site on the 3' side of the 3' terminal SL.

Mutations were next made to the stem of the 3' terminal SL that were predicted to disrupt the A-U base pairs in the predicted tertiary interaction. In Mutant 19, U72 was mutated to a G. This mutation created a large internal loop and produced small plaques (Fig. 3.2). In Mutant 20, U77 was mutated to a G, which was predicted to introduce a bulged G·A near the base of the stem. This mutant produced small plaque virus (Fig. 3.2). After a single passage on BHK cells, large plaques were observed. These plaques were picked and sequenced and the results showed that the mutated nt had reverted to the parental sequence. In Mutant 21, U74 was mutated to a G. In Mutant 22, U74 and U72 were mutated to Gs. Both of these mutants had a lethal phenotype; no plaques were observed and no viral RNA was detected during three blind passages on BHK cells.

To determine whether a tertiary interaction might form between the SSL loop nts and bases on the 3' side of the 3' terminal SL that might be spatially close in a helical structure, mutations were next made either singly or in combination to Cs on both the 5' and 3' sides of the stem. In Mutant 23, the Cs at positions 9, 70 and 73 were changed to Gs. These nt substitutions did not change the predicted secondary structure and the mutant virus produced parental-size plaques (Fig. 3.3). The Cs at position 9, 68, and 73 were substituted with Gs in Mutant 24. These substitutions created a larger loop in the middle of the terminal stem. Plaques produced by this virus were intermediate in size (1.5 mm) (Fig. 3.3). This mutation was stable during three passages on BHK cells, only intermediate-size plaques and mutant sequence was detected. The Cs at positions 9 and 68 were substituted with Gs in Mutant 25,

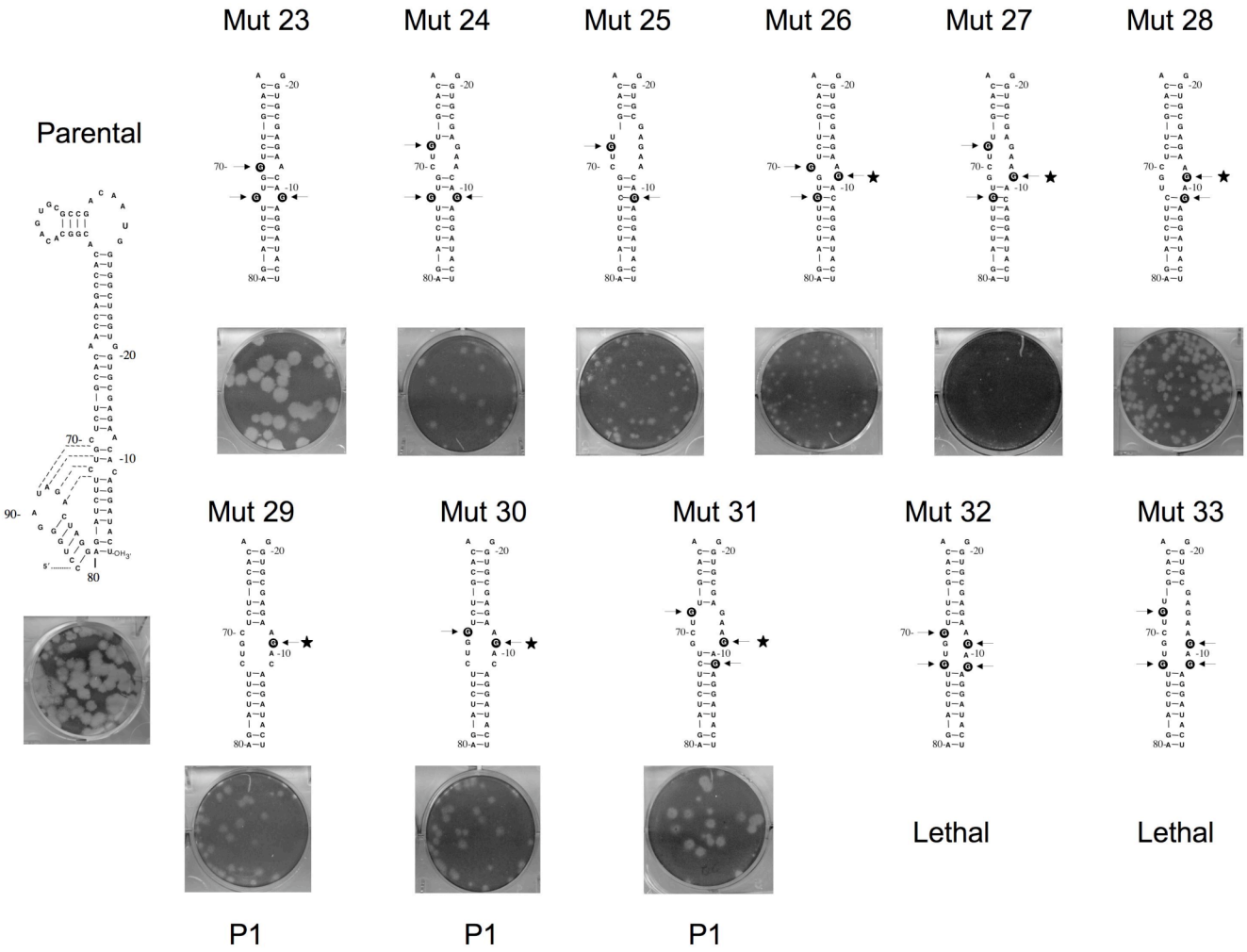

Figure 3.3. Mutagenesis of nts on the 3' and 5' sides of the WNV 3' terminal SL in the region of the predicted tertiary interaction.
Nt substitutions are indicated with an arrow and a black circle. Plaques formed 72 hr after transfection of either 1μg or 0.1 μg of RNA on a 6-well plate are shown.

which was predicted to change the C·C bulge to a G-C base pair and to open the middle of the stem. Mutant 25 virus had an intermediate plaque diameter (Fig. 3.3). This plaque phenotype and the mutated sequence were maintained through three passages. In Mutant 26, the Cs at positions 11, 70 and 73 were mutated to Gs, which was also predicted to change the C·C bulge to a G-C base pair and to increase the size of the internal loop. Mutant 26 produced virus with a small plaque phenotype (Fig. 3.3). Large plaques were observed after one passage on BHK cells and sequencing of viral RNA from picked large plaques revealed that only G11 had reverted to C, restoring the G-C base pair. In mutant 27, the Cs at positions 11, 68 and 73 were changed to Gs, changing the C·C bulge to a G-C base pair and creating a large internal loop in the middle of the stem. Mutant 27 produced pin point plaques (Fig. 3.3). Large plaques were observed after a single passage on BHK cells. These plaques were picked and sequenced. Only the mutated G11 reverted to the parental C. The Cs at positions 9 and 11 were changed to Gs in Mutant 28. This mutant produced plaques with diameters ranging from small to intermediate (0.5-1.5 mm) at 72 hours after transfection (Fig. 3). After a single passage on BHK cells large plaques were observed. These plaques were picked and sequenced. Again only the mutated G11 had reverted to the parental sequence. In Mutant 29, only C11 was changed to a G. A large internal loop was predicted to be created by this mutation. No plaques were observed on the transfection plate. Parental-size plaques observed after one passage on BHK cells, were picked and the viral RNA sequenced. The mutated G11 had reverted to the parental C11. Mutation of the Cs at positions 11 and 70 to Gs in

Mutant 30 were predicted to create a large internal loop. No plaques were observed on the transfection plate, but parental-size plaques appeared after one passage on BHK cells (Fig. 3.3). Only the mutated G11 had reverted to the parental sequence. For Mutant 31, the Cs at positions 9, 11 and 68 were changed to Gs. These mutations were predicted to create a large internal loop. No plaques were observed on the transfection plate. Sequencing of viral RNA from parental-size plaques observed after one passage on BHK cells (Fig. 3.3), revealed that again only the G at position 11 had reverted to the parental C. In Mutant 32, Cs were changed to Gs at positions 9, 11, 70 and 73 and in Mutant 33 Cs were mutated to Gs at positions 9, 11, 68 and 73, respectively. Both of these sets of mutations produced a lethal phenotype. No plaques were detected on the transfection plates, and no plaques or viral RNA were detected after three blind passages on BHK cells.

Mutation of U-A and G-C base pairs.

The mutational analysis described above indicated that C11 was important for efficient viral growth. In many different structural contexts mutation of C11 to a G resulted in rapid reversion of this nt and restoration of a G71-C11 base pair and the parental phenotype. Restoration of the G71-C11 base pair also allowed the adjacent U72-A10 pair to form, which was also shown to be important for efficient viral growth in Mutant 19. Mutations were next made to determine the relative importance of the primary sequence and the predicted secondary structure of these two base pairs. In Mutants 34, 35, 36, 37, the U72-A10 base pair at nt 10 was changed to G-C, C-G, A-U, or G-U, respectively (Fig. 3.4). All these mutations preserved the predicted

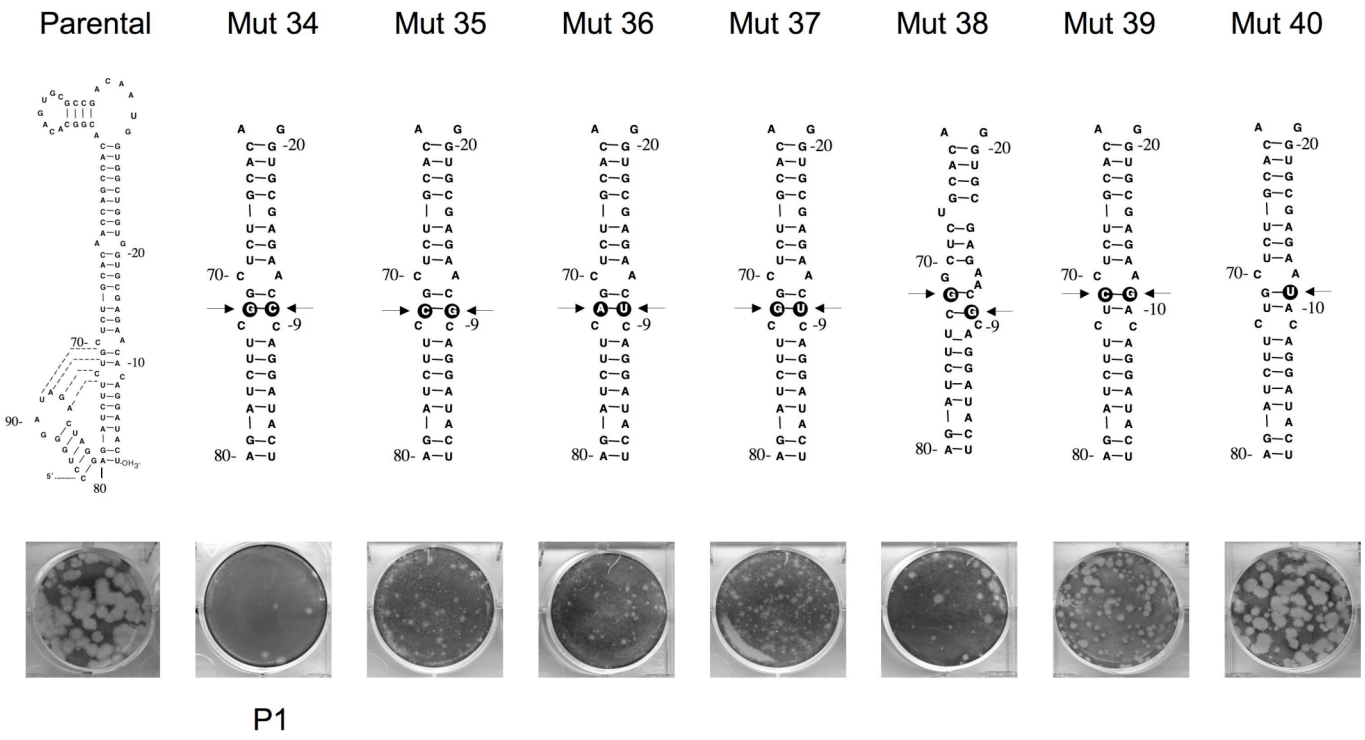

Figure 3.4. Mutagenesis of the U72-A10 and G71-C11 base pairs.
Nt substitutions are indicated with an arrow and a black circle. Nt substitutions are indicated with an arrow and a black circle. Plaques formed 72 hr after transfection of either 1μg or 0.1 μg of RNA on a 6-well plate are shown.

secondary structure of the 3' terminal SL. No plaques were observed on the transfection plate for Mutant 34, but a few small to intermediate size plaques (0.1-1.0 mm) were observed after a single passage on BHK cells (Fig. 3.4). After a second passage on BHK cells, many large plaques were observed and these plaques were picked and sequenced. Both mutated nts had reverted restoring the U-A base pair. Mutants 35 (C72-G10), 36 (A72-U10), and 37 (G72-U10) produced small to intermediate plaques (0.1-1.0 mm) (Fig. 3.4). After two passages on BHK cells, large plaque revertants were observed with each of these mutants. These plaques were picked and the viral RNA sequenced. In each case, both the mutated nts had reverted to the parental U72-A10 sequence. In mutant 38, the U72-A10 base pair was changed to a G72·G10. These substitutions were predicted to shift the predicted base pairing of the stem (Fig. 3.4). Both small and intermediate-sized plaques were observed on the transfection plate (Fig. 3.4). After a single passage on BHK cells, large plaques were observed and these plaques were picked and sequenced. Both mutated nts had reverted to the parental U72-A10. In Mutants 39 and 40, the G71-C11 base pair was changed to C71-G11 and G71-U11, respectively. These mutations were predicted to maintain the RNA secondary structure. Mutant 39 virus, produced both small and intermediate-sized plaques on the tranfection plate, but after two passages on BHK cells, only large plaques were observed (Fig. 3.4). The large plaques were picked and sequenced. Both mutated nts had reverted to the parental G71-C11. Mutant 40 virus produced large plaques on the transfection plate. After three passages, the large plaques were picked and sequenced. Only the mutant sequence was detected

indicating that this mutant was stable. These results indicated that the primary sequence as well as the structure of the U72-A10, G71-C11 base pairs was important. However, as indicated by the results with Mutant 40, replacement of the G71-C11 base pair with a G71-U11 had no effect on viral plaque diameter.

Relative eEF1A in vitro binding activity.

The binding activity of eEF1A to the WNV 3' terminal SL alone was previously shown to be 20% lower than that to the complete 3' (+) SL, which consists of both the SSL and the 3' terminal SL (Blackwell and Brinton, 1997). A gel mobility shift assay was used to compare the relative binding activity of purified recombinant eEF1A for the SL RNAs of Mutants 1, 2, 39 and 40 to that for the parental 3' (+) SL RNA (Fig. 3.5 A). Each of the radiolabeled RNA probes (~2000 CPM) was incubated with 0, 4, 8, or 20 ng of purified recombinant eEF1A for 30 min at room temperature. The RNA-protein complexes formed were separated on 5% non-denaturing polyacrylamide gels and detected by phosphorimaging. The percent of the free probe shifted was calculated as described in the Materials and Methods. A representative gel for each RNA probe is shown in Figure 3.5B. Average relative binding activity for each RNA probe calculated from three replicate assays is shown in Fig. 3.5C. With 20 ng of recombinant eEF1A, 55% of the parental 3' SL RNA probe was shifted, but only 28% of the Mutant 1, 10% of the Mutant 2, 33% of the Mutant 39 and 47% of the Mutant 40 RNA probes were shifted. Deletion of the SSL from the 3'(+) SL RNA in Mutant 1 resulted in a 27% decrease in relative binding activity as compared to the parental 3' (+) SL RNA probe which is similar to the 20% decrease

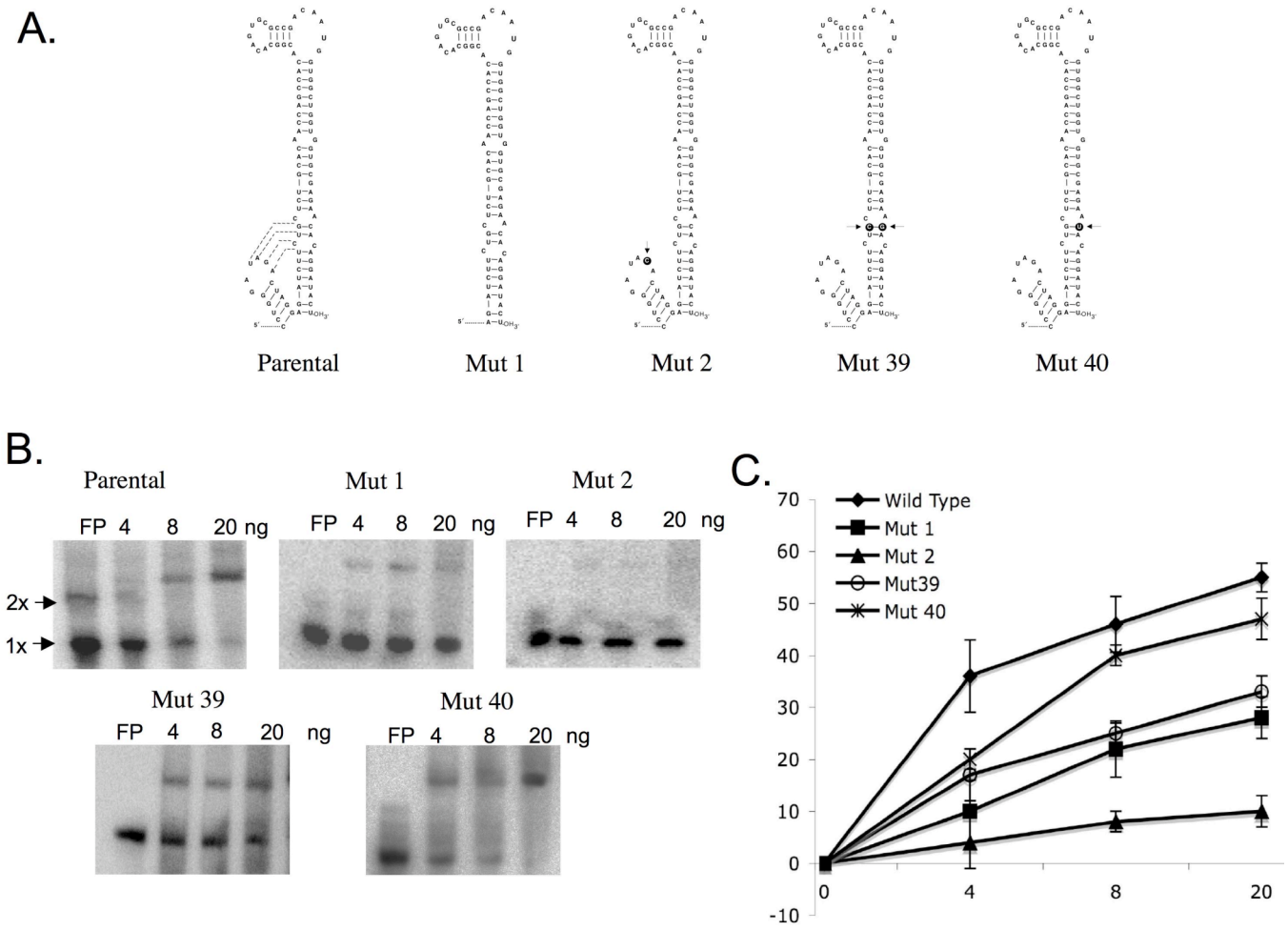

Figure 3.5. Comparison of the *in vitro* binding activity of recombinant eEF1A for parental, mutant and revertant virus 3' (+) SL RNA probes.
(A) RNA probes used for gel mobility shift assays. (B) Gel mobility shift assays done with ^{32}P-radiolabeled WNV 3' (+) SL RNAs (2000 CPM) and recombinant eEF1A purified from *E. coli* extracts. (C) The percent of ^{32}P RNA shifted by recombinant eEF1A. Error bars represent the standard error of the mean (SE) (n=3).

previously observed in a filter binding assay (Blackwell and Brinton, 1997). Interestingly, Mutant 2, in which G87 in the loop of the SSL was changed to a C, showed in a 45% decrease in relative binding activity of eEF1A as compared to the parental RNA. Mutation of the G71-C11 base pair also had a negative affect on *in vitro* eEF1A binding, as indicated by the results obtained with Mutant 39 (22% decrease) and Mutant 40 (8% decrease).

Effect of mutations in the WNV 3' (+) SL on viral RNA translation.

Previous studies have shown that mutations in the 3' terminal regions of some other positive strand viral RNAs could affect viral RNA translation. To analyze the effect of mutations in the WNV 3' (+) SL on viral RNA translation, the parental infectious clone and Mutant 1, 2, 33, 34, 39, and 40 RNAs were *in vitro* transcribed and then used to transfect BHK cells grown on coverslips. At 3 hr after RNA transfection, the cells were fixed and permeabilizeded. Intracellular WNV protein (red) produced was detected by immunofluorescence microscopy using an anti-WNV mouse hyperimmune ascites fluid (MHIAF). Even though these mutants differed in their viability and growth efficiency, Mutant 1 (lethal), Mutant 2 (lethal), Mutant 33 (lethal), Mutant 34 (intermediate-sized plaques only after 1 passage), Mutant 39 (small plaques) and Mutant 40 (large plaques), similar high levels of viral proteins were detected. Relative fluorescence intensity was assessed as described in the Materials and Methods. The transfection efficiencies (80-90%) were similar for all of the viral RNAs (Fig. 3.6A and B). These results demonstrate that none of the mutations had a significant negative affect on the efficiency of viral RNA translation.

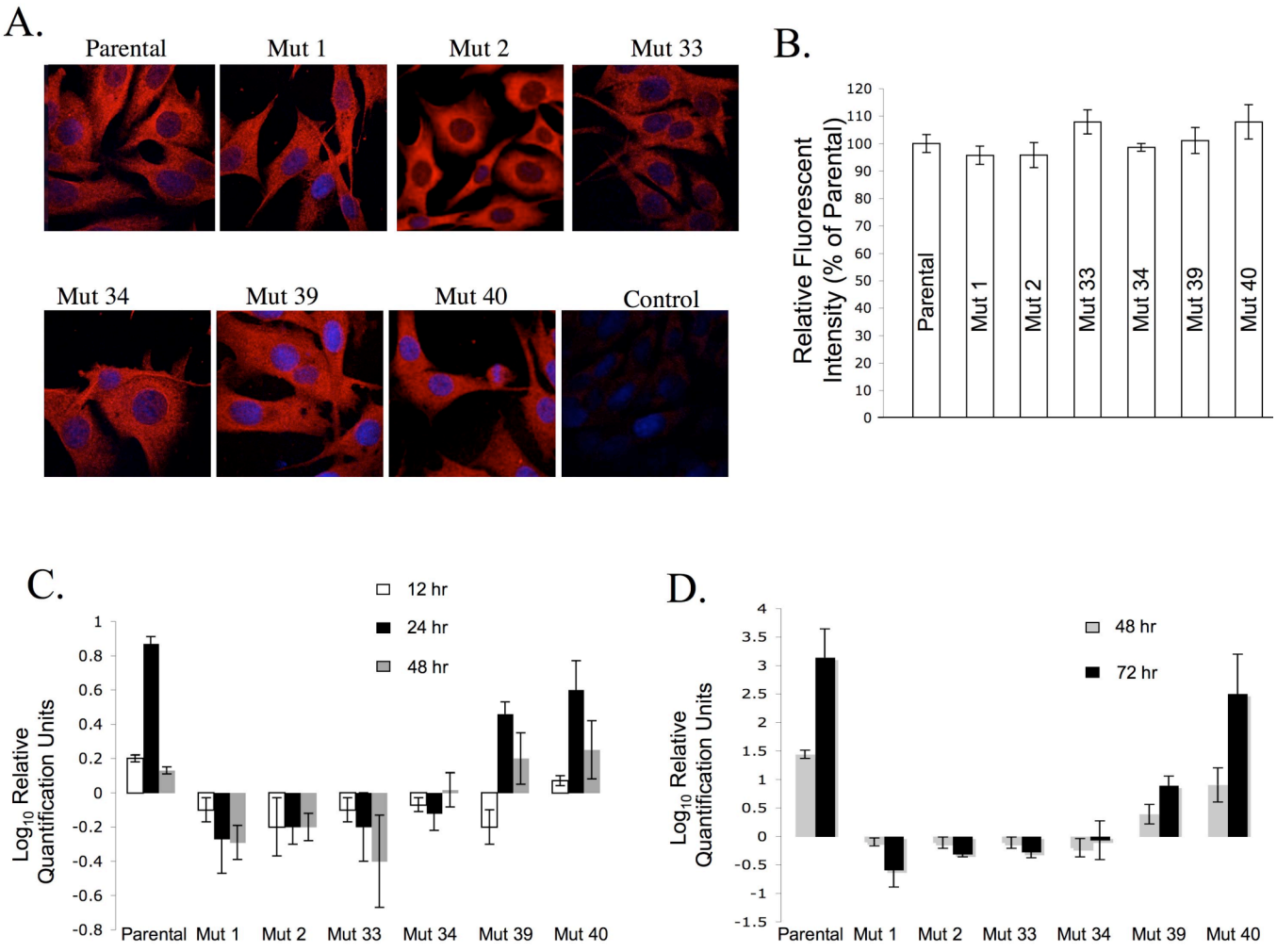

Figure 3.6. Effect of mutations on translation and replication of viral RNA.
(A) As a measure of translation efficiency, translated WNV proteins (red) were detected by confocal microscopy in BHK cells 3 hr after transfection of genomic RNA with anti-WNV MHIAF. (B) Relative fluorescent intensities of WNV proteins in the cytoplasm of transfected BHK cells. (C) Relative quantification of intracellular WNV minus-strand RNA by strand-specific Real-Time RT-PCR. Minus strand RNA levels are expressed as a log fold change of RNA detected at 12, 24 and 48 hr after transfection of viral RNA compared to the level of RNA detected at 2 hr after transfection. Each RNA sample was normalized to cellular GAPDH mRNA. Error bars represent the SE (n=3). (D) Relative quantification of intracellular WNV genomic RNA by Real-Time RT-PCR. Genomic RNA levels are expressed as a log fold change of RNA detected at 48 and 72 hr after transfection compared to the level of RNA present 6 hr after transfection as well as to cellular GAPDH mRNA. Error bars represent the SE (n=3).

Effect of mutations on viral RNA replication.

Relative real time RT-PCR was next used to quantify the intracellular levels of viral plus strand and minus strand RNAs produced within BHK cell monolayers after transfection of various mutant RNAs. Since the 3' (+) SL RNA is thought to contain *cis*-acting elements necesary for minus strand synthesis, the effects of the mutations on viral minus strand RNA synthesis were first investigated using minus strand specific real time RT-PCR. Minus strand RNA in BHK cells was quantified at 12, 24 and 48 hr after transfection by real-time RT-PCR as described in the Materials and Methods. After transfection of the parental infectious clone RNA, minus strand RNA levels peaked at 24 hr and then decreased by 48 hr (Fig. 3.5C). No minus strand RNA amplification above input was detected at 12, 24 or 48 hr after transfection for any of the lethal phenotype mutants (Mutant 1, 2, and 33) (Fig. 3.5C). Although no minus strand synthesis was observed at 12 or 24 hr after transfection of Mutant 34 RNA, by 48 hr, a small increase in minus strand RNA was detected. With Mutant 39, increased levels of minus strand RNA were detected by 24 hr after transfection (Fig. 3.5C). Mutant 40 produced slightly lower levels of minus strand RNA at 12 and 24 hr after transfection than did the parental RNA.

Viral plus strand RNA levels were measured at 48 and 72 hr after transfection, as described in the Materials and Methods. With the parental infectious clone RNA, the levels of viral genomic RNA increased significantly above the level of transfected input RNA present at 6 hr at 48 and 72 hr after transfection (Fig. 3.5D). At both 48 and 72 hr after transfection of RNAs of the lethal Mutants 1, 2 and 33, the

intracellular genomic RNA levels were lower than that of the viral RNA input at 6 hr after transfection, indicating degradation of the input RNA and little if any RNA replication (Fig. 3.5D). With Mutant 34, for which revertant virus was detected after a single passage on BHK cells (Fig. 3.3), the levels of genomic RNA reached input levels by 72 hr after transfection, confirming that some viral RNA replication had occurred but at a much lower level than for the parental genomic RNA. Mutant 39, which produced small plaques on the transfection plate, showed a 10-fold increase in genomic RNA over input RNA by 72 hr after transfection. The stable Mutant 40, which had a plaque phenotype similar to parental virus, showed a slight decrease in genomic RNA levels at both 48 and 72 hr after transfection, compared to the parental infectious clone RNA (Fig. 3.5D). These results indicate that each of the mutations that had a negative affect on viral viability also had a negative effect on viral genomic RNA replication.

DISCUSSION

Two minor binding sites for eEF1A on the WNV 3' (+) SL RNA were previously mapped to the top left loop of the 3' terminal SL and to the SSL and one major binding site was mapped to the 5' side of the stem of the 3' terminal SL RNA (Blackwell and Brinton, 1997). The predicted secondary structures and the majority of the sequences in the minor sites are conserved among divergent mosquito borne flaviviruses. With the high error rate of the viral RNA dependent RNA polymerase, conservation of sequences among flaviviruses especially in a noncoding region strongly suggests that these sequences are important in the flaviviral life cycle.

Mutations of particular nts in the top left loop of the terminal SL or deletion of the SSL had significant negative effects on virus replication even though each of these elements only accounted for about 20% of the *in vitro* eEF1A binding activity for the 3' (+) SL RNA (Blackwell and Brinton, 1997).

The previous study that suggested the possibilty of a tertiary interaction by ribonuclease probing and UV-melting analysis used *in vitro* transcribed RNAs (Shi et al., 1996). A recent NMR analysis of various synthetic model RNAs was performed in collaboration with Dr. M. Germann did not provide supporting evidence for this tertiary interaction (data not shown). Either the higher quality of the synthetic RNA used or the higher sensitivity of the NMR method provided a more accurate and detailed analysis of base pairing in the 3'(+) SL RNA. Data from the mutational studies with the WNV infectious clone also did not support the presence of the tertiary structure. Mutation of C73, which is located on the 3' side of the stem of the terminal SL and predicted to form the strongest base pair in the putative tertiary interaction had no effect on viral growth. This was also the case when C73 was deleted (Mutant 13). The formation of a G9-C73 base pair in the 3' terminal SL RNA was previously reported to disrupt the putative tertiary interaction (Shi et al., 1996). When C9 was mutated to a G in the infectious clone Mutant 14 so that a G9-C73 base pair was predicted to form, no effect on virus growth was observed. However mutation of U72 or U74 to Gs, which would be predicted disrupt the weaker A-U base pairs of the putative tertiary interaction, had a negative affect on virus growth. However, these mutations were also predicted to disrupt the base pairs at the bottom

of the 3' terminal stem (Fig. 3.2). Pairing of the first two bases of the 3' terminal stem was previously shown to be essential for viral RNA replication in a WNV replicon system (Tilgner and Shi, 2004).

The SSL was previously predicted to form in divergent mosquito borne flaviviruses (Olsthoorn and Bol, 2001). As well as in whole genome folds of WNV and dengue 2 virus (J.Y Sgro and A. Palmenberg, data not shown). The hexanucleotide loop of the SSL resembles a GN_NRA motif and this structural motif has been shown to be important for binding eEF1A to ribosomal RNA (Szewczak et al., 1993). Deletion of the SSL in a WNV infectious clone was lethal indicating this SL is essential for virus viability (Fig. 3.1). Deletion of the SSL from a WNV 3'(+) SL RNA probe resulted in a 27% decrease in relative *in vitro* eEF1A binding activity (Fig. 5). Mutation of G87 in the loop of the SSL to a C was also lethal for the virus. This mutation caused a 45% decrease in eEF1A binding activity, suggesting that G87 is also essential for eEF1A binding. Mutation of the first nt in the SSL loop (G91) produced virus with a small plaque phenotype when this nt was changed to either an A (Mutant 3) or a C (Mutant 10) which reverted to parental sequence. Mutation of the last nt in the SSL loop (A86) resulted in small plaques on the transfection plates (Mutant 8, 9 and 10) and the rapid reversion to the parental sequence. The rapid reversion of the first and last nt in the loop to a G and an A respectively, suggests that the SSL may form a GN_NRA loop motif.

Mutational analysis of the lower part of the stem of the WNV 3' terminal SL identified two *cis*-acting base pairs (U72-A10 and G71-C11). Substitutions that

maintained the predicted secondary structure in this region, but changed the primary sequence of either of these base pairs had a negative affect on viral viability with the exception of Mutant 40 (G71-U11) that produced parental-size plaques, indicating that a G-U base pair could substitute for the G71-C11 pair. Mutant 39 (C71-G10) showed a 22% decrease in *in vitro* eEF1A binding and Mutant 40 showed an 8% decrease in *in vitro* eEF1A binding. A decrease of 22% or more in *in vitro* eEF1A binding correlated with reduced viral viability.

The two minor eEF1A binding sites may facilitate the initial interaction between eEF1A and the WNV 3' (+) SL RNA. This initial interaction may lead to conformational changes in the viral 3' RNA as well as in eEF1A that allow eEF1A to recognize the major binding site, which accounts for 60% of the total *in vitro* eEF1A binding activity. Further induced fit may then maximize the contacts between eEF1A and the WNV 3' (+) SL RNA. Most DNA-binding proteins recognize specific sequences located in the major groove of a B-form double helix. The steep and narrow major groove of the RNA A-form double helix prevents the bases in this groove from being easily accessible for interaction with protein. Often RNA-protein interactions are accomplished in two distinct steps. First, positively charged residues on the surface of a protein allow it to rapidly associate with negatively charged RNA. Second, the close proximity of the RNA and protein allow the formation of a stable complex via conformational changes in both the RNA and the protein that lead to sequence specific interactions (Katsamba, Myszka, and Laird-Offringa, 2001).

EF-Tu, the bacterial homolog of eEF1A has been shown to bind to the Qβ viral genomic RNA at the S2 binding site and also to viral proteins in the replication holoenzyme. Both of these interactions were reported to be required for specific initiation of minus strand RNA synthesis (Brown, 1996; Kita et al., 2006). Data from this study and previous studies demonstrated that mutations in the 3' (+) SL RNA that reduced eEF1A binding to this RNA negatively affected the accumulation of viral minus strand RNA, suggesting that this RNA-protein interaction may facilitate the initiation of minus strand synthesis. eEF1A was also shown to colocalize with WNV viral replication complexes in infected cells by confocal microscopy and and anti-eEF1A antibody coprecipitated viral replication complex proteins (data from Chapter 2). These data suggest the possibility that eEF1A may also interact with a viral nonstructural protein. None of the mutations made in the WNV 3'(+) SL RNA that negatively affected eEF1A binding had an effect on the translational efficiency of the WNV viral polyprotein in BHK cells. The function of eEF1A in flaviviral replication appears to be similar to that in Qβ replication but not TYMV replication where eEF1A binding to the terminus of the TYMV viral genome was shown to enhance viral protein translation and a repress viral minus strand RNA synthesis (Matsuda, 2003a; Matsuda, 2003b).

MATERIALS AND METHODS

Cells

Baby hamster kidney-21/WI2 cells (hereafter referred to as BHK cells) were grown at 37^{o} C with 5% CO_2 in Eagle's minimum essential media (MEM) containing

4.5% heat-inactivated fetal bovine serum (FBS) and 10 μg/ml gentamicin (Vaheri et al., 1965).

Mutagenesis of a WNV infectious clone

The construction and characteristics of the chimeric full length WNV infectious clone were previously described (Yamshchikov, 2001). The strategy used to introduce mutations to the terminal SL in the infectious clone was described previously (Elghonemy, Davis, and Brinton, 2005). To introduce mutations into the SSL, a shuttle vector (pWNV-TrunII), which contained 162 5' nt and 207 3'nt of the WNV cDNA, was created by digestion of the infectious clone with the restriction enzyme, SacII, followed by gel purification and ligation of the fragment similar to the method described previously (Elghonemy, Davis, and Brinton, 2005). Mutations were introduced using the Quick-Change Site-Directed Mutagenesis kit (Stratagene) according to the manufacturer's protocol. Primer sequences used to generate the mutant viral cDNAs are available upon request. The mutated infectious clones were generated by restriction digestion with SacII followed by gel purification and ligation with the gel purified internal fragment from the parental infectious clone. All mutations made were confirmed by sequencing.

In vitro transcription of WNV genomic RNA

Parental or mutant infectious clone plasmid DNAs were linearized at the 3' end of the WNV cDNA with Xba I and then purified using a PCR cleanup kit (Qiagen). The *in vitro* transcription of capped viral RNA was performed using the mMessage Machine high yield capped RNA transcription kit (Ambion) or the

Amplicap high yield message maker kit (Epicentre, Madison, WI) according to the manufactures' protocols. RNase-free DNase was then added and the reaction mixture was incubated at 37^{o} C for 30 min followed by heat-inactivation of the DNase at 65^{o}C for 15 min. The transcription reaction mixture was used directly to transfect BHK cells.

Transfection of WNV genomic RNA into BHK cells

RNA transfection was performed as described previously (Elghonemy, Davis, and Brinton, 2005). Briefly, either 0.1 or 1.0 μg of genomic RNA was transfected into BHK cells grown to 80% confluency in 6-well dishes with DMRIE-C according to the manufacturer's protocol (Invitrogen). After a 2 hr incubation at 37^{o}C, the transfection media was removed and the cells were overlayed with either 2 ml of 5% FCS MEM or a 1:1 mixture of 1% agarose and 2X MEM containing 5% FBS. At 72 hr after transfection, the agarose was removed and plaques were visualized using a methyl violet stain (10% ethanol, 0.5% methyl violet), or a second overlay of 0.05% neutral red solution, 0.5% agarose in 1X MEM was applied to the cell monolayers when plaques were to be picked. Virus in growth media harvested from duplicate wells was titered in duplicate by plaque assay on BHK cells.

Analysis of virus revertants

Viral RNA was extracted and purified using TRI Reagent LS (Molecular Research Center, Inc., Cincinnati, OH.) according to the manufacturer's protocol. Extracted RNA was subjected to 3' polyadenylation as described previously using the

Poly A tailing kit (Ambion), amplified by RT-PCR and then sequenced (Tilgner and Shi, 2004). Primers used are available upon request.

Purification of eEF1A

eEF1A cDNA amplified by RT-PCR from BHK cells was cloned into the T7 expression vector pCR T7/CT-TOPO (Invitrogen, Carlsbad, CA.) (Smith, Blackwell, and Brinton, unpublished data). Recombinant eEF1A was expressed in Origami cells (Novagen, Madison, WI.) and induced with 1 mM IPTG. After 4 hr, bacterial cells were pelleted and resuspended in Extraction buffer (50 mM sodium phosphate, 300 mM NaCl, pH 7.6) and then lysed with a French pressure cell press (SIM-AMINCO Spectronic Instrument Inc., Rochester, NY.). The cell lysate was clarified by centrifugation at 3000 x g. Recombinant protein was bound to Talon metal affinity resin (BD Biosciences Clontech, Palo Alto, CA.), washed with Wash buffer (50 mM sodium phosphate, 300 mM NaCl, 20 mM imidazole, pH 7.6), and then eluted with Elution buffer (50 mM sodium phosphate, 300 mM NaCl, 300 mM imidazole, pH 7.6). To remove imidazole, eluted protein was dialyzed against two liters of dialysis buffer (50 mM sodium phosphate, 50 mM NaCl, pH 7.6) in a Slide-A-Lyzer dialysis cassette (Pierce, Rockford, IL.) and concentrated to 200-400 ng/μl using a Centricon 10 concentrator (Amicon, Beverly, MA.).

Gel mobility shift assays.

The WNV infectious clone described above was used to generate PCR templates to generate 3' SL RNA probes that contained a T7 promoter for RNA transcription and specific mutations as described previously (Blackwell and Brinton,

1995). The primers used are available upon request. PCR products were purified using the Qiagen PCR clean up kit (Qiagen, Valencia, CA). The PCR products were transcribed in the presence of (α-^{32}P) GTP using T7 RNA polymerase (50 U) according to the manufacturer's protocol (Ambion, Austin, TX.) for 1 hr at 37^{o} C. Transcription reactions were stopped by the addition of DNase (1 U) for 15 minutes at 37^{o} C, and the RNA was gel purified and precipitated with ethanol as described previously (D'Alessio, 1982). The purified RNAs were resuspended in 100 μl of RNase free water. Radioactivity was measured using a scintillation counter (Beckman LS6500) and the specific activity (~1.3 x 10^{7} cpm/μg) was calculated as described previously (Blackwell and Brinton, 1997).

Purified recombinant eEF1A was incubated in gel shift buffer [(GS buffer) 3% Ficoll 400, 20 mM Sodium phosphate, pH 7.0, 60 mM KCl, 1 mM $MgCl_2$, and 0.5 mM EDTA] with a ^{32}P-labeled 3' viral RNA probe (approximately 2000 cpm or 0.2 nM final concentration per reaction), poly I-C (50 ng), and RNase inhibitor (Ambion) (10 units) for 30 min at room temperature. The RNA-protein complexes were resolved by nondenaturing 5% polyacrylamide gel electrophoresis (PAGE) in 1X TBE buffer. The percent RNA bound was quantified with a Fuji BAS 1800 analyzer (Fuji Photo Film Co., Japan) and Image Gauge software (Science Lab, 98, version 3.12, Fuji Photo Film Co.).

Analysis of intracellular viral RNA by real-time RT-PCR

Replicate BHK monolayers in 6-well tissue culture plates (80% confluency) were washed once with 2 ml of Opti-MEM (Invitrogen) and then transfected with 200

ng of parental or mutant viral RNA in DMRIE-C (Invitrogen). BHK monolayers were washed 3 times with 5 ml of growth media and total intracellular RNA was extracted using TRI Reagent (Molecular Research Center, Inc.) at the times indicated. Using real-time RT-PCR, the relative amount of intracellular viral genomic RNA was determined on an Applied Biosystems 7500 real-time PCR system using 200 ng of total RNA, and the TaqMan one-step RT-PCR kit according to the manufacturer's protocol (Applied Biosystem). The primers used to detect WNV RNA were 5'-GGCGGTTCTAGGAGAAGTCA-3' and 5'-CTCCTGTTGTGGTTGCTTCT-3' and the FRET probe was 5'-Fam-TGCACCTGGCCAGAAACCCACACTCTGT -3'-TAMRA from the NS1 region of the genome.

T7-tagged primer real-time RT-PCR was performed as previously described for specific detection of minus strand RNA (Lanford et al., 1994; Samuel and Diamond, 2005). Briefly, 2 pmol of the minus strand primer, 5'-**GCGTAATACGACTCACTATA**gagggcggttctaggagaagt-3', [T7 tag sequence (uppercase, bold); NS1 specific sequence (lower case, non-bold)] was incubated with 800 ng of total intracellular RNA in a Taqman one-step RT-PCR reaction mixture and incubated at 50^{o}C for 30 min to synthesize cDNA and then at 95^{o}C for 30 min to inactivate the reverse transcriptase. Following inactivation, 20 pmol of each of the following primers 5'-**GCGTAATACGACTCACTATA**-3' and 5'-ctcctgttgtggttgcttc-3' with 5 pmol of the probe, 5'Fam-TGCACCTGGCCAGAAACCCACACTCTGT3'-TAMRA, were added to the reaction mixture. The PCR reaction was performed as

follows: 40 cycles at 95^{o}C for 15 sec and then 60^{o}C for 1 min on an Applied Biosystems 7500 real-time PCR system.

Analysis of all real-time RT-PCR reactions was done using the relative quantification software from Applied Biosystems and the cellular mRNA GAPDH (Applied Biosystems) as the endogenous control. The genomic RNA levels at 48 and 72 hr after transfection were normalized against input RNA present at 6 hr after transfection to remove background. Levels of minus strand RNA at 12, 24 and 48 hr after transfection were also normalized to viral RNA levels present at 2 hr after transfection to remove nonspecific amplification of genomic strand RNA.

Confocal Microscopy

BHK cells were grown to 60% confluency on glass coverslips and then were transfected with 1 μg of *in vitro* transcribed viral RNA. Three hr after transfection, cells were fixed by incubation with 4% paraformaldehyde in PBS for 10 min at room temperature and then permeabilized with methanol at -20^{o}C for 10 min. Coverslips were blocked overnight with 5% horse serum (Invitrogen) in PBS. Coverslips were incubated with a 1:100 dilution of mouse hyper-immune ascitic fluid (MHIAF) against WNV (a gift from Dr. Robert Tesh, UTMB, Galveston, TX) in PBS containing 5% horse serum for 1 hr at 37^{o}C and then washed 4 times with PBS. Coverslips were then incubated with a 1:300 dilution of chicken anti-mouse IgG-TR (Santa Cruz Biotechnology) in PBS containing 5% horse serum at and 0.5 μg/ml Hoechst 33258 (Molecular probes) to stain the nuclei. Coverslips were washed with PBS, mounted on glass slides with Prolong mounting media (Invitrogen) and

visualized with a 100 X oil immersion objective on a LSM 510 laser confocal microscope using LSM 5 (Ver. 3.2) software (Carl Zeiss Inc., Thornwood, NY). Relative fluorescence intensity was measured in equivalent diameter circles in 3 locations in the cytoplasm of 10 representative BHK cells for each transfected viral RNA using LSM 5 (3.2) software. The same camera settings were used for each of the images compared.

RNA secondary structure prediction

Secondary structures were predicted for the 3' terminal 120 nt of the parental and mutant genomic RNAs using the RNA secondary structure predicting program, MFold v3.1 (Zuker, 2003).

REFERENCES

Abramovitz, D. L., and Pyle, A. M. (1997). Remarkable morphological variability of a common RNA folding motif: the GNRA tetraloop-receptor interaction. *J Mol Biol* **266**(3)**,** 493-506.

Blackwell, J. L., and Brinton, M. A. (1995). BHK cell proteins that bind to the 3' stem-loop structure of the West Nile virus genome RNA. *J Virol* **69**(9)**,** 5650-8.

Blackwell, J. L., and Brinton, M. A. (1997). Translation elongation factor-1 alpha interacts with the 3' stem-loop region of West Nile virus genomic RNA. *J Virol* **71**(9)**,** 6433-44.

Blumenthal, T., and Carmichael, G. G. (1979). RNA replication: function and structure of Qbeta-replicase. *Annu Rev Biochem* **48,** 525-48.

Bredenbeek, P. J., Kooi, E. A., Lindenbach, B., Huijkman, N., Rice, C. M., and Spaan, W. J. (2003). A stable full-length yellow fever virus cDNA clone and the role of conserved RNA elements in flavivirus replication. *J Gen Virol* **84**(Pt 5)**,** 1261-8.

Brinton, M. A., Fernandez, A. V., and Dispoto, J. H. (1986). The 3'-nucleotides of flavivirus genomic RNA form a conserved secondary structure. *Virology* **153**(1)**,** 113-21.

Brown, D., and Gold, L. (1996). RNA replication by Qβ replicase: A working model. *Proc. Natl. Acad. Sci. USA* **93,** 11558-11562.

Cimarelli, A., and Luban, J. (1999). Translation elongation factor 1-alpha interacts specifically with the human immunodeficiency virus type 1 Gag polyprotein. *Journal of Virology* **73,** 5388-5401.

Costa, M., and Michel, F. (1995). Frequent use of the same tertiary motif by self-folding RNAs. *Embo J* **14**(6)**,** 1276-85.

D'Alessio, J. A. (1982). "RNA sequencing." Gel electroporesis of nucleic acids (D. R. a. B. D. James, Ed.) IRL Press, Oxford.

Ejiri, S. (2002). Moonlighting Functions of Polypeptide Elongation factor 1: From Actin Bundling to Zinc Finger Protein R1-Associated Nuclear Localization. *Biosciences, Biotechnology, and Biochemistry* **66,** 1-21.

Elghonemy, S., Davis, W. G., and Brinton, M. A. (2005). The majority of the nucleotides in the top loop of the genomic 3' terminal stem loop structure are cis-acting in a West Nile virus infectious clone. *Virology* **331**(2)**,** 238-246.

Gonen, H., Dickman, D.,Schwartz, A.L. and Ciechanover, A. (1996). Protein synthesis elongation factor EF-1α is an isopeptidase essential for ubiquitin-dependent degradation of certain proteolytic substrates. *Adv. Exp. Med. Biol* **389,** 209-219.

Gonen, H., Smith, C.E., Siegel, N.R., Kahana, C., Merrick, W.C., Chakraburtty, K., Schwartz, A.L. and Ciechanover, A. (1994). Protein synthesis elongation factor factor EF-1α is essential for ubiquitin-dependent degredation of certain Na-acetylated proteins and may be substituted for by the bacterial elongation factor EF-Tu. *Proceedings from the National Academy of Sciences USA* **91,** 7648-7652.

Gutell, R. R., Larsen, N., and Woese, C. R. (1994). Lessons from an evolving rRNA: 16S and 23S rRNA structures from a comparative perspective. *Microbiol Rev* **58**(1)**,** 10-26.

Hahn, C. S., Hahn, Y. S., Rice, C. M., Lee, E., Dalgarno, L., Strauss, E. G., and Strauss, J. H. (1987). Conserved elements in the 3' untranslated region of flavivirus RNAs and potential cyclization sequences. *J Mol Biol* **198**(1)**,** 33-41.

Johnson, C. M., Perz, D.R., French, R., Merrick, W.C., and Donis, R.O. (2001). The NS5A protein of bovine viral diarrhoea virus interacts with the a subunit of translation elongation factor-1. *Journal of General Virology* **82,** 2935-2943.

Katsamba, P. S., Myszka, D. G., and Laird-Offringa, I. A. (2001). Two functionally distinct steps mediate high affinity binding of U1A protein to U1 hairpin II RNA. *J Biol Chem* **276**(24)**,** 21476-81.

Kita, H., Cho, J., Matsuura, T., Nakaishi, T., Taniguchi, I., Ichikawa, T., Shima, Y., Urabe, I., and Yomo, T. (2006). Functional Qbeta replicase genetically fusing essential subunits EF-Ts and EF-Tu with beta-subunit. *J Biosci Bioeng* **101**(5)**,** 421-6.

Kou, Y. H., Chou, S. M., Wang, Y. M., Chang, Y. T., Huang, S. Y., Jung, M. Y., Huang, Y. H., Chen, M. R., Chang, M. F., and Chang, S. C. (2006). Hepatitis C virus NS4A inhibits cap-dependent and the viral IRES-mediated translation through interacting with eukaryotic elongation factor 1A. *J Biomed Sci*.

Lanford, R. E., Sureau, C., Jacob, J. R., White, R., and Fuerst, T. R. (1994). Demonstration of in vitro infection of chimpanzee hepatocytes with hepatitis C virus using strand-specific RT/PCR. *Virology* **202**(2)**,** 606-14.

Lo, M. K., Tilgner, M., Bernard, K. A., and Shi, P. Y. (2003). Functional analysis of mosquito-borne flavivirus conserved sequence elements within 3' untranslated region of West Nile virus by use of a reporting replicon that differentiates between viral translation and RNA replication. *J Virol* **77**(18)**,** 10004-14.

Lui, G., Tang, J., Edmonds, B.T., Murray, J., Levin, S., and Condeelis, J. (1996). F-actin Sequesters Elangation Factor 1α from Interaction with Aminoacyl-tRNA in a pH-dependent Reaction. *The Journal of Cell Biology* **135,** 953-963.

Lui, G. G., W.M., Persky, D., Latham, V.M., Singer, R.H. and Condeelis, J. (2002). Interaction of Elongation Factor 1α with F-Actin and β-Actin mRNA: Implications for Anchoring mRNA in Cell Protrusions. *Molecular Biology of the Cell* **13,** 579-592.

Matsuda, D., and T.W. Dreher (2003a). The tRNA-like structure of Turnip yellow mosaic virus RNA is a 3'-translational enhancer. *Virology* **321,** 36-46.

Matsuda, D., S. Yoshinari and T.W. Dreher (2003b). eEF1a binding to aminoacylated viral RNA represses minus strand synthesis by TYMV RNA-dependant RNA polymerase. *Virology* **321,** 47-56.

Mickleburgh, I., Chabanon, H., Nury, D., Fan, K., Burtle, B., Chrzanowska-Lightowlers, Z., and Hesketh, J. (2006). Elongation factor 1alpha binds to the region of the metallothionein-1 mRNA implicated in perinuclear localization--importance of an internal stem-loop. *Rna* **12**(7)**,** 1397-407.

Miranda, G., Schuppli, D., Barrera, I., Hausherr, C., Sogo, J., and Weber, H. (1997). Recognition of bacteriophage Qb replicase: role of RNA interactions mediated by ribosomal proteins S1 and host factor. *Journal of Molecular Biology* **267,** 1089-1103.

Olsthoorn, R. C., and Bol, J. F. (2001). Sequence comparison and secondary structure analysis of the 3' noncoding region of flavivirus genomes reveals multiple pseudoknots. *Rna* **7**(10)**,** 1370-7.

Petersen, L. R., Marfin, A. A., and Gubler, D. J. (2003). West Nile virus. *Jama* **290**(4)**,** 524-8.

Qanungo, K. R., D. Shaji, M. Mathur, and A.K. Banerjee (2004). Two RNA polymerase complexes from vesicular stomatitis virus-infected cells that carry

out transcription and replication of genome RNA. *Proceedings from the National Academy of Sciences USA* **101,** 5952-5957.

Riis, B., Rattan, S. I., Clark, B. F., and Merrick, W. C. (1990). Eukaryotic protein elongation factors. *Trends Biochem Sci* **15**(11)**,** 420-4.

Samuel, M. A., and Diamond, M. S. (2005). Alpha/beta interferon protects against lethal West Nile virus infection by restricting cellular tropism and enhancing neuronal survival. *J Virol* **79**(21)**,** 13350-61.

Schuppli, D., Geogijevic, J., and Weber, H. (2000). Synergism of mutations in the bacteriophage Qb RNA affecting host factor dependence of Qb replicase. *Journal of Molecular Biology* **295,** 149-154.

Schuppli, D., Miranda, G., Qiu, S., and Weber, H (1998). A branched stem-loop structure in the M-site of bacteriophage Qb RNA is important for template recognition by Qb replicase holoenzyme. *Journal of Molecular Biology* **283,** 585-593.

Shi, P. Y., Brinton, M. A., Veal, J. M., Zhong, Y. Y., and Wilson, W. D. (1996). Evidence for the existence of a pseudoknot structure at the 3' terminus of the flavivirus genomic RNA. *Biochemistry* **35**(13)**,** 4222-30.

Shiina, N., Gotoh, y., Kubomura, N., Iwamatsu, A., and Nishida, E. (1994). Microtubule severingby elongation factor 1a. *Science* **266,** 282-285.

Szewczak, A. A., Moore, P. B., Chang, Y. L., and Wool, I. G. (1993). The conformation of the sarcin/ricin loop from 28S ribosomal RNA. *Proc Natl Acad Sci U S A* **90**(20)**,** 9581-5.

Tilgner, M., Deas, T. S., and Shi, P. Y. (2005). The flavivirus-conserved penta-nucleotide in the 3' stem-loop of the West Nile virus genome requires a specific sequence and structure for RNA synthesis, but not for viral translation. *Virology* **331**(2)**,** 375-86.

Tilgner, M., and Shi, P. Y. (2004). Structure and function of the 3' terminal six nucleotides of the west nile virus genome in viral replication. *J Virol* **78**(15)**,** 8159-71.

Vaheri, A., Sedwick, W. D., Plotkin, S. A., and Maes, R. (1965). Cytopathic effect of rubella virus in RHK21 cells and growth to high titers in suspension culture. *Virology* **27**(2)**,** 239-41.

Weaver, S. C., and Barrett, A. D. (2004). Transmission cycles, host range, evolution and emergence of arboviral disease. *Nat Rev Microbiol* **2**(10)**,** 789-801.

Yamaji, Y., Kobayashi, T., Hamada, K., Sakurai, K., Yoshii, A., Suzuki, M., Namba, S., and Hibi, T. (2006). In vivo interaction between Tobacco mosaic virus RNA-dependent RNA polymerase and host translation elongation factor 1A. *Virology* **347**(1)**,** 100-8.

Yamshchikov, V. F., G. Wengler, A.A. Perelygin, M.A. Brinton, and R.W. Compans (2001). An infectious clone of the West Nile flavivirus. *Virology* **281**(2)**,** 294-304.

Yu, L., and Markoff, L. (2005). The topology of bulges in the long stem of the flavivirus 3' stem-loop is a major determinant of RNA replication competence. *J Virol* **79**(4)**,** 2309-24.

Zuker, M. (2003). Mfold web server for nucleic acid folding and hybridization prediction. *Nucleic Acids Res* **31**(13)**,** 3406-15.